Graphical functions in parametric space

MASTERARBEIT

zur Erlangung des akademischen Grades
Master of Science
(M. Sc.)
im Fach Physik

eingereicht an der
Mathematisch-Naturwissenschaftlichen Fakultät
Institut für Physik
Humboldt-Universität zu Berlin

von
Marcel Golz
geboren am 07.07.1989 in Cottbus

Betreuung:

1. *Prof. Dr. Dirk Kreimer*
2. *Dr. Oliver Schnetz*

eingereicht am: *10. Februar 2015*

Abstract

We study graphical functions as defined by Oliver Schnetz and derive an alternative integral representation. Following a brief overview over the physical and mathematical background we introduce all the graph theoretical tools that will be made use of. We then review graphical functions in their original definition, their properties and applications in physics and mathematics. The main result is a detailed derivation of an integral representation of graphical functions in analogy to the well known Feynman parameter integrals from quantum field theory. Using the properties of this new integral representation we then go on to prove two new results in the theory of graphical functions and give an alternative proof of an identity originally due to Schnetz. Additionally we note that the new parametric integral representation makes graphical functions potentially susceptible to the iterated integration algorithm developed by Brown and implemented in Erik Panzer's `HyperInt`. We present many results for certain concrete graphical functions obtained with Panzer's program.

Zusammenfassung

Wir untersuchen die von Oliver Schnetz definierten graphischen Funktionen und leiten eine alternative Integraldarstellung her. Nach einer kurzen Übersicht über den physikalischen und mathematischen Hintergrund führen wir alle graphentheoretischen Werkzeuge ein, die später benutzt werden. Danach besprechen wir graphische Funktionen in ihrer ursprünglichen Definition, ihre Eigenschaften, sowie Anwendungen in Physik und Mathematik. Das Hauptergebnis ist eine detaillierte Herleitung einer Integraldarstellung graphischer Funktionen in Analogie zu den bekannten Feynman Parameterintegralen aus der Quantenfeldtheorie. Unter Benutzung der Eigenschaften dieser neuen Integraldarstellung beweisen wir zwei neue Ergebnisse in der Theorie der graphischen Funktionen und geben einen alternativen Beweis für eine zuvor von Schnetz bewiesene Identität. Zusätzlich bemerken wir, dass die neue parametrische Darstellung potentiell ermöglicht graphische Funktionen mit Browns Algorithmus zur iterierten Integration, der von Erik Panzer in `HyperInt` implementiert wurde, zu behandeln. Wir präsentieren zahlreiche Ergebnisse die mit Panzers Programm für gewisse graphische Funktionen erhalten werden konnten.

Contents

List of Figures

yōgā vē bhūri jāyati
ayōgā bhūrisaṅkhayō
bhavāya vibhavāya ca
ētāṃ dvēdhā pathaṃ ñatvā
yathā bhūri pavaḍḍhati
tathā attānaṃ nivēsēyya

From endeavour wisdom springs,
lacking effort wisdom wanes:
having known this two-fold path
either to progress or decline
so should one exhort oneself
that wisdom may increase.

Siddhārta Gautama
Dhammapada, Ch. XX, Verse 282

Chapter 1

Introduction

1.1 Background

1.1.1 Quantum field theory and Feynman integrals

Quantum field theories are the framework in which physicists describe subatomic particles and their interactions. The goal is to make predictions in the form of scattering probabilities that can be compared with measurements at modern particle accelerators like the LHC. The way from some first principles (the Wightman axioms [44]) to actual natural phenomena is long and laborious and here we will only give a very brief summary of the most important steps. For details we refer to the multitude of textbooks, e.g. [22].

From Lagrangians to amplitudes. A field theory is given by its Lagrangian (density), for example in ϕ^4 theory[1]

$$\mathcal{L}_{\phi^4} = \frac{1}{2}\left((\partial_\mu\phi)(\partial^\mu\phi) - m^2\phi^2\right) - \frac{g}{4!}\phi^4, \tag{1.1}$$

which typically depends on the fields that appear in that particular theory and their derivatives, as well as parameters like the mass m and coupling g. The 'quantum' enters the stage through a quantization process, for example by imposing equal time commutation relations on the fields in canonical quantization. Computing the aforementioned scattering probabilities then essentially boils down to the computation of *vacuum expectation values* of certain time-ordered products of fields. However, actually performing these computations in practice is highly non-trivial and has in one way or another been the main occupation of theoretical high-energy physicists for the better part of a century. By far the most used method is the perturbative approach in which one assumes that the coupling constant (g in the example Lagrangian above) is sufficiently small to justify an expansion in a power series. The result is an infinite series in the coupling constant, whose coefficients are certain integrals (except for the first 'tree-level' term). Since the integrals quickly become more numerous and more complicated in higher orders, one has to cut off that series

[1] ϕ^4 theory and 'scalar theories' in general are typically used as pedagogical examples because they are the least complicated QFTs, conceptually as well as notationally. While they are not themselves 'physical', there are ways to reduce integrals arising in physical theories like quantum electrodynamics to scalar master integrals (e.g. the Passarino-Veltman algorithm [31]), so they are not only important in teaching but also in research.

at some finite order and be content with an approximate result. Extraordinary precision in modern high energy experiments necessitates that theoreticians compute coefficients at higher and higher orders, often approaching, sometimes extending the very boundaries of current mathematical knowledge. Before we elaborate on that last point, we have to clarify the nature of the coefficients in the perturbation expansion.

Feynman rules and diagrams As mentioned above, the coefficients in a perturbation expansion are integrals. Most commonly one uses momentum space, in which a general scalar dimensionally regularized Euclidean Feynman integral has the form

$$I = \int \prod_{l=1}^{L} \mathrm{d}^D k_l \, \frac{1}{(k_l^2 + m^2)^{a_l}} \prod_{v=1}^{V} \delta^D \left(P_v - \sum_{l=1}^{L} \epsilon_{vl} k_l \right). \tag{1.2}$$

Here, P_v are external momenta, i.e. the momenta of interacting particles. The k_l are internal momenta, i.e. the momenta of virtual particles that can appear in an interaction (and $\epsilon_{vl} = \pm 1$, indicating incoming our outgoing momenta). Since none of them can be observed, one has to integrate over all possible values of their momenta and the delta function guarantees conservation of momentum.

Remark 1.1.1. *Convergence of these integrals is not guaranteed, so one often has to first* regularize *and then* renormalize *the integral. In this thesis we will need neither of them, but the interested reader may find the book [16] useful. Moreover, we directly write the integral in a Euclidean space, not in physical Minkowski space. This is done by analytically continuing the time parameter to imaginary values, see 'Wick rotation' in any textbook on quantum field theory.*

Richard Feynman invented mnemonics, called *Feynman rules* - that assign to each part of such an integral a part of a diagram. This not only nicely illustrates the physical processes but also allows the study of the integrals with the tools of graph theory. Nowadays the process is typically reversed and one starts by drawing all non-isomorphic diagrams[2] for a given order in the expansion (= number of integrations left after integrating the momentum conserving delta functions = number of independent loops of the graph = first Betti number h_1 of the graph). Then one translates diagrams to integrals, for example again in a scalar theory one gets a propagator for each edge

$$\frac{1}{q^2 + m^2} \qquad \longleftrightarrow \qquad \overset{q}{\bullet\!\!-\!\!-\!\!-\!\!-\!\!\bullet}$$

where the momenta q may be sums of internal and external momenta $p + k$. Then one integrates each independent internal momentum with $\int_{\mathbb{R}^D} \frac{\mathrm{d}^D k}{(2\pi)^D}$.

While the momentum space integral is the usual way to write Feynman integrals, there are other integral representations that can be useful (see fig. 1.1). In position space, which is related to momentum space via Fourier transformation, propagators are not given by momentum flowing through edges but by the positions of the

[2]Not all graphs are possible. For instance in ϕ^4 theory only 4-valent vertices are allowed, while diagrams in quantum electro dynamics may only have 3-valent vertices with one photon and two electron lines. Furthermore one only considers 2-edge-connected ('one-particle irreducible') graphs.

vertices the edge connects. For example, in a scalar and massless theory

$$\frac{1}{(x_1 - x_2)^2} \quad \longleftrightarrow \quad x_1 \bullet\!\!-\!\!-\!\!\bullet x_2$$

The titular graphical functions are basically special cases, or rather special interpretations, of position space Feynman integrals of such massless scalar theories. The other part of the title of this thesis refers to another possible representation of Feynman integrals. Momentum space integrals can be transformed to parametric integrals by the *Schwinger trick* which consists of replacing all propagators with

$$\frac{1}{q^2 + m^2} = \int_0^\infty e^{-\alpha(q^2+m^2)} \mathrm{d}\alpha \tag{1.3}$$

and then executing the momentum integrals, which have become simple Gaussians. Position space integrals can be transformed analogously and the majority of chapter 2 will be concerned with the application of a more general version of this trick to graphical functions. The parametric analogue of the Fourier transform is the Cremona transform, in this case simply an inversion of each parameter $\alpha_i \to \alpha_i^{-1}$.

Parametric integrals have many properties that make them useful. The integration variables are simple abstract parameters instead of physical momentum vectors. Moreover, they occur in polynomials that are themselves very interesting objects and will be introduced in section 1.2.3. Finally it is possible to rewrite a parametric integral projectively, which makes them well-suited to be treated with the toolbox of algebraic geometry.

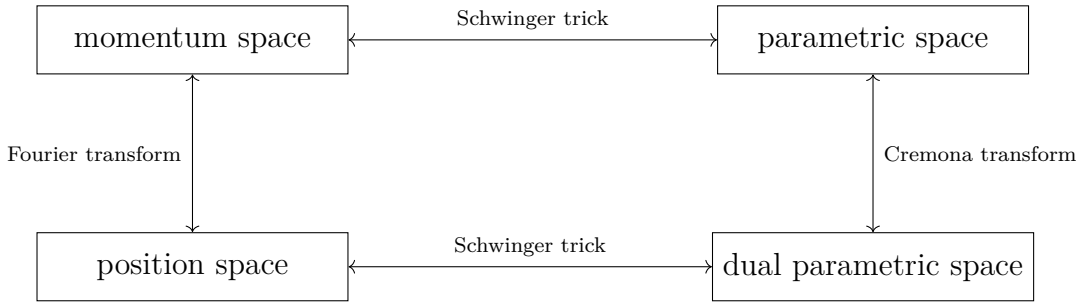

Figure 1.1: Transformations between representations of Feynman integrals

1.1.2 Periods: Multiple zeta values and beyond

Results of Feynman integrals have spawned an almost unprecedented fusion of physics and highly abstract pure mathematics. Even a cursory overview over the number theoretic aspects of Feynman integrals is beyond the scope of this thesis but we will at least explain the terminology that one most often encounters in this context.

The term *period* refers to "a complex number whose real and imaginary parts are values of absolutely convergent integrals of rational functions with rational coefficients, over domains in $\mathbb{R}^n$ given by polynomial inequalities with rational coefficients" [24].

Feynman integrals are periods (or have a period as the first coefficient in their Laurent expansion if they have to be regularized). Only the simplest Feynman graphs evaluate to rational numbers. Starting with the wheel with three spokes graph in ϕ^4 theory one encounters special numbers that are the values of the Riemann zeta function at positive odd integers. At higher loop orders certain more general numbers called *multiple zeta values* appear. For a long time it was suspected that all Feynman graphs might turn out to give multiple zeta values but in recent years it was first proved abstractly and later via explicit counterexamples that even in ϕ^4 other numbers appear (see [12] and references therein). Meanwhile concrete examples of such numbers, e.g. *alternating* sums and *multiple polylogarithms at sixth roots of unity* have been found (cf. [30]). At the time of writing it is completely unclear what else might await us at higher and higher loop orders.

Multiple polylogarithms

What all the special numbers mentioned above have in common is that they are special cases of *multiple polylogarithms* (MPLs). These functions are generalizations of the classical polylogarithm to several arguments and are given by the series

$$\mathrm{Li}_{s_1,...,s_l}(z_1,...,z_l) = \sum_{0<k_1<...<k_l} \frac{z_1^{k_1}...\, z_l^{k_l}}{k_1^{s_1}...\, k_l^{s_l}}, \tag{1.4}$$

in which $s_1,\ldots,s_l \in \mathbb{N}$ and $z_1,\ldots,z_l \in \mathbb{C}$. The number of variables l is called *depth* and the sum of the indices $\sum s_i$ is called the *weight* of the MPL. The special cases that appear as periods result from it as follows:

The Riemann zeta function. The *Riemann zeta function* is the depth 1 MPL (the classical polylogarithm) evaluated at $z = 1$:

$$\zeta(s) = \sum_{k=1}^{\infty} \frac{1}{k^s} \tag{1.5}$$

Such single zeta values appear prominently in the periods of the wheels with three ($6\zeta(3)$) and four ($20\zeta(5)$) spokes. Furthermore, all *zig-zag* graphs have rational multiples of single zeta values as periods (cf. section 1.3.3). Note that even zeta values $\zeta(2n)$ are just rational multiples of π^{2n}.

Multiple zeta values. Allowing depths larger than 1 but still evaluating the multiple polylogarithms at $z_1 = \ldots = z_l = 1$ results in *multiple zeta values (MZVs)*. Thus, they have the series representation

$$\zeta(s_1,...,s_l) = \sum_{0<k_1<...<k_l} \frac{1}{k_1^{s_1}...\, k_l^{s_l}}. \tag{1.6}$$

Alternating sums. If instead of setting all arguments to 1 one also allows -1, then alternating sums are given by the multiple polylogarithms

$$\mathrm{Li}_{s_1,...,s_l}(\xi_1,...,\xi_l) = \sum_{0<k_1<...<k_l} \frac{\xi_1^{k_1}...\, \xi_l^{k_l}}{k_1^{s_1}...\, k_l^{s_l}}, \tag{1.7}$$

with $\xi_1,\ldots,\xi_l \in \{-1,1\}$.

MPLs at roots of unity. The final generalization to be discussed here allows general N-th roots of unity $\mu_N := \{\xi \in \mathbb{C} \mid \xi^N = 1\}$ as arguments. Multiple polylogarithms at roots of unity span a vector space

$$\mathcal{Z}^{(N)} := \mathbb{Q}\langle \mathrm{Li}_{s_1,\ldots,s_l}(\xi_1,...,\xi_l) \mid l \geq 1,\ s_1,\ldots,s_l \in \mathbb{N},\ \xi_1,\ldots,\xi_l \in \mu_N \rangle \tag{1.8}$$

that includes alternating sums $\mathcal{Z}^{(2)}$ and multiple zeta values $\mathcal{Z}^{(1)} \equiv \mathcal{Z}$.

Hyperlogarithms

A different way to generalize the logarithm function are *hyperlogarithms*. We will give only a brief overview. For details we refer to the groundbreaking work by Lappo-Danilevskiy [25]. A wonderful introduction and a multitude of applications can be found in [30].

Let $\Sigma = \{0, \sigma_1, ..., \sigma_N\}$ be a set of distinct points $\sigma_i \in \mathbb{C}$ and associate with it an alphabet $A = \{\mathsf{a}_0, \mathsf{a}_1, ..., \mathsf{a}_N\}$. Then $A^\times$ is the set of all words (concatenations of letters) w over A, including the so-called *empty word* e. Hyperlogarithms are then defined by the four properties

1. $L_e(z) = 1$
2. $L_{\mathsf{a}_0^n}(z) = \frac{1}{n!}\log^n(z) \quad \forall\ n \geq 1$
3. For all $w \in A^\times$ and $0 \leq i \leq N$
$$\frac{\partial}{\partial z} L_{\mathsf{a}_i w}(z) = \frac{1}{z - \sigma_i} L_w(z)$$
4. For all non-empty $w \in A^\times$, $w \neq \mathsf{a}_0^n$
$$\lim_{z \to 0} L_w(z) = 0$$

where $\log(z)$ is the principal branch of the complex logarithm function. This definition can be extended to $\mathbb{Q}\langle A \rangle$ by linearity. With the shuffle product the hyperlogarithms over Σ, written $L(\Sigma)$, form an algebra since

$$L_{w_1 \sqcup\!\sqcup w_2}(z) = L_{w_1}(z) L_{w_2}(z) \quad \forall w_1, w_2 \in A^\times. \tag{1.9}$$

By extending $L(\Sigma)$ with

$$\mathcal{O}_\Sigma^+ = \mathcal{O}_\Sigma \left[\sigma_i, \frac{1}{\sigma_i - \sigma_j}, 0 \leq i < j \leq N \right] \tag{1.10}$$

where we now understand the σ_n as variables and

$$\mathcal{O}_\Sigma := \mathbb{Q}\left[z, \frac{1}{z}, \frac{1}{z - \sigma_1}, ..., \frac{1}{z - \sigma_N} \right] \tag{1.11}$$

denotes the regular functions on $\mathbb{C} \setminus \Sigma$ one even gets an algebra

$$\mathcal{O}_\Sigma^+ \otimes L(\Sigma) \tag{1.12}$$

that is closed under taking primitives. It is possible to write hyperlogarithms in terms of an iterated integral

$$L_{a_{i_1}\dots a_{i_l}}(z) = \int_0^z \frac{\mathrm{d}z_{i_1}}{z_{i_1} - \sigma_{i_1}} \int_0^{z_{i_1}} \frac{\mathrm{d}z_{i_2}}{z_{i_2} - \sigma_{i_2}} \dots \int_0^{z_{i_{l-1}}} \frac{\mathrm{d}z_{i_l}}{z_{i_l} - \sigma_{i_l}}. \tag{1.13}$$

This is the basis for the algorithm due to Francis Brown [8], that allows integration of many Feynman integrals completely symbolically within the hyperlogarithm algebra. However, not all integrals can be written in this form. The property is called *linear reducibility* and checking if certain integrals are linearly reducible will be one of the main concerns in chapter 3.

Using $\Sigma = \{0, 1\}$ and the above integral representation one recovers multiple polylogarithms in one variable from hyperlogarithms by

$$L_{a_0^{s_1-1}a_1\dots a_0^{s_l-1}a_1}(z) = (-1)^l \mathrm{Li}_{s_1,\dots,s_l}(z). \tag{1.14}$$

1.2 Graph theoretic foundations

In this section we briefly review some basics of graph theory, a thorough understanding of which is imperative when talking about graphical functions. In particular we will examine properties of the special class of graphs we will use and give suitable definitions of properties and objects related to them.

1.2.1 Graphs

Definition 1.2.1. (Graphs)
A graph G *is an ordered pair* (V, E) *of the set of* vertices V *and the multiset of* edges E.

- *Elements* $e \in E$ *can be identified with an unordered pair of vertices* $v_1, v_2 \in V$[3]. E *is then called* incident on v_1 *and* v_2.
- *The number of edges incident on a vertex is called its* valence.
- *A graph whose vertices are all* k*-valent is called* k-regular.
- *Two vertices are called* adjacent *if there is an edge incident on both of them.*
- *A* path *of length* k *is a non-empty graph of the form* $P = (\{v_0, v_1, \dots, v_k\}, \{\{v_0, v_1\}, \{v_1, v_2\}, ..., \{v_{k-1}, v_k\}\})$. *If* $v_k = v_0$ *then* P *is called a* cycle *of length* k *or* k-cycle.
- *A graph is called* connected *if there exists a path between any two of its vertices.*
- *A graph that is connected and contains no cycles is called* tree *and a disjoint union of trees is a* forest.

[3] v_1 and v_2 need not be distinct. While graphical functions will turn out to be ill-defined for graphs with self-loops (also known as 1-cycles or, especially in physics literature, tadpoles), certain graphs that appear in intermediate steps might contain them.

- *If a graph is still connected after removal of any k vertices/edges then it is called* k-vertex/edge-connected. *k-vertex connectivity implies k-edge-connectivity. If the type is not specified then k-connected shall always mean k-vertex-connected.*

- *Natural numbers are used to label both, vertices and edges, i.e. we identify each $v \in V$ and $e \in E$ with a certain $v' \in \{1, \ldots, |V|\}$ and $e' \in \{1, \ldots, |E|\}$ respectively*[4].

- *In a* weighted graph *one additionally associates a* weight *given by a complex number $\nu_e \in \mathbb{C}$ to each edge. All graphs in this thesis will be weighted, so from now on we refrain from explicitly stating it whenever graphs are mentioned.*

- *We define the* weight of a vertex *to be the sum of the weights of the edges incident on it*

$$\nu(v) = \sum_{e=\{\bullet,v\}} \nu_e. \tag{1.15}$$

  If all weights are 1*, then the weight is equal to the valence.*

Definition 1.2.2. (Subgraphs)
A subgraph *g of G is a graph $g = (V(g), E(g))$ with $V(g) \subseteq V(G)$ and $E(g) \subseteq E(G)$. Isolated vertices are allowed but isolated edges are not, i.e. $e = \{v_1, v_2\} \in E(g)$ implies $v_1, v_2 \in V(g)$.*

- *If $V(g) = V(G)$, then g is called a* spanning *subgraph of G.*

- *The* complement *g^c of a subgraph g of G is the subgraph of G determined by the complement of the edge set, i.e. $E(g^c) = E(G) \setminus E(g)$. The vertices of g^c are all those that its edges are incident on, so g and g^c may share vertices.*

In addition to those usual graph theory definitions we also demand that the vertices are subdivided into two disjoint sets, internal vertices X and external vertices Z and Z is always assumed to be non-empty.

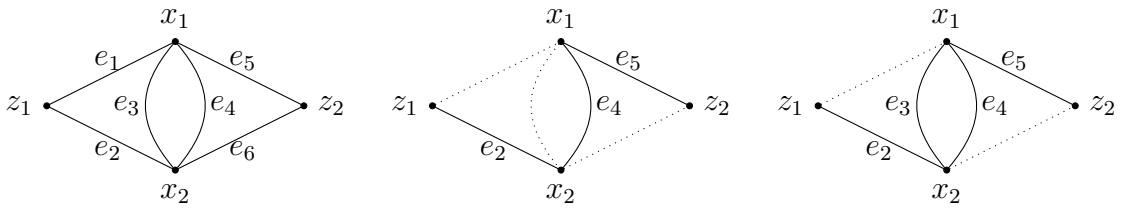

Figure 1.2: A depiction of the "Sauron's eye" graph on the left, a spanning tree subgraph (solid lines) together with its complement (dotted lines) in the middle and a subgraph with cycle on the right.

Example 1.2.3. *The graph on the left-hand side of fig. 1.2 (sometimes called Sauron's eye for obvious reasons) has 4 vertices and 6 edges. It is 2-connected. All vertices are adjacent to all others except z_1 and z_2. No specific weights are assigned to its edges*[5]*. The subgraph $(\{x_1, x_2, z_1, z_2\}, \{e_2, e_4, e_5\})$ (uniquely determined by its*

[4]Note that this induces an ordering on E and V.

[5]All graphs that will be drawn in this thesis will only have edge weights $+1$ or -1, which will be indicated with curly lines.

edge set) depicted with solid lines in the middle of fig. 1.2 is a spanning tree of the graph on the left-hand side. The dotted lines are the complement. The graph drawn with solid lines on the right-hand side is also a spanning subgraph, but not a tree, because it contains the 2-cycle $\{e_3, e_4\}$. Its complement determined by the edges e_1 and e_6 is a spanning 2-forest of Sauron's eye.

Definition 1.2.4. (Operations on graphs)
For a graph G and $E' \subseteq E(G)$, $V' \subseteq V(G)$ subsets of its edges and vertices we define the following operations:

- Deletion of edges:
  $G \setminus E'$ *is the graph G with all edges in E' removed.*
- Identification of vertices:
  G/V' *is the graph G with all vertices in V' identified*[6].
- Contraction of edges:
  $G//E'$ *is the graph G with all edges in E' contracted, i.e. their endpoints identified and the resulting tadpoles deleted.*

Example 1.2.5. *In fig. 1.3 we illustrate the three operations on the same graph used in the example above.*

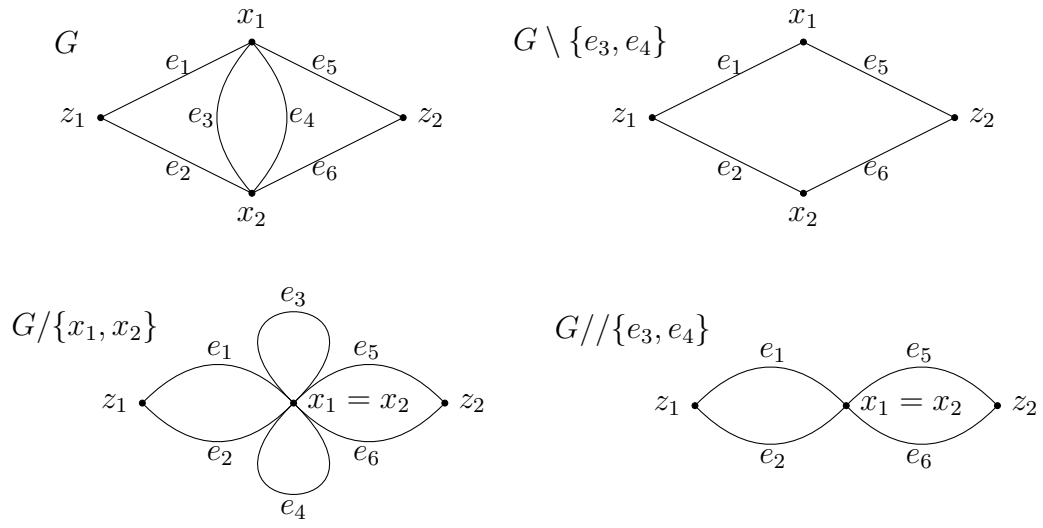

Figure 1.3: The graph operations from definition 1.2.4 illustrated on Sauron's eye.

Since vertex identification does not alter the edge set and all edges have labels, we can uniquely identify edges in G and G/V'. This justifies a certain loose manner of speaking that we will often fall into which treats edge subsets of different graphs as the same objects. For example, taking the graphs from fig. 1.3, we could say that the cycle $\{e_1, e_2\}$ from $G/\{x_1, x_2\}$ is a tree or path in G.

[6]Note that if two adjacent vertices are identified, this results in a tadpole.

The following definitions are concerned with certain types of graphs. Since we introduced the unusual partition of vertices into external and internal, they differ slightly from the common definitions.

Definition 1.2.6. (Planar graph)
We say that a graph is planar *if there exists an embedding of the graph into the plane such that all external vertices are in the unbounded outer face.*

Definition 1.2.7. (Dual graph)
Let G be a planar graph as defined above.Then the dual graph G^* is the graph constructed by the following steps:

1. *For each of the bounded faces i of G add an internal vertex x_i^* to G^*.*
2. *For any edge e that is shared by two bounded faces i and j add an edge $e^* = \{x_i^*, x_j^*\}$ to G^*.*
3. *The edges that are not shared by any bounded faces form $|Z|$ paths P_{kl} between the external vertices k and l. Add an external vertex z_i^* to G^* for each such path and connect it to all internal vertices that correspond to bounded faces that share an edge with the path.*
4. *Assign to each dual edge e^* a new weight $\nu_{e^*} = (\lambda(1-\nu_e)+1)/\lambda$, where λ is a positive half-integer parameter which will be formally introduced in section 1.3.*

Remark 1.2.8. *In the case $|Z| = 3$, where for reasons to be discussed below one typically labels the three external vertices with $0, 1$ and z we shall always label the external vertices in the dual graph such that 0^* corresponds to the path P_{1z}, 1^* to P_{0z} and z^* to P_{01}.*

Example 1.2.9. *Two planar graphs that are dual to each other are drawn in fig. 1.4. The grey letters on the left-hand side label the internal faces of the graph that become internal vertices in the dual graph.*

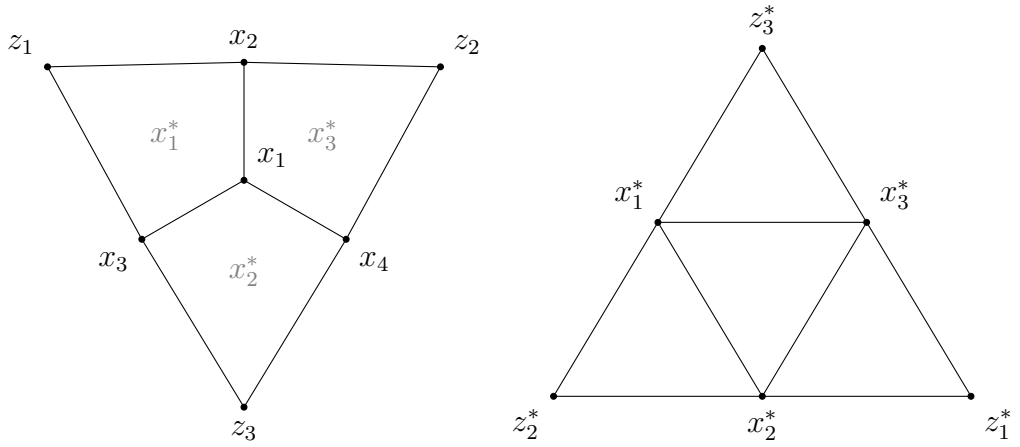

Figure 1.4: Two planar graphs that are dual to each other.

Remark 1.2.10. *Comparing our definition of planar and dual graphs with the usual definitions leads to two findings:*

$$(i)\ G \text{ is planar according to def. 1.2.6.} \implies G \text{ is planar in the usual sense.}$$

$$(ii)\ G^* \text{ is the dual graph of } G \text{ according to def. 1.2.7.} \implies G^*/Z \text{ is a dual graph of } G \text{ in the usual sense.}$$

If not explicitly stated otherwise, planar and dual will from now on always mean planar and dual according to definitions 1.2.6 and 1.2.7.

Remark 1.2.11. *In general there can be several non-isomorphic dual graphs G^*. The dual graph of a planar graph G is unique if G has no* 1*-cycles or* 2*-cycles (multi-edges) and all its internal vertices have valence at least 3. The dual G^* then also has at least 3-valent internal vertices contains neither* 1 *nor* 2*-cycles. Hassler Whitney proved this for the case that all vertices are at least* 3*-valent ([42], Theorem 10 for properties of the dual graph, Theorem 11 for uniqueness). Since in any planar embedding the external vertices have to be in the unbounded outer face in a fixed position relative to each other, the requirement can be dropped for them*[7]*.*

1.2.2 Matrices associated to graphs

Many properties of graphs can be encoded in the form of matrices. This makes them susceptible to the tools of linear algebra which will be highly useful in the following chapters. Thus it is advisable to introduce the matrices that we will encounter in a dedicated section.

Anticipating the needs of chapter 2, we will include parameters $\alpha_e \in \mathbb{R}_+$ associated to each edge e so our definitions of these matrices will differ slightly from standard graph theory definitions, which can be recovered by setting all parameters to 1. For brevity we collect the parameters in $\alpha := (\alpha_1, \cdots, \alpha_{|E|}) \in \mathbb{R}_+^{|E|}$.

Definition 1.2.12. *Let G be a graph according to definition 1.2.1 without* 1*-cycles.*

Its degree matrix *D has the sum over edge parameters of edges incident on v in the diagonal element D_{vv} and is 0 otherwise.*

$$D_{vv'}(\alpha) := \delta_{vv'} \left(\sum_{e=\{\bullet, v\}} \alpha_e \right) \tag{1.16}$$

The adjacency matrix *A of G gives for each pair of vertices v, v' the sum of edge parameters of edges connecting them in the matrix elements $A_{vv'}$ and $A_{v'v}$. Note that we excluded tadpoles, so the diagonal of A contains only zeros and that the empty sum (if no edge $\{v, v'\}$ exists) is zero.*

$$A_{v'v}(\alpha) = A_{vv'}(\alpha) := \sum_{e=\{v,v'\}} \alpha_e \tag{1.17}$$

[7] The statement even holds for isolated external vertices that are not connected to the rest of the graph but such graphs would not make much sense in the context of graphical functions.

For the definition of the incidence matrix I *we have to introduce an arbitrary orientation for each edge*[8]*:*

$$I_{ev}(\alpha) \coloneqq \begin{cases} \alpha_e^{1/2} & \text{if vertex } v \text{ is the initial point of the directed edge } e \\ -\alpha_e^{1/2} & \text{if vertex } v \text{ is the end point of the directed edge } e \\ 0 & \text{if } e \text{ is not incident to } v. \end{cases} \tag{1.18}$$

Finally, we define the Laplacian matrix L *as the difference of* D *and* A*.*

$$L(\alpha) \coloneqq D(\alpha) - A(\alpha) \tag{1.19}$$

Example 1.2.13. *As an example we give incidence, degree and adjacency matrix for the graph from fig. 1.6.*

I	e_1	e_2	e_3	e_4	e_5	e_6
x_1	$-\alpha_{e_1}^{1/2}$	0	$\alpha_{e_3}^{1/2}$	$-\alpha_{e_4}^{1/2}$	$\alpha_{e_5}^{1/2}$	0
x_2	0	$\alpha_{e_2}^{1/2}$	$-\alpha_{e_3}^{1/2}$	$\alpha_{e_4}^{1/2}$	0	$-\alpha_{e_6}^{1/2}$
z_1	$\alpha_{e_1}^{1/2}$	$-\alpha_{e_2}^{1/2}$	0	0	0	0
z_2	0	0	0	0	$-\alpha_{e_5}^{1/2}$	$\alpha_{e_6}^{1/2}$

A	x_1	x_2	z_1	z_2
x_1	0	$\alpha_{e_3} + \alpha_{e_4}$	α_{e_1}	α_{e_5}
x_2	$\alpha_{e_3} + \alpha_{e_4}$	0	α_{e_2}	α_{e_6}
z_1	α_{e_1}	α_{e_2}	0	
z_2	α_{e_5}	α_{e_6}	0	0

D	x_1	x_2	z_1	z_2
x_1	$\alpha_{e_1} + \alpha_{e_3} + \alpha_{e_4} + \alpha_{e_5}$	0	0	0
x_2	0	$\alpha_{e_2} + \alpha_{e_3} + \alpha_{e_4} + \alpha_{e_6}$	0	0
z_1	0	0	$\alpha_{e_1} + \alpha_{e_2}$	0
z_2	0	0	0	$\alpha_{e_5} + \alpha_{e_6}$

Figure 1.5: Incidence, adjacency and degree matrix for Sauron's eye with the orientation and labels as in fig. 1.6.

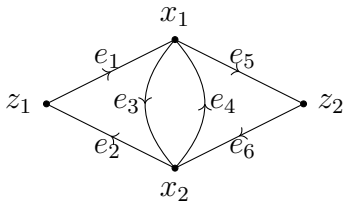

Figure 1.6: Sauron's eye with an additional orientation on all edges

[8]This is just an auxiliary property and does not affect the integrals in which we will later use it.

In the following we will repeatedly need an identity relating Laplace and incidence matrices.

Lemma 1.2.14. *The Laplacian matrix can be written as a product of incidence matrices.*

$$L = I^T I \tag{1.20}$$

Proof. The element of $I^T I$ in the i-th row and j-th column is

$$(I^T I)_{ij} = \sum_{e=1}^{|E|} I_{ei} I_{ej} \tag{1.21}$$

We will see that for $i = j$ we will get the degree matrix while $i \neq j$ gives the adjacency matrix.
a) $i = j$:

$$(I^T I)_{ii} = \sum_{e=1}^{|E|} I_{ei} I_{ei} = \sum_{e=\{\bullet, i\}} \alpha_e = D_{ii} \tag{1.22}$$

b) $i \neq j$:
Since $i \neq j$ we have $I_{ei} = \pm \alpha_e^{1/2}$ and $I_{ej} = \mp \alpha_e^{1/2}$ (such that we always get an over all -1 factor) for the case that i and j are connected by e. If i and j are not adjacent then at least one of those factors is always zero and we get

$$(I^T I)_{ij} = \sum_{e=1}^{|E|} I_{ei} I_{ej} = \sum_{e=\{i,j\}} -\alpha_e = -A_{ij} \tag{1.23}$$

As the adjacency matrix has only zeros on the diagonal while the degree matrix vanishes everywhere but on the diagonal, we indeed see that

$$I^T I = D - A = L. \tag{1.24}$$

□

1.2.3 Graph polynomials

In addition to matrices there are also a multitude of polynomials carrying information about the graph they are associated to. For our purposes, all graph polynomials will be of the form given in the following definition.

Definition 1.2.15. (Graph polynomials)
Let G be any graph and $\alpha = (\alpha_1, \ldots, \alpha_{|E|}) \in \mathbb{R}_+^{|E|}$ parameters associated to each edge. Then a graph polynomial *is defined as*

$$P(G, \alpha) = \sum_{\substack{g \subset G \\ g \in C(G)}} \prod_{e \notin g} \alpha_e \tag{1.25}$$

and its dual graph polynomial *is*

$$\hat{P}(G, \alpha) = \sum_{\substack{g \subset G \\ g \in C(G)}} \prod_{e \in g} \alpha_e, \tag{1.26}$$

where $C(G)$ is a set of subgraphs of G satisfying a certain condition (see examples below). The dependence on α will usually not be written explicitly and the dependence on the graph will often be indicated as subscript P_G or, if there is no danger of ambiguities, also be dropped.

This especially means that all graph polynomials are linear in each variable, in contrast to for example the Tutte polynomial, which, while an important polynomial in graph theory, is not related to graph polynomials in the sense of the above definition[9]. It is also immediately clear that a graph polynomial can be found from its dual via

$$P_G = \left(\prod_{e \in E} \alpha_e \right) \hat{P}_G(\alpha_1^{-1}, \ldots, \alpha_{|E|}^{-1}) \tag{1.27}$$

and vice versa.

Now one has to consider which kind of condition one wants to set for the subgraphs. The broadest class of graph polynomials we will need are the so-called spanning forest polynomials, defined by Brown and Yeats as follows.

Definition 1.2.16. (Spanning forest polynomials [15], Definition 9)
Let $S = S_1 \cup \ldots \cup S_k$ be a set partition of a subset of the vertices of a graph G. Then we define the spanning forest polynomial *of G as*

$$\Phi_G^S = \sum_F \prod_{e \notin F} \alpha_e \tag{1.28}$$

where the sum runs over spanning forests $F = T_1 \cup \ldots \cup T_k$ where each tree T_i of F contains the vertices in S_i and no other vertices of S, i.e. $V(T_i) \supseteq S_i$ and $V(T_i) \cap S_j = \emptyset$ for $i \neq j$. Trees consisting of a single vertex are permitted.

One particularly important example of a spanning forest polynomial is the Kirchhoff polynomial [23].

Definition 1.2.17. (Kirchhoff polynomial)
The Kirchhoff polynomial *is the spanning forest polynomial corresponding to a partition with only one set, i.e.*

$$\Psi_G = \sum_T \prod_{e \notin T} \alpha_e \tag{1.29}$$

where the sum runs over spanning trees T.

While in most applications one uses the above definitions, in chapter 2 we will have to work with dual spanning forest polynomials, defined in the obvious way by replacing $e \notin F$ with $e \in F$ in definition 1.2.16.

The Kirchhoff polynomial is well known to physicists and mathematicians alike [5], [2]. While less well known compared to the Kirchhoff polynomial, special cases of the dual spanning forest polynomials (the same we will encounter in chapter 2) were already known to Nakanishi more than 40 years ago who also found them in the

[9] However, see section 4.3 of the thesis [3] and references therein for an exposition of the Tutte polynomial and an interpretation of it as a vast generalization of the Kirchhoff polynomial with possible applications in physics.

context of position space Feynman integrals [28].

Having defined the objects of interest, we can now collect some of the properties that make them so useful. It is evident from the definition that Φ_G^S and $\hat{\Phi}_G^S$ are linear in every variable and homogenous of degree $|E| - |V| + k$ and $|V| - k$ respectively. This naturally leads to relations between the polynomials of graphs that are related via deletion, contraction and identification, but first we introduce an abbreviating notation.

Notation for graph polynomials of certain subgraphs. Let G be a graph and write $G \setminus \{e\}$, $G//\{e\}$ and G/V' as in definiton 1.2.4. Moreover let Φ_G^S be a (dual) spanning forest polynomial associated to G. If it is clear from context that Φ_G^S is not associated to any other graph we write:

$$\begin{aligned} (i)\ \Phi^S_{G\setminus\{e\}} &\equiv \Phi^{S(e)} \\ (ii)\ \Phi^S_{G//\{e\}} &\equiv \Phi^S_e \\ (iii)\ \Phi^S_{G/V'} &\equiv \Phi^S_{/V'} \end{aligned} \tag{1.30}$$

Proposition 1.2.18. (Deletion and contraction relations)
Let G be a graph and Φ^S, $\hat{\Phi}^S$ a spanning forest polynomial and its dual. Then the following identities hold:

$$\begin{aligned} (i)\ \Phi^{S(e)} &= \frac{\partial}{\partial\alpha_e}\Phi^S & \hat{\Phi}^S_e &= \frac{\partial}{\partial\alpha_e}\hat{\Phi}^S \\ (ii)\ \ \Phi^S_e &= \Phi^S|_{\alpha_e=0} & \hat{\Phi}^{S(e)} &= \hat{\Phi}^S|_{\alpha_e=0} \\ (iii)\ \Phi^S &= \Phi^S_e + \alpha_e\Phi^{S(e)} & \hat{\Phi}^S &= \alpha_e\hat{\Phi}^S_e + \hat{\Phi}^{S(e)} \end{aligned} \tag{1.31}$$

Proof. The case of the Kirchhoff polynomial is well known and the proof generalizes without problems. □

Example 1.2.19. *As an example consider the dual Kirchhoff polynomial of the four graphs from fig. 1.3.*

$$\begin{aligned} \hat{\Psi}_G &= (\alpha_{e_3}+\alpha_{e_4})(\alpha_{e_1}+\alpha_{e_2})(\alpha_{e_5}+\alpha_{e_6}) + \alpha_{e_1}\alpha_{e_2}(\alpha_{e_5}+\alpha_{e_6}) + \alpha_{e_5}\alpha_{e_6}(\alpha_{e_1}+\alpha_{e_2}) \\ \hat{\Psi}_{G\setminus\{e_3,e_4\}} &= \alpha_{e_1}\alpha_{e_2}(\alpha_{e_5}+\alpha_{e_6}) + \alpha_{e_5}\alpha_{e_6}(\alpha_{e_1}+\alpha_{e_2}) = \hat{\Psi}_G\Big|_{\alpha_{e_3},\alpha_{e_4}=0} \\ \hat{\Psi}_{G/\{x_1,x_2\}} &= \hat{\Psi}_{G//\{e_3,e_4\}} = (\alpha_{e_1}+\alpha_{e_2})(\alpha_{e_5}+\alpha_{e_6}) = \frac{\partial}{\partial\alpha_{e_3}}\frac{\partial}{\partial\alpha_{e_4}}\hat{\Psi}_G \end{aligned} \tag{1.32}$$

Another example is the spanning forest polynomial with the partition $S = \{z_1\}\cup\{z_2\}$ and for the same graphs.

$$\hat{\Phi}_G^{\{z_1\},\{z_2\}} = (\alpha_{e_3}+\alpha_{e_4})(\alpha_{e_1}+\alpha_{e_2}+\alpha_{e_5}+\alpha_{e_6}) + \alpha_{e_1}\alpha_{e_6} + \alpha_{e_2}\alpha_{e_5}$$

$$\hat{\Phi}^{\{z_1\},\{z_2\}}_{G\setminus\{e_3,e_4\}} = \alpha_{e_1}\alpha_{e_6} + \alpha_{e_2}\alpha_{e_5} = \hat{\Phi}^{\{z_1\},\{z_2\}}_{G}\Big|_{\alpha_{e_3},\alpha_{e_4}=0}$$

$$\hat{\Phi}^{\{z_1\},\{z_2\}}_{G/\{x_1,x_2\}} = \hat{\Phi}^{\{z_1\},\{z_2\}}_{G//\{e_3,e_4\}} = \alpha_{e_1} + \alpha_{e_2} + \alpha_{e_5} + \alpha_{e_6} = \frac{\partial}{\partial\alpha_{e_3}}\frac{\partial}{\partial\alpha_{e_4}}\hat{\Phi}^{\{z_1\},\{z_2\}}_{G} \tag{1.33}$$

Remark 1.2.20. *It is possible to reinterpret the dual Kirchhoff polynomial of the graph G/Z, which will be of importance in chapter 2, as a spanning forest polynomial of the graph G,*

$$\hat{\Psi}_{/Z} \equiv \hat{\Psi}_{G/Z} = \hat{\Phi}_{G}^{S_{z_1}\cup\ldots\cup S_{z_{|Z|}}} \tag{1.34}$$

where the partition contains exactly one external vertex in each part. This equality holds, even if there are edges between the z_i, because they can never occur in the spanning forests on either side (they are tadpoles in G/Z on the left-hand side and each z_i has to be in a separate part on the right hand side). We will use this for example in the proof of theorem 2.4.2 and in in the following theorem 1.2.21.

Theorem 1.2.21. *Let G be a planar graph, G^* its dual graph, $n \in \{1,\ldots,|Z|\}$ and $S^{(n)}$ a partition of the external vertices into n parts, i.e. $S^{(n)} = S_1,\ldots,S_n$ where each S_i contains at least one external vertex. Then there exists a partition of the external vertices of the dual graph into $|Z|-n+1$ parts such that*

$$\hat{\Phi}_{G}^{S_1,\ldots,S_n}(\alpha_1,\ldots,\alpha_{|E|}) = \left(\prod_{e\in E}\alpha_e\right)\hat{\Phi}_{G^*}^{S^*_1,\ldots,S^*_{|Z|-n+1}}(\alpha_1^{-1},\ldots,\alpha_{|E|}^{-1}) \tag{1.35}$$

In particular, for $n=1$,

$$\hat{\Psi}_{G}(\alpha_1,\ldots,\alpha_{|E|}) = \left(\prod_{e\in E}\alpha_e\right)\hat{\Psi}_{G^*/Z}(\alpha_1^{-1},\ldots,\alpha_{|E|}^{-1}). \tag{1.36}$$

Proof. After first proving the case $n=1$, we subsequently generalize the method to prove the full statement.
Note that for $n=1$ we have $\hat{\Phi}_{G}^{S_1,\ldots,S_n} \equiv \hat{\Psi}_G$ by definition and $\hat{\Phi}_{G^*}^{S^*_1,\ldots,S^*_{|Z|-n+1}} = \hat{\Psi}_{G^*/Z}$ by remark 1.2.20. Whitney's planarity criterion ([43], theorem 29) states that a graph is planar if and only if it has an algebraic dual graph (planar and dual here in the usual sense). As Tutte points out ([40], theorem 2.64), this is equivalent to the statement: Every spanning tree of a planar graph G corresponds to the complement of a spanning tree in its dual G^*. Translating this to graph polynomials while keeping part (ii) of remark 1.2.10 (G^*/Z is a dual graph of G in the usual sense) in mind proves the case $n=1$, i.e. the case of spanning trees.
For the general case one has to consider general spanning n-forests $F_n = \cup_{i=1}^{n} T_i$. Given any such spanning n-forest there exist edges $e_{i_1},\ldots,e_{i_{n-1}}$ such that $F_n = T\setminus\{e_{i_1},\ldots,e_{i_{n-1}}\}$, where T is a spanning tree of G and $e_{i_1},\ldots,e_{i_{n-1}}$ are the $n-1$ edges whose removal from T results in F_n. By the argument above, $F_n\cup\{e_{i_1},\ldots,e_{i_{n-1}}\}$ is the complement of a spanning tree in G^*/Z or in other words, the complement of a spanning $|Z|$-forest $F^*_{|Z|} = \cup_{i=1}^{|Z|} T^*_i$ in G^*. Removing an edge e_{i_j} corresponds to inserting the corresponding edge into $F^*_{|Z|}$, either creating a cycle or turning it into

a $|Z|-1$-forest $F^*_{|Z|-1}$. However, creating a cycle in G^* corresponds to stripping a subgraph of G of all the edges that are connecting it to external vertices. We constructed the partition $S^{(n)}$ and therefore $F_n \cup \{e_{i_1}, \ldots, e_{i_{n-1}}\}$ such that removing the edges $e_{i_1}, \ldots, e_{i_{n-1}}$ leaves a spanning n-forest which has at least one external vertex in every tree. Thus, inserting all the edges $e_{i_1}, \ldots, e_{i_{n-1}}$ into $F^*_{|Z|}$ indeed results in a spanning $|Z|-n+1$-forest $F^*_{|Z|-n+1}$ in G^*. □

In general it is difficult to make a statement about the structure of the partition on the right-hand side. The only case of interest for us is $|Z| = 3$ (see remark 1.2.8) where we find the following corollary, that will be instrumental in the proof of theorem 2.4.4.

Corollary 1.2.22. *Let $Z = \{0, 1, z\}$. For $n = 1$ ($n = 3$) there is a spanning tree on the lhs (rhs) of eq. (1.35) and the partition on the rhs (lhs) has exactly one external vertex in each part. For $n = 2$ one finds for all distinct $i, j, k \in Z$*

$$\hat{\Phi}_G^{\{i,j\}\{k\}}(\alpha_1, \ldots, \alpha_{|E|}) = \left(\prod_{e\in E} \alpha_e\right) \hat{\Phi}_{G^*}^{\{i^*,j^*\}\{k^*\}}(\alpha_1^{-1}, \ldots, \alpha_{|E|}^{-1}) \tag{1.37}$$

Proof. The cases $n = 1, 3$ follow directly from the theorem. The interesting case $n = 2$ becomes obvious with the illustration of the situation in fig. 1.7. Since the external vertices in the dual graph have a canonical position relative to each other and their counterparts in the original graph, one can infer that for each spanning 2-forest $F_1 \cup F_2$ of G there is at least one edge in G that connects F_1 and F_2 and the dual edges corresponding to them connect i^* and j^* in the dual graph. □

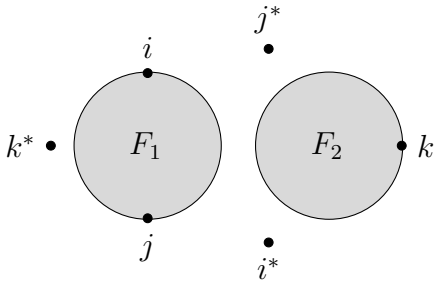

Figure 1.7: Illustration of the case $n = 2$ in corollary 1.2.22. F_1 and F_2 are disconnected trees within G. The vertices with stars represent external vertices of the dual graph. Their position relative to the external vertices of G was fixed in remark 1.2.8. Since G is connected, there must be one or more edges in G connecting F_1 and F_2 exactly such that their dual counterparts connect i^* and j^*.

Example 1.2.23. *Fig. 1.8 illustrates the statement of corollary 1.2.22 on the two dual graphs that we already used as examples earlier.*

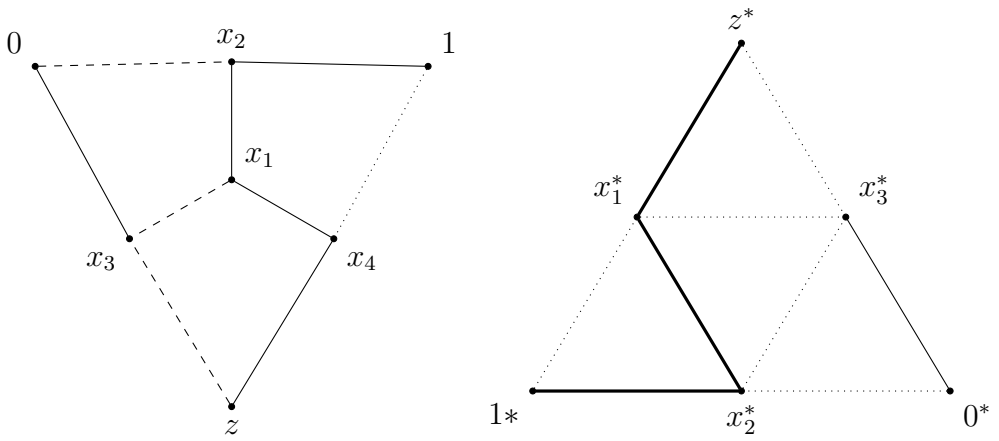

Figure 1.8: Illustration of corollary 1.2.22 on a concrete example. Solid lines in both graphs represent the spanning 2-forests. The dashed lines on the left-hand side are the edges missing from the spanning forest whose counterparts on the right-hand side are the thick lines.

1.3 Graphical functions

1.3.1 Definition and properties

Preliminaries. Before we give a definition of graphical functions we first discuss the setting that we will work in. Our space-time is D-dimensional Euclidean, where D is an integer strictly larger than 2.[10] As the name suggests, graphical functions are always associated to a certain graph and their definition is basically a translation rule from graphs to integrals, similar to the Feynman rules of quantum field theory.

With each vertex we associate a real vector, $x_v \in \mathbb{R}^D$ for $v \in X$ and $z_v \in \mathbb{R}^D$ for $v \in Z$. The x_v will be (vectors of) integration variables, while the z_v will be parameters. For the sake of brevity we collect them in vectors $x = (x_1, ..., x_{|X|})^T \in \mathbb{R}^{D|X|}$ and $z = (z_1, ..., z_{|Z|})^T \in \mathbb{R}^{D|Z|}$.

For each edge there is an associated quadric, defined as

$$Q_e \coloneqq ||u_v - u'_{v'}||^2 \tag{1.38}$$

where $e = \{v, v'\}$, u and u' stand for x or z, depending on the vertex and the norm is Euclidean. The quadrics usually have powers $-\lambda\nu_e$ in which the $\nu_e \in \mathbb{C}$ are precisely the weights of the edge e and $\lambda = \frac{D}{2} - 1 \in \frac{1}{2}\mathbb{N}$ is a dimensional parameter. We do not admit graphs with tadpoles since their quadric is 0. Apart from that restriction, all graphs as defined in the previous section are allowed[11].

Now that we set the stage, we can define graphical functions as follows:

[10] It is possible to define graphical functions for $D = 2$ (see [37]) but that case differs considerably from the cases $D > 2$ and we will not discuss it here. We will also not use dimensional regularization as one often does in quantum field theory. Instead we focus for now on integrals that are convergent in integer dimensions.

[11] While all graphs are allowed, only a small subset of graphs will yield a well-defined graphical function (see lemma 1.3.3).

Definition 1.3.1. (Graphical Functions [37]) *Let G be a graph, $\nu_e \in \mathbb{C}$ for all $e \in E$ and $\lambda = \frac{D}{2} - 1 > 0$ such that the convergence criteria given below are satisfied. Then the graphical function*

$$f_G^{(\lambda)} : \mathbb{R}^{D|Z|} \to \mathbb{C} \tag{1.39}$$

exists and is given by the integral

$$f_G^{(\lambda)}(z) = \int_{\mathbb{R}^{D|X|}} \left(\prod_{v \in X} \frac{\mathrm{d}^D x_v}{\pi^{\frac{D}{2}}} \right) \prod_{e \in E} Q_e^{-\lambda \nu_e}. \tag{1.40}$$

Remark 1.3.2. *The function defined above is what we will later call an* uncompleted *graphical function. Completed graphical functions will be defined below for the special case $Z = \{0, 1, z\}$ whose importance will be discussed later in this section. They will mostly be needed for computations in chapter 3. Chapter 2 will only deal with uncompleted graphical functions. In section 2.3 we will generalize graphical functions to complex arguments, rewriting them as functions depending on complex numbers rather than D-vectors.*

The convergence criterion is based on Weinberg's theorem on power counting for Feynman integrals [41].

Lemma 1.3.3. (Convergence [37], Lemma 3.4)
The integral in definition (1.3.1) is convergent if and only if it is infrared and ultraviolet finite.
It is infrared finite if and only if for every subgraph g of G with $|X(g)|$ vertices whose neighbors all lie in g and $0 < N(g) := \sum_{e \in E(g)} \operatorname{Re} \nu_e$ one has

$$(D-2)N(g) > D|X(g)|. \tag{1.41}$$

It is ultraviolet finite if and only if for every subgraph g of G with $0 < |E(g)|$ and with at most one of its $|V(g)|$ vertices in Z one has

$$(D-2)N(g) < D(|V(g)| - 1). \tag{1.42}$$

If G contains multi-edges (multiple edges between the same two vertices) then the above conditions have to hold only for all those subgraphs g that contain either all edges that are part of a specific multi-edge or none of them.

Remark 1.3.4. *The infrared convergence criterion above contains the set $X(g)$ of internal vertices of g, i.e. vertices whose neighbors all are also in g. It is important not to confuse this set with $X \cap g$, the set of internal vertices of G, that are also in g. These two sets are only the same if $g = G$.*

Conformal parametrization. By far the most important special case of graphical functions is the one with three external vertices $0, 1, z$ parametrized by two complex numbers z, $\bar{z}$,

$$\begin{aligned} 0 &\sim 0 \in \mathbb{R}^D \\ 1 &\sim v_1 = (1, 0, ..., 0) \in \mathbb{R}^D \\ z &\sim v_z = \left(\frac{z + \bar{z}}{2}, \frac{z - \bar{z}}{2i}, 0, ..., 0 \right) \in \mathbb{R}^D. \end{aligned} \tag{1.43}$$

In this form, graphical functions appear in various places in physics (see section 1.3.2). Moreover, many very useful properties, two of which are mentioned in the following two paragraphs, are exclusive to this special case.

Completion. Let G be a graph with three external vertices labeled 0,1 and z and recall that the weight of a vertex v was defined as

$$\nu(v) := \sum_{e=\{v,\bullet\}} \nu_e. \tag{1.44}$$

Then we can complete the graph and define completed graphical functions with the following steps:

- Add another external vertex and label it $'\infty'$.
- Add an edge $\{z, \infty\}$ with weight such that $\nu(z) = 0$.
- For all $v \in X$ add edges $\{v, \infty\}$ with weights such that $\nu(v) = \frac{2D}{D-2}$.
- Add edges $\{0, 1\}$, $\{0, \infty\}$ and $\{1, \infty\}$ such that $\nu(0) = \nu(1) = \nu(\infty) = 0$.

We denote the resulting completed graph by Γ. Completions are unique [37]. Completed graphical functions are defined by applying the definition of uncompleted graphical functions to a completed graph and setting all quadrics $Q_{\{\bullet,\infty\}}$ to 1. Completed graphical functions have various nice properties, most prominently a 24-fold symmetry that relates graphical functions under permutations of the vertices $0, 1, z$ and ∞. An example will be given in section 1.3.3.

Since we set all quadrics of edges incident on ∞ to 1, the graphical function does not change under completion

$$f_G^{(\lambda)}(z) = f_\Gamma^{(\lambda)}(z). \tag{1.45}$$

Appending an edge. There is a useful identity that relates certain graphs with three external vertices $0, 1, z$ (see fig. 1.9) via a differential equation. The identity was previously proved by Schnetz [37]. In section 2.4.1 we give an alternative proof using the parametric version of graphical functions that will be derived in chapter 2. For a graph G and a graph G_z that is G with an additional edge as in fig. 1.9 one has

$$f_G^{(\lambda)}(z) = -\Gamma(\lambda)\left(\partial_z\partial_{\bar{z}} - \frac{\lambda}{z-\bar{z}}(\partial_z - \partial_{\bar{z}})\right) f_{G_z}^{(\lambda)}(z). \tag{1.46}$$

The significance of this identity lies in the fact that it has (under certain quite general assumptions) a unique solution and allows the computation of a large family of periods. This was also independently discovered by James M. Drummond (see section 1.3.2 below). The identity gains further relevance because it is crucial for the proof of theorem 2.4.4 in section 2.4.2.

Figure 1.9: Depiction of the graphs G and G_z. They are almost the same but G_z has an internal vertex where G has z and an edge connecting that vertex to the new z.

1.3.2 Application: Conformally invariant 4-point functions

Conformal symmetry. Extending the usual Poincaré symmetry of space-time by including scale invariance and invariance under so-called *special conformal transformations*

$$x^\mu \to \frac{x^\mu - a^\mu x^2}{1 - 2a \cdot x + a^2 x^2} \tag{1.47}$$

where a is a parameter vector and x^μ is a component of a position vector in the given space-time, results in conformal symmetry. Conformal field theories have a wide range of applications, from statistical mechanics to string theory [19].

Graphical functions are closely related to 4-point functions in that context. Any conformally invariant function of four variables[12] can be written in terms of the two *conformally invariant cross sections*

$$u = \frac{x_{12}^2 x_{34}^2}{x_{13}^2 x_{24}^2} \qquad v = \frac{x_{14}^2 x_{23}^2}{x_{13}^2 x_{24}^2} \tag{1.48}$$

where $x_{ij} = ||x_i - x_j||$ is the usual notation in the literature. This can be related to the conformal parametrization of graphical functions mentioned above by noting that it is possible to map three of the four points to 0, $e_1 = (1, 0, \ldots, 0)$, ∞. Now only rotations that leave e_1 invariant are left as possible transformations which means the remaining point has to be mapped into the plane spanned by e_1 and another base vector, say $e_2 = (0, 1, 0, \ldots, 0)$. For example, choosing

$$\begin{aligned} x_1 &\to \infty \\ x_2 &\to e_1 \\ x_3 &\to r e_1 + s e_2 \quad r, s \in \mathbb{R} \\ x_4 &\to 0 \end{aligned} \tag{1.49}$$

leaves two real parameters as the only functional dependence of such a four-point function. Inserting these points into u and v above shows that the invariant cross sections take the form $u = |x_3|^2$, $v = |e_1 - x_3|^2$. Replacing the two real parameters by a complex parameter $x_3 = z$ returns exactly the case mentioned in the preceding section and discussed in detail in section 2.4.

Generalised ladders. In [17] J.M. Drummond developed the theory of *generalised ladder* type integrals, an infinite family of conformal four-point integrals (see fig. 1.10 and 1.11). They are identical to the special case of *sequential graphical functions*

[12] There are no non-constant conformally invariant functions of less than 4 variables because the conformal symmetry completely fixes all degrees of freedom.

from [37]. Drummond's approach, which amounts to solving a tower of differential equations of the form (1.46), has successfully been applied to 3 and 4 loop integrals arising in $N = 4$ supersymmetric Yang-Mills theory [18].

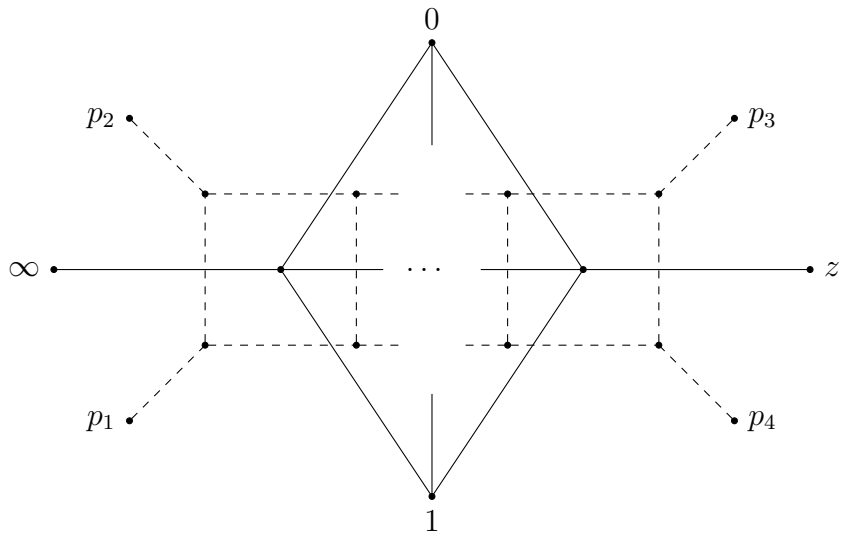

Figure 1.10: A four-point ladder type diagram (solid lines) together with its momentum space dual (dashed lines) whose shape is the origin of the name.

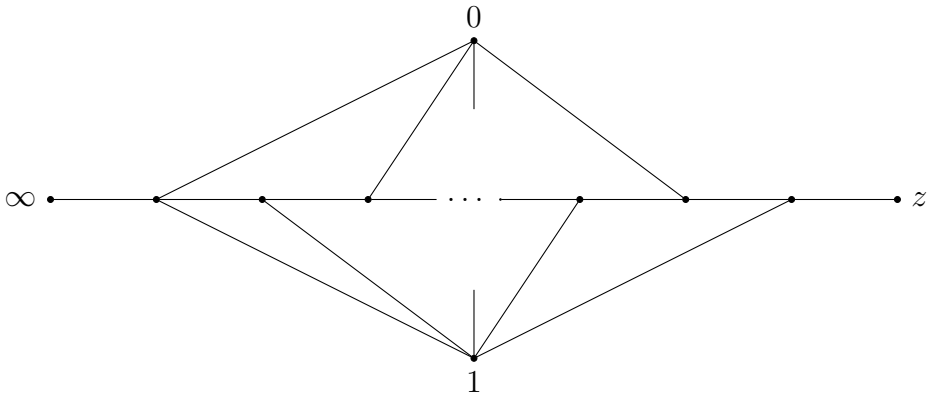

Figure 1.11: A *generalized ladder* type diagram (Drummond, [17]) or *sequential graphical function* (Schnetz, [37]). They differ from the usual ladder diagrams in so far as internal vertices do not have to be adjacent to both 0 and 1 but only at least one of them.

1.3.3 Application: Computation of periods

There are several ways in which graphical functions are useful in the computation of periods. For more theoretical background we refer to [37], where the two examples of this section were taken from. Here we try to focus on illustrating the general concepts on examples.

Constructing periods. The natural way to turn a graphical function into a period is integrating the remaining variable z. In the conformal parametrization this can be achieved by a simple integral over the complex plane instead of an integral over $\mathbb{R}^{D|Z|}$ as one would expect in the general case. This is due to the identity [37]

$$\frac{1}{\pi^{\frac{D}{2}}}\int_{\mathbb{R}^D} f_G^{(\lambda)}(z)\mathrm{d}^D z = \frac{1}{(2i)^{D-2}\sqrt{\pi}\Gamma(\frac{D-1}{2})}\int_{\mathbb{C}} f_G^{(\lambda)}(z)(z-\bar{z})^{D-2}\mathrm{d}^2 z \tag{1.50}$$

which relates the two kinds of integrals in the case of a conformally symmetric function. The steps from an arbitrary (4-regular ϕ^4) graph G to its period are as follows:

1. Label any 4 vertices with $\{0, 1, z, \infty\}$. Denote the resulting graph with Γ.
2. Take the connected components G_i of $\Gamma \setminus \{0, 1, z, \infty\}$.
3. Complete each connected component by adding $\{0, 1, z, \infty\}$ and connecting them to the same vertices of each G_i that they were connected to in Γ. Add edges between 0 and 1 or edges incident on ∞ as necessary such that each G_i becomes a completed graph Γ_i.
4. Integrate

$$P(\Gamma) = \int \frac{\mathrm{d}^D z}{\pi^{\frac{D}{2}}} \frac{\prod_i f_{\Gamma_i}^{(\lambda)}(z)}{||z||^{2\lambda\nu_{0z}}||z-1||^{2\lambda\nu_{1z}}}. \tag{1.51}$$

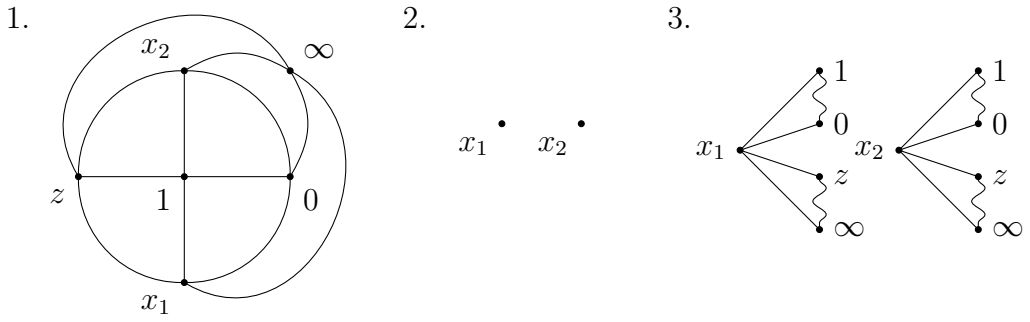

Figure 1.12: Depiction of the steps in the construction of the periods of WS_4.

Exploiting the permutation symmetry of completed graphical functions. Another possibility lies in using the remarkable symmetry under permutation of external vertices that graphical functions satisfy. The following example nicely illustrates the general principle.

Example 1.3.5. (Period of the the complete graph K_5)
We want to find the period of the complete graph K_5. The strategy is to use the permutation symmetry and the fact that edges connected to ∞ just give a factor 1 in order to reduce K_5 to a smaller graph with a known period. Denote with $G_1, \ldots, G_6$

the graphs from fig. 1.13. Let $f^{(\lambda)}_{K_5}(z) = f^{(\lambda)}_{G_1}(z)$ *be the graphical function of* K_5*. Since edges between external vertices give constant factors one has*

$$f^{(\lambda)}_{K_5}(z) = \frac{f^{(\lambda)}_{G_2}(z)}{z\bar{z}(1-z)(1-\bar{z})}. \tag{1.52}$$

where $G_2 = K_5 \setminus \{e_{01}, e_{0z}, e_{1z}\}$*. Now,* G_3 *is the completion of* $K_5 \setminus \{e_{01}, e_{0z}, e_{1z}\}$*. Since completion only adds edges between* 0 *and* 1 *or edges incident on* ∞ *it follows that*

$$f^{(\lambda)}_{K_5}(z) = \frac{f^{(\lambda)}_{G_3}(z)}{z\bar{z}(1-z)(1-\bar{z})}. \tag{1.53}$$

In the next step we use the permutation symmetry. Swap $0 \leftrightarrow 1$ *and* $z \leftrightarrow \infty$*. Then*[13]

$$f^{(\lambda)}_{K_5}(z) = \frac{f^{(\lambda)}_{G_4}(z)}{z\bar{z}(1-z)(1-\bar{z})}. \tag{1.54}$$

From G_4 *to* G_5 *one once again 'decompletes' the graph by deleting* ∞ *and all edges incident on it, as well as all edges between* 0 *and* 1*. This still does not change the graphical function, i.e.* $f^{(\lambda)}_{G_5}(z) = f^{(\lambda)}_{G_4}(z) = f^{(\lambda)}_{G_3}(z) = f^{(\lambda)}_{G_2}(z)$*.*

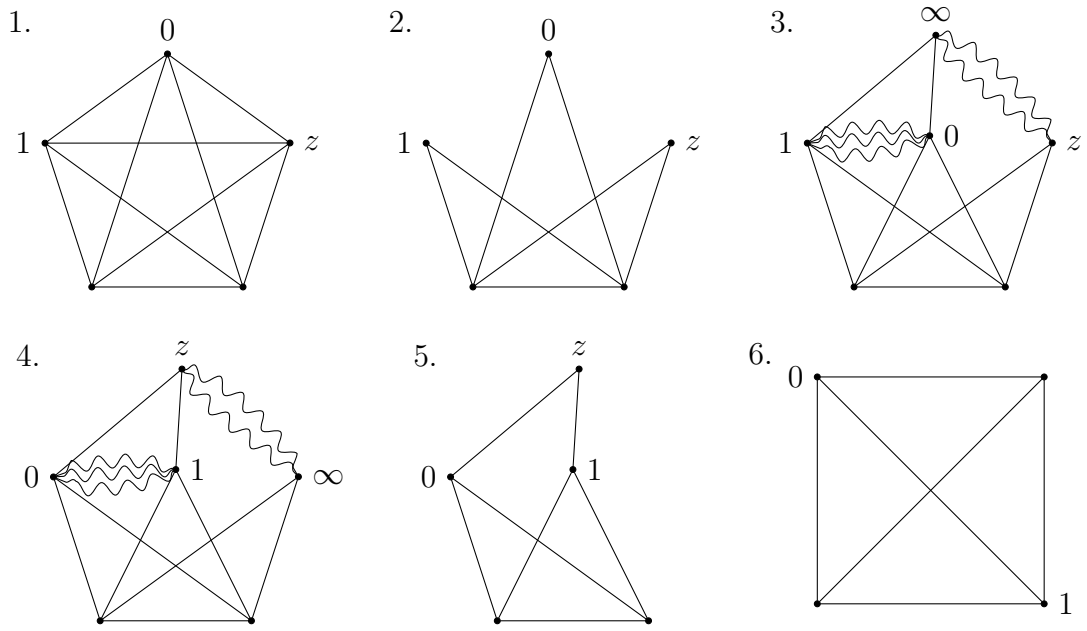

Figure 1.13: Depiction of the 6 steps in the computation of the period of K_5 from the period of K_4 using the permutation symmetry of completed graphical functions.
1.+2.: The complete graph K_5 before and after removal of edges $\{0, z\}, \{1, z\}, \{0, 1\}$.
3.+4.: K_5 after completion and permutations $0 \leftrightarrow 1$, $z \leftrightarrow \infty$.
5.: The graph after removal of all edges connected to ∞.
6.: The graph $K_4 \cong WS_3$ which has the known period $6\zeta(3)$.
Curly lines denote an edge with negative weight.

[13]Actually, completed graphical functions are only invariant under permutations of external vertices *together with* a Möbius transformation of the argument z. This particular double transposition, however, leaves the argument untouched [37].

In the last step one first notes that we can again remove the two edges incident on z, which results in another factor $(z\bar{z}(1-z)(1-\bar{z}))^{-1}$. Finally, adding an edge between 0 and 1 turns $G_5 \setminus \{e_{0z}, e_{1z}\}$ into the graph $G_6 = K_4 \cong WS_3$ which has the well-known period $6\zeta(3)$. All together, the result is

$$f^{(\lambda)}_{K_5}(z) = \frac{6\zeta(3)}{(z\bar{z}(1-z)(1-\bar{z}))^2}. \tag{1.55}$$

Now it is possible to integrate $f^{(\lambda)}_{K_5}(z)$ over the complex plane as in eq. (1.50) and get the period P_{K_5}

The zig-zag conjecture. The zig-zag conjecture, due to Broadhurst and Kreimer [7], states that for $n \geq 3$ the periods of the zig-zag graphs Z_n (two examples of which are given in fig. 1.14) are

$$P(Z_n) = \frac{4(2n-n2)!}{n!(n-1)!}\left(1 - \frac{1-(-1)^n}{2^{2n-3}}\right)\zeta(2n-3). \tag{1.56}$$

Schnetz [37] noticed that his method of solving towers of differential equations implied the conjecture up to multiplication with products of multiple zeta values. The full proof of the conjecture by Brown and Schnetz [14] takes a slightly different approach and is too voluminous for this brief exposition but certainly a great demonstration of the utility of graphical functions.

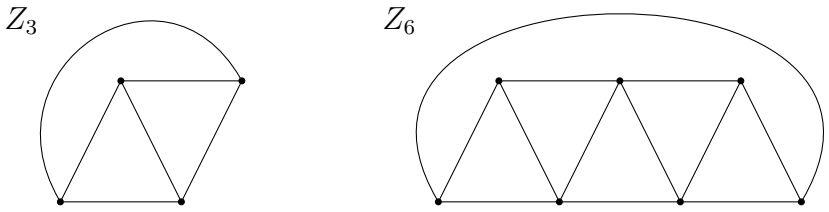

Figure 1.14: The zig-zag graphs Z_3 and Z_6.

Chapter 2

A parametric integral representation for graphical functions

2.1 Derivation of the parametric integral

2.1.1 Schwinger trick and integration of position space variables

Graphical functions were originally defined analogous to position space Feynman integrals and we can rewrite them as an integral depending on abstract parameters, similar to what was mentioned for Feynman integrals in the introduction. However, there are some notable and very important differences that make it worthwhile to discuss the derivation of the parametric integral representation of graphical functions in full detail.

A somewhat less general version of the result that we will arrive at was already briefly discussed by Nakanishi in [28] but the book appears to be long out of print and not well known among physicists, which gives us another reason to thoroughly explain how to write graphical functions in parametric space.

Remark 2.1.1. *Note that in accordance with standard physics terminology as visualized in fig. 1.1 the integral derived in the following is actually* dual parametric *and to go to the* parametric *integral one would have to include a Cremona transformation. This, however, unnecessarily complicates things - especially if one wants to allow quadrics in the numerator, i.e. negative edge weights - and brings no discernible advantage. Since there is no conceptual difference between parametric and dual parametric integrals - apart from their derivation from position space or momentum space integrals via the Schwinger trick - the term 'parametric' will be used loosely to refer to either of the two versions.*

We assume G to be connected and chosen such that $f_G^{(\lambda)}$ satisfies the UV and IR convergence conditions (1.3.3), but otherwise arbitrary. In particular we allow both, arbitrary edge weights $\nu_e \in \mathbb{C}$ and multiple edges between the same vertices. While the equivalence of multiple edges and a single edge with the same total weight is completely obvious in the position space definition 1.3.1 where the exponents of the quadrics can be added up directly, it is somewhat veiled in the parametric version

we are about to derive. For that reason and to check our parametric integral for consistency an explicit proof will be given in proposition 2.2.3.

Given such a graph G, its graphical function is defined according to def. 1.3.1 by the integral

$$f_G^{(\lambda)}(z) = \int_{\mathbb{R}^{D|X|}} \left(\prod_{v \in X} \frac{\mathrm{d}^D x_v}{\pi^{\frac{D}{2}}} \right) \prod_{e \in E} Q_e^{-\lambda \nu_e} \tag{2.1}$$

where G is a graph, X and E are sets containing the graphs internal vertices and edges respectively, $D = 2\lambda + 2$ with a positive half-integer parameter λ is the dimension, $\nu_e \in \mathbb{C}$ and Q_e are the weight and quadric associated to the edge $e \in E$ and the argument $z = (z_i)_{i \in Z} = (z_{i_1}, \ldots, z_{i_D})_{i \in Z} \in \mathbb{R}^{D|Z|}$ consists of variables associated to external vertices of the graph G. We will now replace all quadrics by expressions depending on parameters $\alpha_1, \ldots, \alpha_{|E|}$ and integrate the position space variables x_v as was outlined for Feynman integrals in the introduction.

Treatment of negative edge weights. Since the Schwinger trick relies on the Γ-function, more specifically, the integral representation

$$\Gamma(z) = \int_0^\infty \mathrm{d}x \; x^{z-1} e^{-x} = \int_0^\infty \mathrm{d}x \; a^z x^{z-1} e^{-ax} \quad a, \operatorname{Re} z > 0 \tag{2.2}$$

which demands a positive real part of the argument, one has to replace quadrics with non-positive real parts of their edge weights differently. If the weight is a negative integer or at least a negative rational number such that $\lambda \nu_e$ is a negative integer, then it is possible to write

$$Q_e^{-\lambda \nu_e} = (-1)^{\lambda |\nu_e|} \frac{\partial^{\lambda |\nu_e|}}{\partial \alpha_e^{\lambda |\nu_e|}} \bigg|_{\alpha_e = 0} \exp(-\alpha_e Q_e). \tag{2.3}$$

Any edge weight $\nu_e \in \mathbb{C}$ with $\operatorname{Re} \nu_e \leq 0$ can be decomposed into two parts $\nu_{e_1} + \nu_{e_2} = \nu_e$ with $0 > \nu_{e_1} \in \mathbb{Q}$ and $\nu_{e_2} \in \mathbb{C}$ such that $0 > \lambda \nu_{e_1} \in \mathbb{Z}$ and $\operatorname{Re} \nu_{e_2} > 0$. Therefore, after splitting edges into parallel edges if necessary and naming $E_\pm := \{e \in E \mid \operatorname{Re} \nu_e \gtrless 0\}$, we replace each $Q_e^{-\lambda \nu_e}$ as follows:

$$Q_e^{-\lambda \nu_e} = \begin{cases} \displaystyle\int_0^\infty \mathrm{d}\alpha_e \frac{\alpha_e^{\lambda \nu_e - 1}}{\Gamma(\lambda \nu_e)} \exp(-\alpha_e Q_e) & \text{if } e \in E_+ \\ \displaystyle (-1)^{\lambda |\nu_e|} \frac{\partial^{\lambda |\nu_e|}}{\partial \alpha_e^{\lambda |\nu_e|}} \bigg|_{\alpha_e = 0} \exp(-\alpha_e Q_e) & \text{if } e \in E_- \end{cases} \tag{2.4}$$

The graphical function is then

$$\begin{aligned} f_G^{(\lambda)}(z) = \int_{\mathbb{R}^{D|X|}} \left(\prod_{v \in X} \frac{\mathrm{d}^D x_v}{\pi^{\frac{D}{2}}} \right) \left(\int_0^\infty \prod_{e \in E_+} \mathrm{d}\alpha_e \frac{\alpha_e^{\lambda \nu_e - 1}}{\Gamma(\lambda \nu_e)} \right) \\ \times \left(\prod_{e \in E_-} (-1)^{\lambda |\nu_e|} \frac{\partial^{\lambda |\nu_e|}}{\partial \alpha_e^{\lambda |\nu_e|}} \bigg|_{\alpha_e = 0} \right) \prod_{e \in E} \exp(-\alpha_e Q_e) \\ = \frac{\pi^{-\frac{D}{2}|X|}}{\prod_{e \in E_+} \Gamma(\lambda \nu_e)} \left(\int_0^\infty \prod_{e \in E_+} \frac{\mathrm{d}\alpha_e}{\alpha_e^{1 - \lambda \nu_e}} \right) \left(\prod_{e \in E_-} (-1)^{\lambda |\nu_e|} \frac{\partial^{\lambda |\nu_e|}}{\partial \alpha_e^{\lambda |\nu_e|}} \bigg|_{\alpha_e = 0} \right) \\ \times \int_{\mathbb{R}^{D|X|}} \left(\prod_{v \in X} \mathrm{d}^D x_v \right) \exp\left(- \sum_{e \in E} \alpha_e Q_e \right). \end{aligned} \tag{2.5}$$

Remark 2.1.2. *Let us discuss in detail what one has to check to move the position space integral past both, parameter integration and differentiation. As part of the integrand of the position space integration, parameter integrals and derivatives can be freely exchanged but if we want to move the position space integration past them, we always have to write the parameter integrals to the left of the parameter derivatives. This is due to the fact that while exchanging integrals only requires absolute convergence (which is a given since we required the graphical function to be convergent and the integrand is strictly positive), exchanging the position space integration and the derivatives requires that the integrand (the exponential) and its derivatives are continuous. If we first exchange integrations, then integration and differentiation we have continuous terms of the form*

$$\left(\prod_{e\in E_-} Q_e^{\lambda|\nu_e|}\right)\exp\left(-\sum_{e\in E_+}\alpha_e Q_e\right), \tag{2.6}$$

but trying to do it the other way around gives terms

$$\left(\prod_{e\in E_+} Q_e^{-\lambda\nu_e}\right)\exp\left(-\sum_{e\in E_-}\alpha_e Q_e\right) \tag{2.7}$$

and derivatives thereof. Having quadrics in the denominator they are clearly not continuous everywhere in $\mathbb{R}^{D|X|}$. Consequently, we will from now on always write the parameter integrals to the left of the parameter derivatives.

The exponent. The sum over all edges in the exponent can be rearranged. Each quadric can be written as

$$Q_e = ||u_v - u_{v'}||^2 = u_v^2 - 2u_v \cdot u_{v'} + u_{v'}^2, \tag{2.8}$$

where v and v' are the two endpoints of the edge e and the dot represents the standard scalar product. Any variable vector u_v appears squared exactly once for every edge incident on it. The mixed term containing the standard scalar product of two real vectors appears once for each edge connecting a pair of vertices that are adjacent to each other, with a factor 2 due to symmetry. This means the exponent can be rewritten in terms of the Laplace matrix L from section 1.2.2. We can assume that the labels of the vertices are sorted such that entries for internal vertices form a $|X|\times|X|$ block matrix $L_{(X,X)}$ in the upper left of L while the mixed entries form $|X|\times|Z|$ and $|Z|\times|X|$ block matrices $L_{(X,Z)}$ and $L_{(Z,X)} = L_{(X,Z)}^T$ in the upper right and lower left of L. We can therefore write

$$L = \begin{pmatrix} L_{(X,X)} & L_{(X,Z)} \\ L_{(Z,X)} & L_{(Z,Z)} \end{pmatrix}. \tag{2.9}$$

It is clear from the structure of the Euclidean norm, i.e. from the fact that

$$Q_e = ||u_v - u_{v'}||^2 = u_v^2 - 2u_v \cdot u_{v'} + u_{v'}^2 = \sum_{i=1}^{D} u_{v_i}^2 - 2u_{v_i}\cdot u_{v_i'} + u_{v_i'}^2 \tag{2.10}$$

that the exponential in eq. (2.5) factorizes into D identical factors. To treat all dimensions simultaneously we introduce the scaled Laplace matrix

$$L^{(D)}(\alpha) \coloneqq (L_{ij}(\alpha)\mathbb{I}_D)_{i,j\in V} \tag{2.11}$$

which has a $D \times D$ diagonal matrix with identical entries where the Laplace matrix has a scalar entry. Note that this means that their determinants are related by

$$(\det L)^D = \det L^{(D)}. \tag{2.12}$$

This leads to

$$\sum_{e \in E} \alpha_e Q_e = x^T L^{(D)}_{(X,X)} x + 2 z^T L^{(D)}_{(Z,X)} x + z^T L^{(D)}_{(Z,Z)} z. \tag{2.13}$$

The x_v integrations. Since we started with well defined integrals the Gaussian integral with this exponent is convergent, i.e. $L^{(D)}_{(X,X)}$ (or equivalently $L_{(X,X)}$) is positive definite. We confirm this in the following Lemma.

Lemma 2.1.3. *The matrix $L_{(X,X)}$ is positive definite.*

Proof. One of the characterizations of a positive definite matrix is that it is the Gram matrix of linearly independent vectors. Since $L = I^T I$ each element of L is the inner product of the vectors I_v which are the v-th columns of the incidence matrix, and therefore both L and $L_{(X,X)}$ are Gram matrices. If the vectors are linearly dependent then there are scalars λ_v such that $\sum \lambda_v I_v = 0$ where not all λ_v are zero. Since the underlying graph is connected there are exactly two non-zero elements with the same value but opposite signs in every row of I that corresponds to an internal edge, so all λ_v have to be equal. Because the graph also contains at least one edge connecting to an external vertex, the restriction of L to $L_{(X,X)}$, i.e. to $v \in |X|$ means that at least one λ_v has to be zero. Therefore all λ_v have to vanish to fulfill $\sum \lambda_v I_v = 0$, which means that the the vectors I_v are linearly independent and $L_{(X,X)}$ is hence positive definite. □

Now we can compute the Gaussian integral with the standard result

$$\begin{aligned}\int_{\mathbb{R}^{D|X|}} \left(\prod_{v \in X} \mathrm{d}^D x_v \right) \exp\left(-x^T L^{(D)}_{(X,X)} x - 2 z^T L^{(D)}_{(Z,X)} x - z^T L^{(D)}_{(Z,Z)} z \right) \\ = \left(\frac{\pi^{D|X|}}{\det L^{(D)}_{(X,X)}} \right)^{\frac{1}{2}} \exp\left(\left(z^T L^{(D)}_{(Z,X)} \right) \left(L^{(D)}_{(X,X)} \right)^{-1} \left(z^T L^{(D)}_{(Z,X)} \right)^T - z^T L^{(D)}_{(Z,Z)} z \right)\end{aligned} \tag{2.14}$$

2.1.2 Combinatorics and graph polynomials

Next we discuss how to write the above result in terms of spanning forest polynomials. Specifically, we will find $\hat{\Psi}_{/Z}$ and one that is a linear combination of spanning forest polynomials with partitions of the form $S = \{z_i, z_j\} \cup (Z \setminus \{z_i, z_j\})$ for z_i, z_j two distinct external vertices. The first step will be to evaluate the determinant of $L^{(D)}_{(X,X)}$. This is done in full detail in the following theorem 2.1.4 which is essentially the well known matrix tree theorem (see e.g. [39]). The second step is then the application of the same techniques to the much more complicated expression in the exponential function.

Theorem 2.1.4. (First graph polynomial for graphical functions)
Let G be a graph such that its graphical function $f^{(\lambda)}_G$ exists and G/Z the graph

which can be found from G by identifying all external vertices of G. Furthermore let L be the Laplace matrix of G and $L_{(X,X)}$ the sub matrix corresponding to internal vertices of G. Then

$$\det L_{(X,X)}(\alpha) = \sum_{\substack{T\subset E \\ T \text{ spanning tree of } G/Z}} \prod_{e\in T} \alpha_e = \hat{\Psi}_{/Z} \tag{2.15}$$

Proof. Let $I_{(K,X)}$, $K \subseteq E$ be the $|K| \times |X|$-submatrix of I that contains only the columns corresponding to internal vertices and the rows corresponding to edges in K. Then $L_{(X,X)} = I^T_{(E,X)} I_{(E,X)}$ is the submatrix of L that contains the rows and columns corresponding to internal vertices. Due to the Binet-Cauchy theorem we can write

$$\det L_{(X,X)} = \sum_{\substack{K\in\mathcal{P}(E) \\ |K|=|X|}} \det I^T_{(K,X)} \det I_{(K,X)} \tag{2.16}$$

The determinant of $I_{(K,X)}$ vanishes if its columns or rows are linearly dependent. Next we show that this is the case if the edges $e \in K$ form a cycle in G/Z.

a) The edges in K form a cycle G and therefore also in G/Z:
This means that if the cycle contains $2 \leq q \leq |X|$ of the edges, there are q rows in $I_{(K,X)}$ that have (up to permutation of columns and rows) the form

$$\begin{aligned} e_{i_1} &= \pm\alpha_{i_1}^{1/2}(1,-1,0,...,0) \\ e_{i_2} &= \pm\alpha_{i_2}^{1/2}(0,1,-1,0,...,0) \\ &... \\ e_{i_q} &= \pm\alpha_{i_q}^{1/2}(1,\underbrace{0,...,0}_{\substack{q-2\\ \text{times}}},-1,0,...,0) \end{aligned} \tag{2.17}$$

and are therefore linearly dependent.

b) The edges in K form a cycle in G/Z but not in G:
In this case, if the cycle contains $2 \leq q \leq |X|$ of the edges, there are q rows in $I_{(K,X)}$ that have (up to permutation of columns and rows) the form

$$\begin{aligned} e_{i_1} &= \pm\alpha_{i_1}^{1/2}(1,-1,0,...,0) \\ e_{i_2} &= \pm\alpha_{i_2}^{1/2}(0,1,-1,0,...,0) \\ &... \\ e_{i_{q-2}} &= \pm\alpha_{i_{q-2}}^{1/2}(\underbrace{0,...,0}_{\substack{q-3\\ \text{times}}},1,-1,0,...,0) \\ e_{i_{q-1}} &= \pm\alpha_{i_{q-1}}^{1/2}(1,0,...,0) \\ e_{i_q} &= \pm\alpha_{i_q}^{1/2}(\underbrace{0,...,0}_{\substack{q-2\\ \text{times}}},1,0,...,0) \end{aligned} \tag{2.18}$$

where the last two edges are the ones that contain the merged external vertex of G/Z. These rows are clearly linearly dependent, too. Since edges between external vertices are allowed, there may be tadpoles (loops with only one edge) in G/Z. They correspond to a row of only zeros and therefore also a vanishing determinant.

The remaining edge subsets are trees in G/Z with $|X|$ edges connecting $|X|+1$ vertices. They are the spanning trees T of G/Z.
$I_{(T,X)}$ for a spanning tree T has at least one row with only one non-zero entry in row m, column n. The determinant of $I_{(T,X)}$ is then

$$\det I_{(T,X)} = \pm\alpha_m^{1/2} \det I_{(T,X)}^{(m,n)} \tag{2.19}$$

where the superscript means that the m-th row and n-th column are removed from the matrix. $I_{(T,X)}^{(m,n)}$ has at least one row with only one non-zero entry. Repeating this until only a 1×1 matrix remains gives

$$\det I_{(T,X)}(\alpha) = \pm \prod_{e\in T} \alpha_e^{1/2}. \tag{2.20}$$

Therefore,

$$\det L_{(X,X)}(\alpha) = \sum_{\substack{T\subset E \\ T \text{ spanning tree of } G/Z}} \prod_{e\in T} \alpha_e. \tag{2.21}$$

which is the definition of the dual Kirchhoff polynomial of G/Z. □

Remark 2.1.5. *The dual Kirchhoff polynomial of G/Z will ubiquitous all throughout the rest of this thesis. In order to reduce notation we will from now on identify $\hat{\Psi} \equiv \hat{\Psi}_{G/Z} = \hat{\Psi}_{/Z}$. Should we need the dual Kirchhoff polynomial of G proper, which would normally be equivalent to $\hat{\Psi}$ without indices we will explicitly write $\hat{\Psi}_G$ instead.*

Spanning forest polynomials in the exponent. We will now show that the expression

$$\left(z^T L_{(Z,X)}^{(D)}\right)\left(L_{(X,X)}^{(D)}\right)^{-1}\left(z^T L_{(Z,X)}^{(D)}\right)^T - z^T L_{(Z,Z)}^{(D)} z \tag{2.22}$$

can be written as a linear combination of certain spanning forest polynomials with coefficients that depend only on the external vertex parameters. The inverse matrix in eq. (2.22) can be written using cofactors:

$$\left(L_{(X,X)}^{(D)^{-1}}\right)_{ij} = \frac{(-1)^{i+j}}{\det(L_{(X,X)}^{(D)})} \det(L_{(X,X)}^{(D)(j,i)}) \tag{2.23}$$

As noted earlier, $\det(L_{(X,X)}^{(D)})$ is the D-th power of the determinant of $L_{(X,X)}$ and one quickly confirms that $\det(L_{(X,X)}^{(D)(j,i)}) = (\det(L_{(X,X)}))^{D-1}\det(L_{(X,X)}^{(j,i)})$. So we have

$$\begin{aligned}\left(L_{(X,X)}^{(D)^{-1}}\right)_{ij} &= \frac{(-1)^{i+j}}{(\det L_{(X,X)})^D} \det(L_{(X,X)}^{(D)(j,i)}) \\ &= \frac{(-1)^{i+j}}{\hat{\Psi}} \det(L_{(X,X)}^{(j,i)}).\end{aligned} \tag{2.24}$$

That remaining determinant is

$$\det L_{(X,X)}^{(j,i)} = \sum_{\substack{K\in\mathcal{P}(E) \\ |K|=|X|-1}} \det(I_{(K,X)}^{(j)})^T \det I_{(K,X)}^{(i)}. \tag{2.25}$$

The superscript with only one index on the rhs means that no row is deleted, only the column j or i, respectively. Again, if K has a cycle in G/Z, the determinant of $I^{(i)}_{(K,X)}$ vanishes. The remaining possible sets K are the spanning 2-forests of G/Z because they have $|X|-1$ edges in a graph with $|X|+1$ vertices and no cycles. The incidence matrix $I_{(K,X)}$ for such spanning 2-forest consists of two blocks

$$I_{(K,X)} = \left(\begin{array}{c|c} I(T_{int}) & 0 \\ \hline 0 & I^{(v_{ext})}(T_{ext}) \end{array}\right) \tag{2.26}$$

where T_{int} denotes the tree with only internal vertices, T_{ext} is the tree that contains the external vertex v_{ext} and $I^{(v_{ext})}$ means that the column of v_{ext} is deleted. $I(T_{int})$ has one more columns than rows while $I^{(v_{ext})}(T_{ext})$ is quadratic. Therefore, if $i \in T_{ext}$ then $I^{(i)}_{(K,X)}$ consists of two non-quadratic block matrices so its determinant vanishes. If, on the other hand, $i \in T_{int}$, then the two sub matrices are quadratic and consist of linearly independent columns (because they are incident matrices of trees), so their determinant does not vanish.

We collect all spanning 2-forests which lead to non vanishing determinants by defining

$$\mathcal{F}^{(i,j)}_{G/Z} := \{F = T_{int} \cup T_{ext} \subset G/Z \mid i,j \in T_{int}\} \quad \forall\, i,j \in X. \tag{2.27}$$

One can now introduce for each pair i,j (which need not be distinct) another polynomial similarly to the way the dual Kirchhoff polynomial was found in the proof of theorem 2.1.4, albeit with an additional argument regarding the sign of $\det L^{(j,i)}_{(X,X)}$. $L_{(X,X)}$ is a Stieltjes matrix (real, symmetric and with non-positive off-diagonal entries), so its inverse is a non-negative matrix. Since each entry of the inverse is given by

$$\left(L^{-1}_{(X,X)}\right)_{ij} = \frac{(-1)^{i+j}}{\hat{\Psi}} \det(L^{(j,i)}_{(X,X)}). \tag{2.28}$$

one sees that the sign of $\det(L^{(j,i)}_{(X,X)})$ always cancels the $(-1)^{i+j}$. Consequently one again finds a polynomial with positive coefficients, namely

$$\hat{\chi}_{ij} := (-1)^{i+j} \det L^{(j,i)}_{(X,X)} = \sum_{F \in \mathcal{F}^{(i,j)}} \prod_{e \in F} \alpha_e = \hat{\Phi}^{\{i,j\}\{k\}}_{/Z} \tag{2.29}$$

where $\hat{\Phi}^{\{i,j\}\{k\}}_{/Z}$ is a dual spanning forest polynomial and k in its partition stands for the single external vertex of G/Z. The inverse matrix therefore can be written as

$$\left(L^{(D)}_{(X,X)}\right)^{-1}_{ij} = \frac{\hat{\chi}_{ij}}{\hat{\Psi}}. \tag{2.30}$$

Now one needs to multiply this matrix from both sides with the vector

$$z^T L_{(Z,X)} = \left(- \sum_{\substack{i \in Z \\ i \text{ adj. } k}} z_i \alpha_{e=\{i,k\}} \right)_{k \in X} \in \mathbb{R}^{D|X|} \tag{2.31}$$

which gives the result

$$\left(z^T L^{(D)}_{(Z,X)}\right)\left(L^{(D)}_{(X,X)}\right)^{-1}\left(z^T L^{(D)}_{(Z,X)}\right)^T = \frac{1}{\hat{\Psi}} \sum_{i,j\in Z} z_i^T z_j \sum_{\substack{k,l\in X \\ k \text{ adj. } i \\ l \text{ adj. } j}} \hat{\chi}_{kl} \sum_{\substack{e_1,e_2\in E \\ e_1=\{i,k\} \\ e_2=\{j,l\}}} \alpha_{e_1}\alpha_{e_2}. \quad (2.32)$$

$\hat{\chi}_{kl}$ contains the product of all edge parameters that are in a given spanning 2-forest of G/Z, summed over all spanning 2-forests that have k and l in one tree and the merged external vertex in the other. We have to distinguish three cases:

(a) $i \neq j$:
Multiplying by $\alpha_{e=\{i,k\}}\alpha_{e=\{j,l\}}$ corresponds to adding the two edges $\{i,k\}$ and $\{j,l\}$ to the spanning 2-forest. Since k and l were in the same tree, i and j are in the same tree. For each spanning 2-forest $F \in \mathcal{F}^{(k,l)}_{G/Z}$ one gets $F \cup \{i,k\} \cup \{j,l\}$ which is a spanning $|Z|-1$-forest in G. It is important to note that added edges always connect an external and an internal vertex of G. Purely external edges $e = \{z_{v_1}, z_{v_2}\}$ with $v_1, v_2 \in Z$ do not appear in this case. We will later find them when examining the term $z^T L^{(D)}_{(Z,Z)} z$. The sum over all possible added edges can hence be written as a sum over elements of the set

$$\mathcal{F}^{(i,j)}_{G\setminus E_Z} := \{F \cup \{i,k\} \cup \{j,l\} \mid F \in \mathcal{F}^{(k,l)}_{G/Z},\ i,j \in Z \text{ and } k,l \in X\} \quad (2.33)$$

where $E_Z \subset E$ shall denote the set of purely external edges. The sum from eq. (2.32) is then

$$\sum_{\substack{i,j\in Z \\ i\neq j}} z_i^T z_j \sum_{\substack{k,l\in X \\ k \text{ adj. } i \\ l \text{ adj. } j}} \hat{\chi}_{kl} \sum_{\substack{e_1,e_2\in E \\ e_1=\{i,k\} \\ e_2=\{j,l\}}} \alpha_{e_1}\alpha_{e_2} = \sum_{\substack{i,j\in Z \\ i\neq j}} z_i^T z_j \sum_{F\in\mathcal{F}^{(i,j)}_{G\setminus E_Z}} \prod_{e\in F} \alpha_e = \sum_{\substack{i,j\in Z \\ i\neq j}} z_i^T z_j \ \hat{\Phi}^{\{i,j\}\{k\}}_{G\setminus E_Z} \quad (2.34)$$

where the k in the partition of the dual spanning forest polynomial is again any vertex of $G \setminus E_Z$ which is neither i nor j.

(b) $i = j$ and $k \neq l$:
For any $F \in \mathcal{F}^{(k,l)}_{G/Z}$ adding the two edges results in a subgraph that has a loop in G because the two vertices k and l which where already in the same tree are now connected via the external vertex $i = j$ too. We will see below that all the terms of this case cancel.

(c) $i = j$ and $k = l$:
Here we get the terms

$$\sum_{i\in Z} z_i^2 \sum_{\substack{k\in X \\ k \text{ adj. } i}} \hat{\chi}_{kk} \sum_{\substack{e\in E \\ e=\{i,k\}}} \alpha_e^2. \quad (2.35)$$

Below we will see that these terms also get canceled.

Lastly, we have to take into account the terms that we called $z^T L^{(D)}_{(Z,Z)} z$ in eq. (2.14).

$$z^T L^{(D)}_{(Z,Z)} z = \frac{1}{\hat{\Psi}_{/Z}} \sum_{\substack{i,j\in Z \\ i\neq j}} z_i^T z_j \left(\sum_{T \text{ s. t. of } G/Z} \prod_{e\in T} \alpha_e \right) \cdot \begin{cases} -\sum\limits_{\substack{e\in E \\ e=\{i,j\}}} \alpha_e & \text{if } i \neq j \\ \sum\limits_{\substack{k\in V \\ k \text{ adj. } i}} \sum\limits_{\substack{e\in E \\ e=\{i,k\}}} \alpha_e & \text{if } i = j \end{cases} \quad (2.36)$$

After lifting to G we have to distinguish three cases again:

(a) $i, j \notin T \subset G$:
If $i \neq j$, then the spanning tree $T \subset G/Z$ is by the above considerations a spanning $|Z|$-forest in G. Since neither i nor j are in T, the edge connecting them (if there is one) makes $T \cup \{i, j\}$ a spanning $(|Z| - 1)$-forest of G. In fact, this case contains all the terms corresponding to spanning $(|Z| - 1)$-forest of G with purely external edges that were missing in case (a) above.

If $i = j$, the edge $\{i, k\}$ connects the external vertex i with the tree T. T might contain any (but at most one) external vertex or only internal vertices so this gives *all* spanning $|Z| - 1$-forest of G which have i and another external vertex in one tree and the others in the other tree. All in all we have for $i, j \notin T$

$$- \sum_{\substack{i,j \in Z \\ i \neq j}} z_i^T z_j \sum_{F \in \mathcal{F}_G^{(i,j)} \setminus \mathcal{F}_{G \setminus E_Z}^{(i,j)}} \prod_{e \in F} \alpha_e + \sum_{i \in Z} z_i^2 \sum_{j \in Z} \sum_{F \in \mathcal{F}_G^{(i,j)}} \prod_{e \in F} \alpha_e \tag{2.37}$$

(b) $i = j$, $i \in T \subset G$ and $e = \{i, k\} \notin T$:
We can write

$$\left(\prod_{e \in T} \alpha_e \right) \alpha_{e=\{i,k\}} = \prod_{e \in T \cup \{e\}} \alpha_e \tag{2.38}$$

$T \cup \{e\}$ now contains a cycle, so terms of this kind will cancel the terms one gets from case (b) above. (c) $i = j$, $i \in T \subset G$ and $e = \{i, k\} \in T$:
Because $e \in T$, α_e also occurs in the corresponding monomial of $\hat{\Psi}$, which we can rearrange to make it obvious that these terms cancel those from (2.35):

$$\left(\prod_{e \in T} \alpha_e \right) \alpha_{e=\{i,k\}} = \left(\prod_{e \in (T \setminus \{\{i,k\}\})} \alpha_e \right) \alpha_{e=\{i,k\}}^2 \tag{2.39}$$

Summarized we now have that in the expression (2.22) everything but the results of (2.34) and (2.37) cancels. The non-vanishing terms are

$$\begin{aligned} &\left(z^T L_{(Z,X)} \right) L_{(X,X)}^{-1} \left(z^T L_{(Z,X)} \right)^T - z^T L_{(Z,Z)} z \\ &\qquad = \frac{1}{\hat{\Psi}} \sum_{\substack{i,j \in Z \\ i \neq j}} (z_i^T z_j - z_i^2) \sum_{F \in \mathcal{F}_G^{(i,j)}} \prod_{e \in F} \alpha_e \\ &\qquad = -\frac{1}{\hat{\Psi}} \sum_{i \prec j \in Z} ||z_i - z_j||^2 \hat{\Phi}_G^{\{i,j\}\{k\}} \end{aligned} \tag{2.40}$$

Note that to avoid double counting of terms we make use of the ordering $\prec$ that was induced on Z by labeling the vertices with natural numbers.

Now we can define the second important polynomial.

Definition 2.1.6. (Second graph polynomial for graphical functions)
Let G be a graph with $|Z|$ external vertices, $\mathcal{F}_G^{(i,j)}$ the set of $|Z|-1$-forests of G that have the external vertices i and j in one tree and the remaining external vertices in the other trees (necessarily exactly one per tree). Then we define the second graph polynomial for graphical functions as

$$\hat{\Phi}_G(\alpha, z) := \sum_{i \prec j \in Z} ||z_i - z_j||^2 \sum_{F \in \mathcal{F}_G^{(i,j)}} \prod_{e \in F} \alpha_e = \sum_{i \prec j \in Z} ||z_i - z_j||^2 \hat{\Phi}_G^{\{i,j\}\{k\}}.$$

and as a shorthand notation we will often use

$$\hat{\Phi}_G(\alpha, z) := \sum_{i \prec j \in Z} z_{ij} \hat{\Phi}_{ij}. \tag{2.41}$$

Furthermore the dependence on α, z and usually also G will not be written explicitly.

Using these results one can write the graphical function from eq. (2.5) as

$$f_G^{(\lambda)}(z) = \frac{1}{\prod_{e \in E_+} \Gamma(\lambda \nu_e)} \left(\int_0^\infty \prod_{e \in E_+} \frac{\mathrm{d}\alpha_e}{\alpha_e^{1-\lambda\nu_e}} \right) \left(\prod_{e \in E_-} (-1)^{\lambda|\nu_e|} \frac{\partial^{\lambda|\nu_e|}}{\partial \alpha_e^{\lambda|\nu_e|}} \bigg|_{\alpha_e = 0} \right) \frac{\exp\left(-\frac{\hat{\Phi}}{\hat{\Psi}}\right)}{\hat{\Psi}^{\lambda+1}}. \tag{2.42}$$

2.1.3 The exponential, affine and projective integral

There are two more possible modifications to the parametric integral. Firstly, we can of course execute the derivations but this will lead to a polynomial which is in general neither homogenous nor linear in any particular variable and which - as many examples seem to indicate - does not have a handy factorization like the Dodgson polynomial either. Due to these complications, the integral as it stands is already quite useful in the case of $E_- \neq \emptyset$ and we will from now on refer to

$$f_G^{(\lambda)}(z) = \frac{1}{\prod_{e \in E_+} \Gamma(\lambda \nu_e)} \left(\int_0^\infty \prod_{e \in E_+} \frac{\mathrm{d}\alpha_e}{\alpha_e^{1-\lambda\nu_e}} \right) \left(\prod_{e \in E_-} (-1)^{\lambda|\nu_e|} \frac{\partial^{\lambda|\nu_e|}}{\partial \alpha_e^{\lambda|\nu_e|}} \bigg|_{\alpha_e = 0} \right) \frac{\exp\left(-\frac{\hat{\Phi}}{\hat{\Psi}}\right)}{\hat{\Psi}^{\lambda+1}}. \tag{2.43}$$

as the *exponential integral representation* of graphical functions. The second possible modification is making the integrand rational, which naturally leads to a projective integral. It is in principle possible to do this without first executing the derivatives (see [21]) but here we will make the integrand derivative free, complification notwithstanding.

The partial derivatives. We already mentioned that executing the partial derivatives in eq. (2.43) results in a very inconvenient polynomial as prefactor of the exponential that complicates practical computations considerably (cf. chapter 3). We introduce that polynomial into the graphical function in the following proposition.

Proposition 2.1.7. *Let*

$$N_- := \sum_{e \in E_-} |\nu_e| \tag{2.44}$$

such that λN_- is the total number of partial differentiations and let

$$\hat{\psi} := \hat{\Psi}\Big|_{\alpha_e=0 \ \forall \ e\in E_-}$$

$$\hat{\phi} := \hat{\Phi}\Big|_{\alpha_e=0 \ \forall \ e\in E_-} \tag{2.45}$$

be the graph polynomials as above but with all parameters corresponding to negative integer edge weights set to zero. Then we can write graphical functions as

$$f_G^{(\lambda)}(z) = \frac{1}{\prod_{e\in E_+}\Gamma(\lambda\nu_e)} \int_0^\infty \left(\prod_{e\in E_+} \frac{\mathrm{d}\alpha_e}{\alpha_e^{1-\lambda\nu_e}}\right) \frac{\eta \exp\left(-\frac{\hat{\phi}}{\hat{\psi}}\right)}{\hat{\psi}^{\lambda+1+2\lambda N_-}}. \tag{2.46}$$

where $\eta \equiv \eta(\alpha, z, \lambda)$ is a polynomial of degree $2\lambda N_-|X|$ in the remaining edge parameters $\{\alpha_e \mid e \in E_+\}$.

Proof. We prove by induction over the number of differentiations. For $\lambda N_- = 0$ one has $\eta = 1$ and nothing else to prove. The λN_--th differentiation, say in the variable α_{e_1} is

$$\begin{aligned}
&-\frac{\partial}{\partial\alpha_{e_1}} \frac{\eta^{(\lambda N_- -1)} \exp\left(-\frac{\hat{\Phi}}{\hat{\Psi}}\right)}{\Psi^{\lambda+1+2\lambda N_- -2}} \\
&= \left(\eta^{(\lambda N_- -1)} \frac{\hat{\Phi}_{e_1}\hat{\Psi} - \hat{\Phi}\hat{\Psi}_{e_1} + (\lambda+1+2\lambda N_- -2)\hat{\Psi}_{e_1}\hat{\Psi}}{\hat{\Psi}^2} + \frac{\partial}{\partial\alpha_{e_1}}\eta^{(\lambda N_- -1)}\right) \\
&\qquad\qquad \times \frac{\exp\left(-\frac{\hat{\Phi}}{\hat{\Psi}}\right)}{\hat{\Psi}^{\lambda+1+2\lambda N_- -2}}.
\end{aligned} \tag{2.47}$$

The degree of both $\hat{\Phi}_{e_1}\hat{\Psi} - \hat{\Phi}\hat{\Psi}_{e_1} + (\lambda+1+2\lambda N_- -2)\hat{\Psi}_{e_1}\hat{\Psi}$ and $\hat{\Psi}^2$ is $2|X|$. After pulling $\hat{\Psi}^{-2}$ out of the bracket we can identify the polynomial

$$\eta^{(\lambda N_-)} := \left(\eta^{(\lambda N_- -1)}\left(\hat{\Phi}_{e_1}\hat{\Psi} - \hat{\Phi}\hat{\Psi}_{e_1} + (\lambda+1+2\lambda N_- -2)\hat{\Psi}_{e_1}\hat{\Psi}\right) + \hat{\Psi}^2\frac{\partial}{\partial\alpha_{e_1}}\eta^{(\lambda N_- -1)}\right) \tag{2.48}$$

which is indeed of degree $2\lambda N_-|X|$. Therefore,

$$-\frac{\partial}{\partial\alpha_{e_1}} \frac{\eta^{(\lambda N_- -1)} \exp\left(-\frac{\hat{\Phi}}{\hat{\Psi}}\right)}{\Psi^{\lambda+1+2\lambda N_- -2}} = \frac{\eta^{(\lambda N_-)} \exp\left(-\frac{\hat{\Phi}}{\hat{\Psi}}\right)}{\Psi^{\lambda+1+2\lambda N_-}}. \tag{2.49}$$

□

Projectivization. We will now rewrite the integral in eq. (2.46) in a certain way that will be very useful, for explicit computation as well as for more abstract reasons. First we rescale the variables by[1]

$$\alpha_e \to \alpha_1\alpha_e \quad \forall \ e > 1 \tag{2.50}$$

[1]This will lead to an affine integral, which can be interpreted as a special case of a projective integral. Equivalently one could scale all α_e by a new variable t which one introduces together with a side constraint and directly find the projective integral. See [20] for a detailed explanation and case (b) of the proof of proposition 2.2.3 for an application of this method to a partial integral of the exponential integral representation.

which, remembering that the degrees of $\hat{\psi}$ and $\hat{\phi}$ are $|X|$ and $|X|+1$ respectively, gives

$$f_G^{(\lambda)}(z) = \frac{1}{\prod_{e\in E_+}\Gamma(\lambda\nu_e)} \int_0^\infty \left(\prod_{e>1} \frac{\mathrm{d}\alpha_e}{\alpha_e^{1-\lambda\nu_e}}\right) \int_0^\infty \mathrm{d}\alpha_1 \alpha_1^{\lambda N_+ - |X|(\lambda+1+2\lambda N_-)-1} \times \eta(\alpha_1, \alpha_1\alpha_2, \ldots, \alpha_1\alpha_{|E|}) \frac{\exp\left(-\alpha_1 \left.\frac{\hat{\phi}}{\hat{\psi}}\right|_{\alpha_1=1}\right)}{\hat{\psi}|_{\alpha_1=1}^{\lambda+1+2\lambda N_-}}. \tag{2.51}$$

Here we introduced $N_+ = \sum \nu_e + N_-$, the sum of all edge weights that are not negative integers. Furthermore we will from now on use the abbreviation

$$Y \coloneqq \lambda N_+ - |X|(\lambda+1) \tag{2.52}$$

and $Y_n \coloneqq Y - 2|X|\lambda N_- + n$, which will be useful in the next step.

To integrate α_1 one has to look at the terms in η with different powers of α_1 separately. Write

$$\eta(\alpha_1, \alpha_2, \ldots, \alpha_{|E|}) = \sum_{n=0}^{2|X|\lambda N_-} \eta_n \tag{2.53}$$

where η_n contains all degree n monomials of η. Then

$$\eta(\alpha_1, \alpha_1\alpha_2, \ldots, \alpha_1\alpha_{|E|}) = \sum_{n=0}^{2|X|\lambda N_-} \alpha_1^n \cdot \eta_n|_{\alpha_1=1} \tag{2.54}$$

and the graphical function contains a sum of integrals which give different Γ-functions,

$$\begin{aligned} f_G^{(\lambda)}(z) &= \frac{1}{\prod_{e\in E_+}\Gamma(\lambda\nu_e)} \int_0^\infty \left(\prod_{e>1} \frac{\mathrm{d}\alpha_e}{\alpha_e^{1-\lambda\nu_e}}\right) \\ &\qquad \times \sum_{n=0}^{2|X|\lambda N_-} \eta_n \int_0^\infty \mathrm{d}\alpha_1 \alpha_1^{Y-2|X|\lambda N_- +n-1} \frac{\exp\left(-\alpha_1 \left.\frac{\hat{\phi}}{\hat{\psi}}\right|_{\alpha_1=1}\right)}{\hat{\psi}|_{\alpha_1=1}^{\lambda+1+2\lambda N_-}} \\ &= \frac{1}{\prod_{e\in E_+}\Gamma(\lambda\nu_e)} \int_0^\infty \left(\prod_{e>1} \frac{\mathrm{d}\alpha_e}{\alpha_e^{1-\lambda\nu_e}}\right) \sum_{n=0}^{2|X|\lambda N_-} \left. \frac{\Gamma(Y_n)\eta_n}{\hat{\phi}^{Y+n}\ \hat{\psi}^{\lambda+1-Y_n}} \right|_{\alpha_1=1}. \end{aligned} \tag{2.55}$$

The function in (2.55) will be referred to as *affine integral representation* of graphical functions. It is scale invariant in every variable and can be interpreted as one realization of the *projective integral*,

$$f_G^{(\lambda)}(z) = \frac{1}{\prod_{e\in E_+}\Gamma(\lambda\nu_e)} \int_{\Delta_{\mathbb{P}}} \sum_{n=0}^{2|X|\lambda N_-} \frac{\Gamma(Y_n)\eta_n \prod_e \alpha_e^{\lambda\nu_e-1}}{\hat{\phi}^{Y+n}\ \hat{\psi}^{\lambda+1-Y_n}} \Omega. \tag{2.56}$$

where $\Omega = \sum_e (-1)^{e-1}\alpha_e \mathrm{d}\alpha_1 \wedge \ldots \wedge \widehat{\mathrm{d}\alpha_e} \wedge \ldots \wedge \mathrm{d}\alpha_{|E|}$ is the projective volume form and one integrates over the subset of real projective space in which all parameters are positive

$$\Delta_{\mathbb{P}} = \{[\alpha_1 : \ldots : \alpha_{|E|}] \mid \alpha_i > 0 \ \forall\ i = 1, \ldots, |E|\ \}. \tag{2.57}$$

These two versions of graphical functions are needed for explicit integrations which are practically impossible in the exponential version. The affine integral (2.55) is useful for concrete calculations because it effectively reduces the number of variables by one. It is therefore of course the version of graphical functions most commonly used in calculations with computer algebra (see chapter 3). The projective version (2.56) is more commonly used if one needs the abstract framework of algebraic geometry and wants to use properties that were lost in the affine integral, e.g. homogeneity of the spanning forest polynomials.

Since the polynomial due to negative edge weights complicates things so much, we will mostly use the projective version of graphical functions for the case $E_- = \emptyset$, in which (2.56) takes on the form

$$f_G^{(\lambda)}(z) = \frac{\Gamma(Y)}{\prod_{e\in E}\Gamma(\lambda\nu_e)} \int_{\Delta_{\mathbb{P}}} \frac{\prod_e \alpha_e^{\lambda\nu_e - 1}}{\hat{\Phi}^Y \ \hat{\Psi}^{\lambda+1-Y}} \Omega. \tag{2.58}$$

2.2 Properties of the parametric integrals

In this section we will explicitly show that the parametric graphical function derived above indeed treats edges between external vertices and multi-edges just like the position space graphical function, even though it is everything but obvious from the parametric integral representations introduced above. On the one hand this serves as a consistency check, on the other hand it is an opportunity to familiarize ourselves with the parametric integrals we just derived.

2.2.1 Insertion of purely external edges

From the position space definition (1.3.1) we know that inserting an edge e between external vertices i and j only changes the graphical function by a constant factor

$$||z_i - z_j||^{-2\lambda\nu_e} = z_{ij}^{-\lambda\nu_e}. \tag{2.59}$$

Such a factor can be incorporated into the parametric integral with an additional integration or differentiation. We will explain below how we can use this fact to simplify matters in many situations and in section 2.4 will see this principle applied but first let us check that the parametric graphical function is indeed consistent for graphs with trivial edges.

Let G be a graph such that $f_G^{(\lambda)}$ exists and G' be the graph G with an additional edge e between external vertices, say i and j. Note that G may already contain other edges between any two external vertices, including i and j. We can recover the fact

$$f_{G'}^{(\lambda)}(z) = z_{ij}^{-\lambda\nu_e} f_G^{(\lambda)}(z) \tag{2.60}$$

from the parametric integral as follows. An edge between external vertices becomes a tadpole in G'/Z and is therefore never in one of its spanning trees. Hence,

$$\hat{\Psi}_{G'/Z} = \hat{\Psi}_{G/Z}. \tag{2.61}$$

With the contraction/deletion relations 1.2.18 we find that the polynomial in the integrand of $f_{G'}^{(\lambda)}(z)$ can be written

$$\hat{\Phi}_{G'} = \alpha_e \hat{\Phi}_{G'//e} + \hat{\Phi}_{G'\setminus\{e\}} \tag{2.62}$$

where one also directly finds $\hat{\Phi}_{G'\setminus\{e\}} = \hat{\Phi}_G$. Since α_e, i.e. the parameter of an edge directly connecting i and j, may only occur in a single polynomial $\hat{\Phi}_{ij}$ from the sum $\hat{\Phi} = \sum z_{mn}\hat{\Phi}_{mn}$, one has

$$\hat{\Phi}_{G'//e} = \frac{\partial}{\partial \alpha_e}\hat{\Phi}_{G'} = z_{ij}(\hat{\Phi}_{ij})_{G'//e}. \tag{2.63}$$

Moreover, when using spanning forest polynomial notation with S_{res} a partition of all external vertices except i and j into disjoint sets, one has

$$(\hat{\Phi}_{ij})_{G'} = \hat{\Phi}_{G'}^{\{i,j\},S_{res}} \tag{2.64}$$

and consequently

$$(\hat{\Phi}_{ij})_{G'//e} = \hat{\Phi}_{G'//e}^{\{i=j\},S_{res}} = \hat{\Phi}_{G'/\{i,j\}}^{\{i=j\},S_{res}} = \hat{\Phi}_{G/\{i,j\}}^{\{i=j\},S_{res}} \tag{2.65}$$

Here, the second and third equality are due to the fact that contracting $e = \{i, j\}$ gives a tadpole that can never be part of a spanning forest. Finally we find that we can write (following remark 1.2.20)

$$\hat{\Phi}_{G/\{i,j\}}^{\{i=j\},S_{res}} = \hat{\Phi}_{\tilde{G}}^{\{i\},\{j\},S_{res}} = \hat{\Psi}_{G/Z} \tag{2.66}$$

such that the second polynomial now is

$$\hat{\Phi}_{G'} = \alpha_e z_{ij}\hat{\Psi}_{G/Z} + \hat{\Phi}_G \tag{2.67}$$

Now, starting from the graphical function as in (2.43) an additional edge either gives an integral

$$\begin{aligned}\frac{1}{\Gamma(\lambda\nu_e)}\int_0^\infty \mathrm{d}\alpha_e \alpha_e^{\lambda\nu_e-1}\frac{\exp\left(-\frac{\hat{\Phi}_{G'}}{\hat{\Psi}_{G'/Z}}\right)}{\hat{\Psi}_{G'/Z}^{\lambda+1}} &= \frac{1}{\Gamma(\lambda\nu_e)}\frac{\exp\left(-\frac{\hat{\Phi}_G}{\hat{\Psi}_{G/Z}}\right)}{\hat{\Psi}_{G/Z}^{\lambda+1}}\int_0^\infty \mathrm{d}\alpha_e \alpha_e^{\lambda\nu_e-1}e^{-\alpha_e z_{ij}} \\ &= z_{ij}^{-\lambda\nu_e}\frac{\exp\left(-\frac{\hat{\Phi}_G}{\hat{\Psi}_{G/Z}}\right)}{\hat{\Psi}_{G/Z}^{\lambda+1}}\end{aligned} \tag{2.68}$$

or a differentiation

$$\begin{aligned}(-1)^{\lambda|\nu_e|}\frac{\partial^{\lambda|\nu_e|}}{\partial\alpha_e^{\lambda|\nu_e|}}\bigg|_{\alpha_e=0}\frac{\exp\left(-\frac{\hat{\Phi}_{G'}}{\hat{\Psi}_{G'/Z}}\right)}{\hat{\Psi}_{G'/Z}^{\lambda+1}} &= z_{ij}^{\lambda|\nu_e|}\left.\frac{\exp\left(-\frac{\hat{\Phi}_{G'}}{\hat{\Psi}_{G'/Z}}\right)}{\hat{\Psi}_{G'/Z}^{\lambda+1}}\right|_{\alpha_e=0} \\ &= z_{ij}^{-\lambda\nu_e}\frac{\exp\left(-\frac{\hat{\Phi}_G}{\hat{\Psi}_{G/Z}}\right)}{\hat{\Psi}_{G/Z}^{\lambda+1}}.\end{aligned} \tag{2.69}$$

In both cases one finds the integrand for $f_G^{(\lambda)}(z)$ and the correct constant factor.

Remark 2.2.1. *Note that for these particular integrations and differentiations the caveat from remark 2.1.2 does not apply since they just give a constant factor that does neither affect convergence nor continuousness in any way. Therefore it is justified to look at them isolated from the other integrations and differentiations as we just did.*

This property can be exploited to simplify a graphical function. Provided that $f_G^{(\lambda)}$ exists with $Y < \lambda + 1$ and there are no inverse propagators, it is always possible to insert an edge with weight such that for the new graph $Y = \lambda + 1$ and $\hat{\Psi}$ vanishes from the integrand in (2.56) or (2.55). Then one can do all calculations or proofs for that graphical function and recover the result for the original graphical function by simply dividing through a constant. This will be used in the proof of theorem 2.4.4. If the graph contains inverse propagators this is only possible for one of the Y_n but might still be helpful, depending on the complexity and number of terms in the sum.

Example 2.2.2. *Consider the graph G from the left-hand side of fig. 2.1 in the case $\lambda = 1$ and with all edge weights $\nu_e = 1$. It has three edges and one internal vertex, giving*

$$Y = 3\lambda - (\lambda + 1) = 2\lambda - 1 \overset{\lambda=1}{=} 1 \tag{2.70}$$

and a graphical funtion

$$f_G^{(1)}(z) = \int_{\Delta_{\mathbb{P}}} \frac{1}{\hat{\Phi}\hat{\Psi}}\Omega. \tag{2.71}$$

The graph on the right hand side has an extra edge such that $Y' = Y + 1 = 2$ and we can write

$$f_G^{(1)}(z) = \frac{\Gamma(Y)}{\Gamma(Y')}||z_2 - z_3||^2 f_{G'}^{(1)}(z) = \frac{1}{2}||z_2 - z_3||^2 \int_{\Delta_{\mathbb{P}}} \frac{1}{\hat{\Phi}^2}\Omega. \tag{2.72}$$

We see that the integrand only depends on one polynomial which is a situation that is combinatorially much easier to handle, as we will see below.

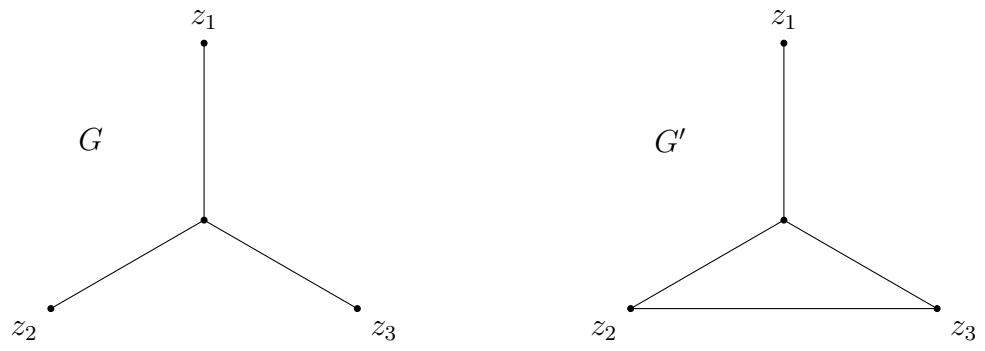

Figure 2.1: Graphs G with $Y = 1$ and G' with $Y' = 2$ for the case $\lambda = 1$.

2.2.2 Equivalence of multi-edges and a single weighted edge

Proposition 2.2.3. *Let G be a graph with $n > 1$ edges with weights $\nu_{e_1}, \dots, \nu_{e_n}$ between two of its vertices such that $f_G^{(\lambda)}(z)$ exists and the sum of the weights either has positive real part or is in $\lambda^{-1}\mathbb{Z}$.[2] Furthermore let G' be the same graph as G but with the multiple edges replaced by a single edge with weight $\nu_{e_1} + \ldots + \nu_{e_n}$. Then their parametric integral representations are equivalent.*

Proof. Firstly we note that it suffices to prove the case $n = 2$ because if there are more edges one can successively merge them pairwise. Secondly, no tree or $|Z| - 1$-forest can ever contain more than one edge between the same two vertices and for each tree or forest containing one edge from a pair of multi-edges there is another tree or forest that contains the other edge but is otherwise identical. In equations that means we can write

$$\begin{aligned}\hat{\Psi} &= \hat{\Psi}_{e_1}(\alpha_{e_1} + \alpha_{e_2}) + \hat{\Psi}^{(e_1e_2)} = \hat{\Psi}_{e_2}(\alpha_{e_1} + \alpha_{e_2}) + \hat{\Psi}^{(e_1e_2)} \\ \hat{\Phi} &= \hat{\Phi}_{e_1}(\alpha_{e_1} + \alpha_{e_2}) + \hat{\Phi}^{(e_1e_2)} = \hat{\Phi}_{e_2}(\alpha_{e_1} + \alpha_{e_2}) + \hat{\Phi}^{(e_1e_2)}. \end{aligned} \tag{2.73}$$

There are several cases to investigate separately. In all of them we use the exponential integral representation as written in (2.43):

(a) $e_1, e_2 \in E_-$:
In order to prove this case we look at the derivatives:

$$(-1)^{\lambda|\nu_{e_1}|+\lambda|\nu_{e_2}|} \left.\frac{\partial^{\lambda|\nu_{e_1}|}}{\partial\alpha_{e_1}^{\lambda|\nu_{e_1}|}}\right|_{\alpha_{e_1}=0} \left.\frac{\partial^{\lambda|\nu_{e_2}|}}{\partial\alpha_{e_2}^{\lambda|\nu_{e_2}|}}\right|_{\alpha_{e_2}=0} \frac{\exp\left(-\frac{\hat{\Phi}}{\hat{\Psi}}\right)}{\hat{\Psi}^{\lambda+1}} \tag{2.74}$$

Due to the relations (2.73), the above expression is equivalent to

$$(-1)^{\lambda|\nu_{e_1}+\nu_{e_2}|} \left.\frac{\partial^{\lambda|\nu_{e_1}+\nu_{e_2}|}}{\partial\alpha_{e_1}^{\lambda|\nu_{e_1}+\nu_{e_2}|}}\right|_{\alpha_{e_1},\alpha_{e_2}=0} \frac{\exp\left(-\frac{\hat{\Phi}}{\hat{\Psi}}\right)}{\hat{\Psi}^{\lambda+1}}, \tag{2.75}$$

which is exactly what appears in $f_{G'}^{(\lambda)}(z)$.

(b) $e_1, e_2 \in E_+$:
We cannot exchange integration and partial derivatives, but can execute them as in eq. 2.46. The relevant partial integral is then

$$\frac{1}{\Gamma(\lambda\nu_{e_1})\Gamma(\lambda\nu_{e_2})} \int_0^\infty \mathrm{d}\alpha_{e_1} \int_0^\infty \mathrm{d}\alpha_{e_2} \alpha_{e_1}^{\lambda\nu_{e_1}-1} \alpha_{e_2}^{\lambda\nu_{e_2}-1} f(\alpha_{e_1} + \alpha_{e_2}), \tag{2.76}$$

where we abbreviated

$$f(\alpha_{e_1} + \alpha_{e_2}) := \eta \frac{\exp\left(-\frac{\hat{\phi}}{\hat{\psi}}\right)}{\hat{\psi}^{\lambda+1+2\lambda N_-}} = \eta(\alpha_{e_1} + \alpha_{e_2}) \frac{\exp\left(-\frac{\hat{\phi}_{e_1}(\alpha_{e_1}+\alpha_{e_2})+\hat{\phi}^{(e_1e_2)}}{\hat{\psi}_{e_1}(\alpha_{e_1}+\alpha_{e_2})+\hat{\psi}^{(e_1e_2)}}\right)}{\left(\hat{\psi}_{e_1}(\alpha_{e_1} + \alpha_{e_2}) + \hat{\psi}^{(e_1e_2)}\right)^{\lambda+1+2\lambda N_-}} \tag{2.77}$$

[2] At the beginning of this chapter we noted that we always split edges that do not have such a weight into two parallel edges and use the resulting graph for our graphical functions. For such a case this proposition simply states that an n-fold multi-edge with $n > 2$ is equivalent to a double edge.

A change of coordinates

$$\begin{aligned}\alpha_{e_1} &\to \alpha t\\ \alpha_{e_2} &\to \alpha(1-t)\end{aligned}$$

gives

$$\begin{aligned}&\int_0^\infty \mathrm{d}\alpha_{e_1}\int_0^\infty \mathrm{d}\alpha_{e_2}\alpha_{e_1}^{\lambda\nu_{e_1}-1}\alpha_{e_2}^{\lambda\nu_{e_2}-1}f(\alpha_{e_1}+\alpha_{e_2})\\ &\quad=\int_0^\infty \mathrm{d}\alpha\ \alpha^{\lambda(\nu_{e_1}+\nu_{e_2})-1}f(\alpha)\int_0^1 \mathrm{d}t\ t^{\lambda\nu_{e_1}-1}(1-t)^{\lambda\nu_{e_2}-1}\end{aligned}\tag{2.78}$$

The t integration is now exactly the Euler-Beta-function

$$\frac{\Gamma(a)\Gamma(b)}{\Gamma(a+b)}=\mathrm{B}(a,b)=\int_0^1 \mathrm{d}x\ x^{a-1}(1-x)^{b-1}\tag{2.79}$$

which exists for $\mathrm{Re}\,a,\mathrm{Re}\,b>0$. This is the case for $\lambda\nu_{e_1}$ and $\lambda\nu_{e_2}$, so

$$\begin{aligned}&\frac{1}{\Gamma(\lambda\nu_{e_1})\Gamma(\lambda\nu_{e_2})}\int_0^\infty \mathrm{d}\alpha_{e_1}\int_0^\infty \mathrm{d}\alpha_{e_2}\alpha_{e_1}^{\lambda\nu_{e_1}-1}\alpha_{e_2}^{\lambda\nu_{e_2}-1}f(\alpha_{e_1}+\alpha_{e_2})\\ &\quad=\frac{1}{\Gamma(\lambda\nu_{e_1}+\lambda\nu_{e_2})}\int_0^\infty \mathrm{d}\alpha\ \alpha^{\lambda(\nu_{e_1}+\nu_{e_2})}f(\alpha)\end{aligned}\tag{2.80}$$

and after appropriate renaming of α, this is exactly what one would expect in $f^{(\lambda)}_{G'}(z)$.

(c) $e_1\in E_-, e_2\in E_+, \mathrm{Re}\,\nu_{e_2}>|\nu_{e_1}|$:
Here one has both, a partial integral and a differentiation. Since the merged edge would still have positive real part, the integration has to remain but the weight of the corresponding edge has to be changed due to the differentiation. Due to case (a) we can assume without loss of generality that $\lambda\nu_{e_1}=-1$. Let $f(\alpha_{e_1}+\alpha_{e_2})$ be as above and denote the polynomials corresponding to G' with primed variables. Then, using again (2.73),

$$\begin{aligned}&\frac{-1}{\Gamma(\lambda\nu_{e_2})}\int_0^\infty \frac{\mathrm{d}\alpha_{e_2}}{\alpha_{e_2}^{1-\lambda\nu_{e_2}}}\left.\frac{\partial}{\partial\alpha_{e_1}}\right|_{\alpha_{e_1}=0} f(\alpha_{e_1}+\alpha_{e_2})\\ &\quad=\frac{1}{\Gamma(\lambda\nu_{e_2})}\int_0^\infty \mathrm{d}\alpha_{e_2}\frac{\hat\phi_{e_1}\hat\psi^{(e_1)}-\hat\phi^{(e_1)}\hat\psi_{e_1}+(\lambda+1)\hat\psi_{e_1}\hat\psi^{(e_1)}}{(\hat\psi^{(e_1)})^2}\cdot\frac{f(\alpha_{e_2})}{\alpha_{e_2}^{1-\lambda\nu_{e_2}}}\\ &\quad=\frac{1}{\Gamma(\lambda\nu_{e_2})}\int_0^\infty \mathrm{d}\alpha_{e_2}\frac{\hat\phi'_{e_2}\hat\psi'-\hat\phi'\hat\psi'_{e_2}+(\lambda+1)\hat\Psi'_{e_2}\hat\psi'}{(\hat\psi')^2}\cdot\frac{f(\alpha_{e_2})}{\alpha_{e_2}^{1-\lambda\nu_{e_2}}}\\ &\quad=\frac{1}{\Gamma(\lambda\nu_{e_2})}\int_0^\infty \mathrm{d}\alpha_{e_2}\alpha_{e_2}^{\lambda\nu_{e_2}-1}\frac{\partial}{\partial\alpha_{e_2}}f(\alpha_{e_2})\\ &\quad=\frac{1}{\Gamma(\lambda\nu_{e_2}-1)}\int_0^\infty \mathrm{d}\alpha_{e_2}\alpha_{e_2}^{\lambda\nu_{e_2}-2}f(\alpha_{e_2})\end{aligned}\tag{2.81}$$

which is the correct partial integral from $f^{(\lambda)}_{G'}(z)$.

(d) $e_1\in E_-, e_2\in E_+, \lambda|\nu_{e_1}|>\lambda\nu_{e_2}\in\mathbb{Z}$:
Due to case (b) we can assume that $\lambda\nu_{e_2}=1$. Then one has

$$(-1)^{\lambda|\nu_{e_1}|}\int_0^\infty \mathrm{d}\alpha_{e_2}\left.\frac{\partial^{\lambda|\nu_{e_1}|}}{\partial\alpha_{e_1}^{\lambda|\nu_{e_1}|}}\right|_{\alpha_{e_1}=0} f(\alpha_{e_1}+\alpha_{e_2}).\tag{2.82}$$

Let

$$\tilde{f}(\alpha_{e_1}+\alpha_{e_2}) := \frac{\partial^{\lambda|\nu_{e_1}|-1}}{\partial\alpha_{e_1}^{\lambda|\nu_{e_1}|-1}} f(\alpha_{e_1}+\alpha_{e_2}), \tag{2.83}$$

such that we can use again the trick from case (c),

$$\frac{\partial}{\partial\alpha_{e_1}}\bigg|_{\alpha_{e_1}=0} \tilde{f}(\alpha_{e_1}+\alpha_{e_2}) = \frac{\partial}{\partial\alpha_{e_2}}\tilde{f}(\alpha_{e_1}+\alpha_{e_2})\bigg|_{\alpha_{e_1}=0} \tag{2.84}$$

and find

$$\begin{aligned}
(-1)^{\lambda|\nu_{e_1}|}\int_0^\infty \mathrm{d}\alpha_{e_2}\, \frac{\partial^{\lambda|\nu_{e_1}|}}{\partial\alpha_{e_1}^{\lambda|\nu_{e_1}|}}\bigg|_{\alpha_{e_1}=0} & f(\alpha_{e_1}+\alpha_{e_2}) \\
&= (-1)^{\lambda|\nu_{e_1}|}\int_0^\infty \mathrm{d}\alpha_{e_2}\frac{\partial}{\partial\alpha_{e_2}}\tilde{f}(\alpha_{e_2})\bigg|_{\alpha_{e_1}=0} \\
&= (-1)^{\lambda|\nu_{e_1}|}\left(\lim_{\alpha_{e_2}\to\infty}\tilde{f}(\alpha_{e_1}+\alpha_{e_2})-\tilde{f}(\alpha_{e_1})\right)_{\alpha_{e_1}=0} \\
&= (-1)^{\lambda|\nu_{e_1}|}\,\frac{\partial^{\lambda|\nu_{e_1}|}}{\partial\alpha_{e_1}^{\lambda|\nu_{e_1}|}}\bigg|_{\alpha_{e_1}=0} f(\alpha_{e_1})
\end{aligned} \tag{2.85}$$

which is the desired integrand for $f_{G'}^{(\lambda)}(z)$. The limit is evident when one observes that in the denominator α_{e_2} always occurs with a power that is by $\lambda+1$ larger than it can be in the numerator polynomial one gets from the differentiations and the exponential converges to a constant. □

2.3 Analytic Continuation

So far, graphical functions were always treated as functions

$$f_G^{(\lambda)} : \mathbb{R}^{D|Z|} \to \mathbb{C}. \tag{2.86}$$

In position space the z-dependence was possibly distributed over many quadrics and in differences of z_v and x_v vectors. In the parametric integral all z-dependence is contained in quadrics of the form $||z_i - z_j||^2 =: z_{ij} \in \mathbb{R}_+$, i.e. $f_G^{(\lambda)}$ is effectively not a function of $|Z|$ D-vectors but of $\binom{|Z|}{2}$ positive real numbers. This naturally leads to an analytic continuation to complex arguments as follows.

Definition 2.3.1. (Analytically continued graphical functions)
Let $f_G^{(\lambda)}(z) : \mathbb{R}^{D|Z|} \to \mathbb{C}$ be a graphical function as given by one of the formulae (2.43), (2.55) or (2.56). By replacing all positive real z_{ij} in the second graph polynomial with $z_{ij} \in \mathbb{C}$ we define the corresponding analytically continued graphical function (using the same notation)

$$f_G^{(\lambda)} : \mathbb{C}^n \setminus \Sigma \to \mathbb{C} \tag{2.87}$$

where $n = \binom{|Z|}{2}$ and Σ is the subset of $\mathbb{C}^n$ on which the analytic continuation does not exist.

Σ is the zero locus of a set of polynomials in the z_{ij}, i.e. the polynomials that remain in the denominator of the graphical function after integrating all variables α_i. It is a representation of a *Landau variety*, a hypersurface in $\mathbb{P}^1(\mathbb{C}) \times \ldots \times P^1(\mathbb{C})$ (n times), where each z_{ij} is a coordinate on its individual copy of the Riemann sphere. For detailed technical background we refer to the book [33] and the article [10]. The latter reference also contains explicit computations of Landau varieties in some small cases. In general, however, Landau varieties are immensely difficult to compute. In chapter 3, upper bounds for the Landau varieties of certain graphical functions are studied.

Remark 2.3.2. *For simplicity we will often relabel the arguments and corresponding spanning forest polynomials with a single index $i \in \{1, \ldots, n\}$ instead of the double index.*

2.3.1 Analyticity

To show analyticity of graphical functions in $z = (z_1, \ldots, z_n)$ we will make use of the following standard theorem:

Theorem 2.3.3. (Holomorphic parameter integrals)
Let $R \subset \mathbb{R}^m$ and $S \subset \mathbb{C}^n$ be domains with $m, n \in \mathbb{N}$. Furthermore be

$$I(\alpha, z) = I(\alpha_1, \ldots, \alpha_m, z_1, \ldots, z_n) : R \times S \to \mathbb{C} \tag{2.88}$$

a continuous function with the following properties:
(a) For every fixed $\alpha \in R$,

$$\iota(z) := I(\alpha, z) \tag{2.89}$$

is holomorphic for all $z \in S$.

(b) There is a continuous function $F(\alpha) : R \to [0, \infty)$ with

$$\int_R F(\alpha)\, \mathrm{d}\alpha < \infty \tag{2.90}$$

such that

$$|I(\alpha, z)| \leq F(\alpha) \text{ for all } (\alpha, z) \in R \times S. \tag{2.91}$$

Then the function

$$f(z) \ := \int_R I(\alpha, z)\, \mathrm{d}\alpha \tag{2.92}$$

is holomorphic in S.

Proof. The theorem can be proven by construction of a sequence of holomorphic functions which is then shown to converge to the desired function $f(z)$. See [34], p. 231 for details. □

We will now show that graphical functions satisfy the conditions of the above theorem if we demand positive real parts for all z_i. We restrict ourselves to the case of non-negative edge weights only. A more elaborate proof that includes negative edge weights will appear in [21].

Theorem 2.3.4. (Analyticity of graphical functions)
Let G be a graph in which all edge weights have positive real part (i.e. $E_- = \emptyset$), that satisfies the convergence conditions 1.3.3 such that its graphical function $f_G^{(\lambda)}(z)$ exists for $z \in \mathbb{R}^{D|Z|}$. Then its continuation is holomorphic in $\mathbb{C}_+^n$.

Proof. Take the exponential parametric version of the graphical function as in (2.43),

$$f_G^{(\lambda)}(z) = \frac{1}{\prod_{e\in E_+}\Gamma(\lambda\nu_e)}\left(\int_0^\infty \prod_{e\in E}\frac{\mathrm{d}\alpha_e}{\alpha_e^{1-\lambda\nu_e}}\right)\frac{\exp\left(-\frac{\hat{\Phi}}{\hat{\Psi}}\right)}{\hat{\Psi}^{\lambda+1}}. \tag{2.93}$$

Because $f_G^{(\lambda)}$ exists, there are $z_i^0 > 0,\ i = 1,\dots,n$ such that $f_G^{(\lambda)}(z^0) < \infty$. To satisfy condition (a) of theorem 2.3.3 we choose the domain of the complex parameters to be a strip with finite width along the real axis

$$S \coloneqq \{z \in \mathbb{C}_+^n \mid 0 < z_i^0 - l_i < \operatorname{Re} z_i < z_i^0 + L_i \quad \forall\ i = 1,\dots,n\}. \tag{2.94}$$

for fixed $l_i, L_i \in \mathbb{R}_+$ and $R = \mathbb{R}_+^{|E|}$ as the domain of the real integration variables. For (b) we need the following estimate. Let $A = \min\{z_i^0 - l_i \mid i = 1,\dots,n\}$ and set $\xi_A = \max\left\{\frac{z_i^0}{A} \mid i = 1,\dots,n\right\}$. Then we have

$$\hat{\Phi}(A) = \sum_{i=1}^n A\hat{\Phi}_i \geq \sum_{i=1}^n \frac{z_i^0}{\xi_A}\hat{\Phi}_i = \hat{\Phi}(z^0/\xi_A), \tag{2.95}$$

With this bound one has

$$\left(\int_0^\infty \prod_{e\in E}\frac{\mathrm{d}\alpha_e}{\alpha_e^{1-\lambda\nu_e}}\right)\frac{\exp\left(-\frac{\hat{\Phi}(A)}{\hat{\Psi}}\right)}{\hat{\Psi}^{\lambda+1}} \leq \left(\int_0^\infty \prod_{e\in E}\frac{\mathrm{d}\alpha_e}{\alpha_e^{1-\lambda\nu_e}}\right)\frac{\exp\left(-\frac{\hat{\Phi}(z^0/\xi_A)}{\hat{\Psi}}\right)}{\hat{\Psi}^{\lambda+1}} < \infty \tag{2.96}$$

where the integral on the right hand side exists because scaling each z_i^0 with ξ_A^{-1} corresponds to scaling each original variable vector from $\mathbb{R}^{D|Z|}$ with $\xi_A^{-1/2}$ and does not change the convergence behaviour. Furthermore,

$$\hat{\Phi}(A) \leq \operatorname{Re}\hat{\Phi}(z) \tag{2.97}$$

which means that the second condition

$$\begin{aligned}\left(\int_0^\infty \prod_{e\in E_+}\frac{\mathrm{d}\alpha_e}{\alpha_e^{1-\lambda\nu_e}}\right)\frac{\exp\left(-\frac{\hat{\Phi}(A)}{\hat{\Psi}}\right)}{\hat{\Psi}^{\lambda+1}} &\geq \left(\int_0^\infty \prod_{e\in E_+}\frac{\mathrm{d}\alpha_e}{\alpha_e^{1-\lambda\nu_e}}\right)\frac{\exp\left(-\frac{\operatorname{Re}\hat{\Phi}(z)}{\hat{\Psi}}\right)}{\hat{\Psi}^{\lambda+1}} \\ &= \left(\int_0^\infty \prod_{e\in E_+}\frac{\mathrm{d}\alpha_e}{\alpha_e^{1-\lambda\nu_e}}\right)\frac{\left|\exp\left(-\frac{\hat{\Phi}(z)}{\hat{\Psi}}\right)\right|}{\hat{\Psi}^{\lambda+1}} \\ &\geq \left|\left(\int_0^\infty \prod_{e\in E_+}\frac{\mathrm{d}\alpha_e}{\alpha_e^{1-\lambda\nu_e}}\right)\frac{\exp\left(-\frac{\hat{\Phi}(z)}{\hat{\Psi}}\right)}{\hat{\Psi}^{\lambda+1}}\right|\end{aligned} \tag{2.98}$$

is also fulfilled. Because l_i and L_i are arbitrary, $f_G^{(\lambda)}(z)$ is analytic in all of $\mathbb{C}_+^n$. □

2.4 The conformal parametrization

An especially interesting case of graphical functions is given by the set of external vertices $Z = \{0, 1, z\}$. The vertices can be parametrized as follows [37]:

$$\begin{aligned} 0 &\sim 0 \in \mathbb{R}^D \\ 1 &\sim v_1 = (1, 0, ..., 0) \in \mathbb{R}^D \\ z &\sim v_z = \left(\frac{z+\bar{z}}{2}, \frac{z-\bar{z}}{2i}, 0, ..., 0\right) \in \mathbb{R}^D \end{aligned} \tag{2.99}$$

The graphical function is now neither a function of D-vectors nor of $\binom{3}{2} = 3$ numbers z_{01}, z_{0z}, z_{1z} but only of the complex variable z and its complex conjugate $\bar{z}$ because the dependence on external vertices in $\hat{\Phi}$ is now

$$\begin{aligned} \hat{\Phi} &= \sum_{i \prec j \in Z} ||z_i - z_j||^2 \hat{\Phi}_{ij} \\ &= \hat{\Phi}_{1z}||v_z - v_1||^2 + \hat{\Phi}_{0z}||v_z - 0||^2 + \hat{\Phi}_{01}||v_1 - 0||^2 \\ &= \hat{\Phi}_{1z}(z-1)(\bar{z}-1) + \hat{\Phi}_{0z} z\bar{z} + \hat{\Phi}_{01}. \end{aligned} \tag{2.100}$$

The analytically continued graphical function arises naturally from treating z and $\bar{z}$ as independent variables instead of complex conjugates, which we will always do from now on. The complex conjugate, if needed, will be denoted by z^* to avoid confusion.

In this special case we immediately find a corollary to theorem 2.3.4:

Corollary 2.4.1. *If* $\operatorname{Re} z\bar{z} > 0$ *and* $\operatorname{Re}(z-1)(\bar{z}-1) > 0$*, then* $f_G^{(\lambda)}(z, \bar{z})$ *is analytic in* z *and* $\bar{z}$*. In particular,* $f_G^{(\lambda)}(z, z^*)$ *is real analytic in* $\mathbb{C} \setminus \{0, 1\}$

Proof. The first part is true because for $z_{0z} = z\bar{z}$, $z_{1z} = (z-1)(\bar{z}-1)$, $z_{01} = 1$ $f_G^{(\lambda)}(z_{0z}, z_{1z}, z_{01})$ is analytic in $\mathbb{C}^3_+$ and the three complex variables z_{1z}, z_{0z} and z_{01} are themselves analytic functions in z and $\bar{z}$. The second part follows since $zz^* > 0 \; \forall \; z \neq 0$ and $(z-1)(z^*-1) > 0 \; \forall \; z \neq 1$. □

In the following sections we will discuss properties that are unique to graphical functions in this parametrization. Section 2.4.1 contains a new proof of a previously known identity. Both the result and the techniques of the proof are instrumental in section 2.4.2 where they will be used to prove a new identity between graphical functions of dual planar graphs.

Figure 2.2: The graphs G and G_z from theorem 2.4.2.

2.4.1 Appending an edge

In this section we give an alternative proof for an identity that relates the graphical functions of certain graphs via a differential equation. The original proof is due to Oliver Schnetz [37].

Theorem 2.4.2. (Appending an edge)
Let G, G_z be graphs such that their graphical functions exist and G_z is the graph G with an edge e_z with weight $\nu_{e_z} = 1$ appended to the external vertex z as in fig. 2.2, i.e. such that $G_z//\{\{\bullet, z\}\} = G$. Then[3],

$$f_G^{(\lambda)}(z) = -\Gamma(\lambda)\left(\partial_z\partial_{\bar{z}} - \frac{\lambda}{z-\bar{z}}(\partial_z - \partial_{\bar{z}})\right) f_{G_z}^{(\lambda)}(z). \tag{2.101}$$

Proof. Let α_{e_z} denote the appended edge's parameter and mark all remaining variables associated to G_z with a subscript z. Starting from the exponential parametric integral (2.43) it suffices to prove the case $E_-(G) = \emptyset$ because derivatives with respect to edge parameters can be exchanged with ∂_z and $\partial_{\bar{z}}$. For the graph polynomials of G_z one finds from the usual contraction-deletion relations (1.2.18) and observing how an appended edge affects trees and forests that they can be written as:

$$\begin{aligned}\hat{\Psi}_z &= \alpha_{e_z}\partial_{\alpha_{e_z}}\hat{\Psi}_z + \hat{\Psi}_z|_{\alpha_{e_z}=0} \\ &= \alpha_{e_z}\hat{\Psi} + \hat{\Phi}_{0z} + \hat{\Phi}_{1z}\end{aligned} \tag{2.102}$$

$$\begin{aligned}\hat{\Phi}_z &= \alpha_{e_z}\partial_{\alpha_{e_z}}\hat{\Phi}_z + \hat{\Phi}_z|_{\alpha_{e_z}=0} \\ &= \alpha_{e_z}\hat{\Phi} + \hat{\Psi}_G \\ &= \alpha_{e_z}(z\bar{z}\hat{\Phi}_{0z} + (z-1)(\bar{z}-1)\hat{\Phi}_{1z} + \hat{\Phi}_{01}) + \hat{\Psi}_G\end{aligned} \tag{2.103}$$

Some parts of that deserve a more detailed explanation. As we observed several times already, $\hat{\Psi}_z = \hat{\Phi}_{G_z}^{\{0\},\{1\},\{z\}}$. Setting α_{e_z} to zero corresponds to deleting all the spanning 3-forests of G_z that have the three external vertices in different trees and contain the edge e_z. In the remaining spanning 3-forests z is necessarily an isolated vertex, so the vertex that was z in G must be contained in one of the other two trees, i.e. it is connected to either 0 or 1. For the polynomials this means

$$\hat{\Psi}_z|_{\alpha_{e_z}=0} = \hat{\Phi}_{0z} + \hat{\Phi}_{1z} \tag{2.104}$$

as above. In $\hat{\Phi}_z$, setting α_{e_z} to zero only leaves spanning 2-forests of G_z that do not contain e_z. Seen instead as subgraphs of G they are the spanning trees, so $\hat{\Phi}_z|_{\alpha_{e_z}=0} = \hat{\Psi}_G$.

The appended edge corresponds to an integration

$$\frac{1}{\Gamma(\lambda)}\int_0^\infty \mathrm{d}\alpha_{e_z}\alpha_{e_z}^{\lambda\nu_{e_z}-1}\frac{\exp\left(-\frac{\hat{\Phi}_z}{\hat{\Psi}_z}\right)}{\hat{\Psi}_z^{\lambda+1}}. \tag{2.105}$$

[3] In [37], the identity was formulated as $f_G^{(\lambda)}(z) = -\Gamma(\lambda)\left(\frac{1}{(z-\bar{z})^\lambda}\partial_z\partial_{\bar{z}}(z-\bar{z})^\lambda + \frac{\lambda(\lambda-1)}{(z-\bar{z})^2}\right) f_{G_z}^{(\lambda)}(z)$. Here we prefer a shorter but equivalent version.

Applying $\left(\partial_z\partial_{\bar{z}} - \frac{\lambda}{z-\bar{z}}(\partial_z - \partial_{\bar{z}})\right)$ to the $z, \bar{z}$ dependent part gives

$$\begin{aligned}
&\left(\partial_z\partial_{\bar{z}} - \frac{\lambda}{z-\bar{z}}(\partial_z - \partial_{\bar{z}})\right) \exp\left(-\frac{\alpha_{e_z}(z\bar{z}\hat{\Phi}_{0z} + (z-1)(\bar{z}-1)\hat{\Phi}_{1z} + \hat{\Phi}_{01}) + \hat{\Psi}_G}{\hat{\Psi}_z}\right) \\
&\quad = \alpha_{e_z}\hat{\Psi}_z^{-2}\left(\alpha_{e_z} z\bar{z}\hat{\Phi}_{0z}(\hat{\Phi}_{0z} + \hat{\Phi}_{1z}) + \alpha_{e_z}(z\bar{z} - z - \bar{z})\hat{\Phi}_{1z}(\hat{\Phi}_{0z} + \hat{\Phi}_{1z})\right. \\
&\qquad \left. -(\lambda+1)(\hat{\Phi}_{0z} + \hat{\Phi}_{1z})\hat{\Psi}_z + \alpha_{e_z}\hat{\Phi}_{1z}^2\right) \exp\left(-\frac{\hat{\Phi}_z}{\hat{\Psi}_z}\right). \qquad (2.106)
\end{aligned}$$

A tedious computation best left to a computer then shows that the full integrand can be written as

$$\begin{aligned}
&\left(\partial_z\partial_{\bar{z}} - \frac{\lambda}{z-\bar{z}}(\partial_z - \partial_{\bar{z}})\right)\alpha_{e_z}^{\lambda\nu_{e_z}-1}\frac{\exp\left(-\frac{\hat{\Phi}_z}{\hat{\Psi}_z}\right)}{\hat{\Psi}^{\lambda+1}} \\
&\quad = \alpha_{e_z}^{\lambda\nu_{e_z}}\left(\alpha_{e_z} z\bar{z}\hat{\Phi}_{0z}(\hat{\Phi}_{0z} + \hat{\Phi}_{1z}) + \alpha_{e_z}(z\bar{z} - z - \bar{z})\hat{\Phi}_{1z}(\hat{\Phi}_{0z} + \hat{\Phi}_{1z})\right. \\
&\qquad \left. -(\lambda+1)(\hat{\Phi}_{0z} + \hat{\Phi}_{1z})\hat{\Psi}_z + \alpha_{e_z}\hat{\Phi}_{1z}^2\right)\frac{\exp\left(-\frac{\hat{\Phi}_z}{\hat{\Psi}_z}\right)}{\hat{\Psi}^{\lambda+3}} \\
&\quad = -\alpha_{e_z}^{\lambda(\nu_{e_z}-1)}\left(\partial_{\alpha_{e_z}}\left(\alpha_{e_z}^{\lambda+1}\frac{\exp\left(-\frac{\hat{\Phi}_z}{\hat{\Psi}_z}\right)}{\hat{\Psi}^{\lambda+1}}\right)\right. \\
&\qquad \left. -\alpha_{e_z}(\hat{\Phi}_{0z}\hat{\Phi}_{1z} + \hat{\Phi}_{0z}\hat{\Phi}_{01} + \hat{\Phi}_{1z}\hat{\Phi}_{01} - \hat{\Psi}\hat{\Psi}_G)\frac{\exp\left(-\frac{\hat{\Phi}_z}{\hat{\Psi}_z}\right)}{\hat{\Psi}^{\lambda+3}}\right) \qquad (2.107)
\end{aligned}$$

With the identity ([15], proposition 22)

$$\hat{\Phi}_{0z}\hat{\Phi}_{1z} + \hat{\Phi}_{0z}\hat{\Phi}_{01} + \hat{\Phi}_{1z}\hat{\Phi}_{01} = \hat{\Psi}\hat{\Psi}_G \qquad (2.108)$$

which is essentially the Dodgson identity formulated in terms of spanning forest polynomials[4], we see that only the term which is a partial derivative in the new edge variable remains. This allows evaluation of the integral

$$\begin{aligned}
&\int_0^\infty \mathrm{d}\alpha_{e_z}\alpha_{e_z}^{\lambda(\nu_{e_z}-1)}\partial_{\alpha_{e_z}}\left(\alpha_{e_z}^{\lambda+1}\frac{\exp\left(-\frac{\hat{\Phi}_z}{\hat{\Psi}_z}\right)}{\hat{\Psi}^{\lambda+1}}\right) \\
&\quad = \frac{\alpha_{e_z}^{\lambda+1}}{(\alpha_{e_z}\hat{\Psi} + \hat{\Phi}_{0z} + \hat{\Phi}_{1z})^{\lambda+1}}\exp\left(-\frac{\alpha_{e_z}(z\bar{z}\hat{\Phi}_{0z} + (z-1)(\bar{z}-1)\hat{\Phi}_{1z} + \hat{\Phi}_{01}) + \hat{\Psi}_G}{\alpha_{e_z}\hat{\Psi} + \hat{\Phi}_{0z} + \hat{\Phi}_{1z}}\right)\Bigg|_0^\infty \\
&\quad = -\frac{\exp\left(-\frac{\hat{\Phi}}{\hat{\Psi}}\right)}{\hat{\Psi}^{\lambda+1}}. \qquad (2.109)
\end{aligned}$$

Including the factor -1 from eq. (2.107) and the factor $\Gamma(\lambda\nu_{e_z}) = \Gamma(\lambda)$ from eq. (2.105) proves the statement. □

[4]In [15] the identity was formulated for spanning forest polynomials. It is clear that it also holds for dual spanning forest polynomials.

2.4.2 Fourier identity

We will prove an identity on graphical functions of a certain class of graphs - planar graphs, that are dual to each other. The name stems from the theory of Feynman integrals, where the Fourier transform of a momentum space integral of a planar graph gives the position space integral of a dual graph (cf. the ladder box graph from fig. 1.10). In the parametric analog something similar but somewhat more convenient happens. Cremona transforms take the place of Fourier transforms when going from parametric to dual parametric space or vice versa. Such a transformation effectively replaces the graph polynomials in the integrand by their complements, which, by Tutte's observation [40] already mentioned in the proof of theorem 1.2.21, are exactly the graph polynomials of the dual graph.

For the case $\lambda = 1$ it was previously proved by O. Schnetz [38] using position and momentum space methods. Here we will give a proof for general positive half-integer λ in the parametric representation which mainly uses identities on graphs and their associated polynomials as well as the above identity for graphs with an appended edge.

Before stating the main theorem of this section we need a lemma to establish two simple facts about planar graphs and their graphical functions.

Lemma 2.4.3. *Let G be a planar graph with only positive weights such that $f_G^{(\lambda)}$ and $f_{G^*}^{(\lambda)}$ exist, and $Y = Y(G) = \lambda N(G) - (\lambda+1)|X(G)|$, $Y^* = Y(G^*)$. Then*

$$\textit{(i)}\ Y + Y^* = 2(\lambda+1),$$

$$\textit{(ii)}\ Y, Y^* > 0.$$

Proof. The first fact follows from the definition of the edge weights in the dual graph $\lambda\nu_{e^*} = \lambda(1-\nu_e)+1$ (which in turn was chosen that way because one wants both weights positive *and* $\lambda\nu_e, \lambda\nu_{e^*} < \lambda+1$ for UV convergence) applied to the sum of all edges

$$\lambda N^* = \sum_{e^*} \lambda\nu_{e^*} = \sum_{e} (\lambda(1-\nu_e)+1) = -\lambda N + (\lambda+1)|E| \tag{2.110}$$

together with Euler's formula for planar graphs (where internal vertices of G^* are internal faces of G and the 'outside' of the graph counts as one additional face)

$$|X^*| = |E| - |X| - 2. \tag{2.111}$$

Inserting both into the formula for $Y^* = Y(G^*)$ gives

$$\begin{aligned} Y^* &= \lambda N^* - (\lambda+1)|X^*| \\ &= -\lambda N + (\lambda+1)|E| - (\lambda+1)(|E| - |X| - 2) \\ &= -Y + 2(\lambda+1). \end{aligned} \tag{2.112}$$

Lastly, the second claim follows from the convergence conditions. Take the IR condition

$$(D-2)N(g) > D|X(g)|, \tag{2.113}$$

which has to hold for all subgraphs $g \subseteq G$ (G^*) and consider the case $g = G$ (G^*). Substituting $D = 2\lambda + 2$ and dividing by 2 directly gives

$$0 < \lambda N - |X|(\lambda + 1) = Y \tag{2.114}$$

and Y^* analogously. □

Theorem 2.4.4. (Fourier identity)
Let G be a planar graph with three external vertices labeled $0, 1$ and z, weights such that $0 < \lambda\nu_e < \lambda + 1$ for all edges $e \in E$, $\lambda \in \frac{1}{2}\mathbb{N}$, $f_G(z)$ and $f_{G^*}(z)$ exist, and Y and Y^* are positive integers. Then

$$f_G^{(\lambda)}(z) = \frac{\Gamma(\lambda+1)\prod_{e^*\in E^*}\Gamma(\lambda\nu_{e^*})}{\Gamma(Y^*)\prod_{e\in E}\Gamma(\lambda\nu_e)}\left(\frac{\lambda}{z-\bar{z}}(\partial_z - \partial_{\bar{z}}) - \partial_z\partial_{\bar{z}}\right)^{Y-\lambda-1} f_{G^*}^{(\lambda)}(z) \tag{2.115}$$

if $Y^* \leq Y$, and

$$f_{G^*}^{(\lambda)}(z) = \frac{\Gamma(\lambda+1)\prod_{e\in E}\Gamma(\lambda\nu_e)}{\Gamma(Y)\prod_{e^*\in E^*}\Gamma(\lambda\nu_{e^*})}\left(\frac{\lambda}{z-\bar{z}}(\partial_z - \partial_{\bar{z}}) - \partial_z\partial_{\bar{z}}\right)^{Y^*-\lambda-1} f_G^{(\lambda)}(z) \tag{2.116}$$

if $Y^* \geq Y$.

Proof. First we prove the case $Y = \lambda + 1 = Y^*$, i.e. we prove that

$$\frac{\Gamma(Y)}{\prod_{e\in E}\Gamma(\lambda\nu_e)}\int_{\Delta_{\mathbb{P}}}\frac{\prod_e \alpha_e^{\lambda\nu_e-1}}{\Phi_G^{\lambda+1}}\Omega = \frac{\Gamma(Y^*)}{\prod_{e^*\in E^*}\Gamma(\lambda\nu_{e^*})}\int_{\Delta_{\mathbb{P}}}\frac{\prod_{e^*}\alpha_{e^*}^{\lambda\nu_{e^*}-1}}{\Phi_{G^*}^{\lambda+1}}\Omega. \tag{2.117}$$

The prefactors are already part of the identity. What remains to be shown is the relation between the integrals. An inversion of all parameters turns the projective volume form into

$$\Omega = \sum_e (-1)^{e-1}\alpha_e \mathrm{d}\alpha_1 ... \widehat{\mathrm{d}\alpha_e} ... \mathrm{d}\alpha_{|E|}$$

$$\to \sum_e (-1)^{e-1}\frac{1}{\alpha_e}\frac{-\mathrm{d}\alpha_1}{\alpha_1^2}\wedge ... \wedge \frac{-\widehat{\mathrm{d}\alpha_e}}{\alpha_e^2}\wedge ... \wedge \frac{-\mathrm{d}\alpha_{|E|}}{\alpha_{|E|}} = (-1)^{|E|-1}\frac{\Omega}{(\prod_e \alpha_e)^2}. \tag{2.118}$$

The sign that one picks up if $|E|$ even is canceled by the orientation reversal of $\Delta_{\mathbb{P}}$ in that case.[5] Thence such a Cremona transformation applied to the integral on the

[5] In the special case of the affine integral, where one sets one parameter to 1 this is rather obvious, since $\Delta_{\mathbb{P}}$ is then just $\mathbb{R}_+^{|E|-1}$ and one gets the correct sign because one has to change the integration boundaries after the Cremona transformation, i.e. one gets $|E|-1$ times a -1 from $\int_\infty^0 \ldots = -\int_0^\infty \ldots$. For the abstract projective case the argument is more difficult. For $|E|$ odd, $\Delta_{\mathbb{P}}$ has even dimension and is therefore not orientable (see e.g. [26], ch. 13). If $|E|$ is even, one can consider the $(|E|-1)$-sphere $S^{|E|-1}$ which is orientable if and only if $|E|-1$ is odd. For the sphere one can explicitly check that the Cremona transformation reverses the orientation (e.g. in the charts given by the stereographic projection). Then one can construct $\mathbb{P}^{|E|-1}(\mathbb{R})$ from the sphere by identification of antipodal points and go further to $\Delta_{\mathbb{P}}$ by restricting to positive values of the homogenous coordinates, neither of which changes the orientation behavior one found for the sphere.

left hand side of eq. (2.117) gives

$$\left(\prod_{e\in E}\Gamma(\lambda\nu_e)\right) f_G^{(\lambda)}(z) = \int_{\Delta_{\mathbb{P}}} \frac{\prod_e \alpha_e^{\lambda\nu_e-1}}{\Phi_G^{\lambda+1}}\Omega = \int_{\Delta_{\mathbb{P}}} \frac{\prod_e \alpha_e^{1-\lambda\nu_e}}{(\prod_e \alpha_e)^2\Phi_G^{\lambda+1}(\alpha_1^{-1},\cdots,\alpha_{|E|}^{-1})}\Omega$$

$$= \int_{\Delta_{\mathbb{P}}} \frac{\prod_e \alpha_e^{\lambda(1-\nu_e)}}{(\prod_e \alpha_e)^{\lambda+1}\Phi_G^{\lambda+1}(\alpha_1^{-1},\cdots,\alpha_{|E|}^{-1})}\Omega$$

$$\overset{\text{corollary 1.2.22}}{=} \int_{\Delta_{\mathbb{P}}} \frac{\prod_{e^*} \alpha_{e^*}^{\lambda\nu_{e^*}-1}}{\Phi_{G^*}^{\lambda+1}}\Omega$$

$$= \left(\prod_{e^*\in E^*}\Gamma(\lambda\nu_{e^*})\right) f_{G^*}^{(\lambda)}(z), \tag{2.119}$$

Now we prove the other cases. Due to the symmetry under exchange of G and G^* it suffices to prove the cases $Y > Y^*$. From lemma 2.4.3 we know that

$$1 \leq Y, Y^* \leq 2\lambda + 1 \tag{2.120}$$

and $Y + Y^* = 2(\lambda + 1)$. Consider the pair $(Y = \lambda + 1 + n, Y^* = \lambda + 1 - n)$ for any $n \in \{1, \ldots, \lambda\}$. By inserting n trivial edges with weight $1/\lambda$ between 0^* and 1^* in G^* we can turn it into a graph $G^*_{01^n}$ such that $Y^*_{01^n} := Y(G^*_{01^n}) = \lambda + 1$. The new graph $G^*_{01^n}$ is still planar and has a dual graph. Moreover, from the construction of the dual graphs (see definition 1.2.7 and remark 1.2.8) one finds that this dual graph is in fact G_{z^n}, the graph G on which an edge was appended as in the previous section n times (cf. fig. 2.3). That means we have so far

$$f_{G^*}^{(\lambda)}(z) = \frac{\Gamma(Y^*)}{\Gamma(Y^*_{01^n})} f^{(\lambda)}_{G^*_{01^n}}(z) = \frac{\Gamma(Y^*)}{\Gamma(\lambda+1)} \frac{\Gamma(\lambda)^n \prod_{e\in E}\Gamma(\lambda\nu_e)}{\prod_{e^*\in E^*}\Gamma(\lambda\nu_{e^*})} f^{(\lambda)}_{G_{z^n}}(z) \tag{2.121}$$

where E and E^* denote the edge sets of G and G^* respectively. The gamma factors of the trivial edges only contribute $\Gamma(\lambda\frac{1}{\lambda}) = 1$ for each edge and the gamma factors of the appended edges are written separately as $\Gamma(\lambda)^n$. Now we apply the differential operator of the appending an edge identity 2.4.2 n times and find

$$\left(-\Gamma(\lambda)\left(\partial_z\partial_{\bar{z}} - \frac{\lambda}{z-\bar{z}}(\partial_z - \partial_{\bar{z}})\right)\right)^n f_{G^*}^{(\lambda)}(z) = \frac{\Gamma(Y^*)}{\Gamma(\lambda+1)} \frac{\Gamma(\lambda)^n \prod_{e\in E}\Gamma(\lambda\nu_e)}{\prod_{e^*\in E^*}\Gamma(\lambda\nu_{e^*})} f_G^{(\lambda)}. \tag{2.122}$$

which, after canceling $\Gamma(\lambda)^n$ on both sides and bringing all other gamma factors on the left-hand side, proves the statement.

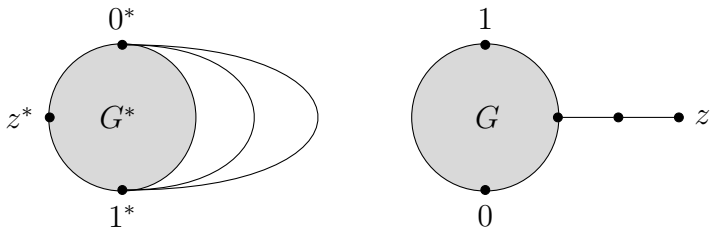

Figure 2.3: Illustration showing how multiple inserted trivial edges in G^* correspond to successively appended edges in G.

□

Chapter 3

Computational aspects

In this chapter we turn our backs on the general analytic considerations of the preceding chapter and instead focus on the question what insights can be gained from concrete computations via computer algebra. There are two main directions to explore. The first is the establishment of a database, collecting properties of as many graphical functions as possible. This is done in the hope that it will help gain intuition and fuel and direct future research into graphical functions. The other option is to concentrate all computing power on a few graphical functions that are - for reasons to be discussed below - especially interesting.

The computations in this chapter were performed using `Maple`[1] [1] and Erik Panzer's `Maple` implemented program `HyperInt` [29].

Conventions. Graphical functions as treated so far are quite general objects. For the remainder of this chapter we will use the following constraints to reduce the number of graphical functions to a manageable amount and concentrate on cases that have immediate applications.

1. Constraints that give conformal 4-point functions and ϕ_4^4-periods:
   (a) space time dimension $D = 4 \Leftrightarrow \lambda = 1$
   (b) external vertices $Z = \{0, 1, z\}$
   (c) conformal parametrization $z_{01} = 1$, $z_{0z} = z\bar{z}$, $z_{1z} = (z-1)(\bar{z}-1)$
   (d) all internal vertices 4-valent: $\nu(v) = 4 \; \forall \; v \in X$
   (e) edge weight only $+1$ ('propagator') or -1 ('inverse propagator')
2. Constraints that reduce the number of graphical functions by known identities and symmetries:
   (a) all external vertices are at least 2-valent: $\nu(v) \geq 2 \; \forall \; v \in Z$
   (see 'appending an edge', section 2.4.1)
   (b) use only one of the 24 graphs that are related via permutation of external vertices when completed (see 'completion', section 1.3.1)

[1] `Maple`™ is a trademark of Waterloo Maple Inc.

3.1 Graph generation

In order to investigate them, one first has to generate an exhaustive list of all graphical functions that fulfill the restrictions mentioned above. This was done with a python script based on Michael Borinsky's Feynman graph generator `feyngen` [6] which in turn makes use of the graph theoretical tools in Brendan McKay's `nauty` [27]. The script works as follows

1. Generate all graphs with a given number of vertices as lists of edges, where edges are sets (propagators) or lists (inverse propagators) of two vertices.
2. Assign external vertices, including '∞' and permutations.
3. Check constraints (vertex valence) and convergence conditions.
4. Complete the graphs that remain after step 3.
5. Check if the graph or a graph that is the same up to permutation of $(0, 1, z, \infty)$ is already in the list of graphical functions. If not, add the graph to the list.

The script takes the total number of vertices ($0, 1, z, \infty$ + internal vertices) as input and returns a list of all completed graphs with convergent graphical functions with that number of vertices that satisfy the above constraints. For 6 and less vertices there are no such graphs. The results for 7-10 vertices are discussed below. For 11 and more vertices we have not yet created a list on the one hand due to the considerable amount of time the program needs for such large graphs on the other hand because there is at the time of this writing no use for such graphical functions in practical calculations. Already the 10-vertex graphical functions are both too numerous and too complicated to treat with currently available programs and computers.

Grouping according to inverse propagator structure. We will classify graphs into three different sets, the criterion being the occurrence and position of inverse propagators. Type 1 graphs have no inverse propagators anywhere, type 2 consists of graphs that have inverse propagators, but *only* between internal vertices. Graphs of the third type have at least one inverse propagator between an internal and an external vertex and may additionally have them between internal vertices.
The reason for this categorization of graphs into three groups is the fact that inverse propagators produce huge polynomials in the numerators of the integrands. In the first type there are no inverse propagators, so these are typically the easiest to handle. The graphs from the second and third type are the more complicated, because more inverse propagators also means that the graph can have more edges in total while still giving a convergent graphical function and in the case of the third type also because the numerator structure now explicitly depends on z.

Having generated the graphs, one can then - among other things that we will do - check if they are *linearly reducible*. What that means will be explained in the following section.

3.2 Linear Reducibility

Let

$$I_G = \int_{\mathbb{R}_+^n} \frac{1}{P_G^2} \prod_{i=1}^{n} \mathrm{d}\alpha_i \tag{3.1}$$

be a convergent integral over some graph polynomial P_G (typically the Kirchhoff polynomial) in variables $\alpha_1, \ldots, \alpha_n$. We say that the integral ($\Leftrightarrow$ polynomial $\Leftrightarrow$ graph) is *linearly reducible* if there exists an order of integration $\alpha_{i_1}, \ldots, \alpha_{i_n}$ such that at each integration step the denominator of the integrand factors into products of polynomials that are linear in the next variable. The significance of this concept is that such integrals can be evaluated step by step in terms of hyperlogarithms and eventually result in multiple zeta values or MPLs at roots of unity.

The notion of linear reducibility was introduced by Brown [10]. In the same article he also gave the so far only sufficient combinatorial criterion for a graph to be linearly reducible, which sadly cannot be further strengthened due to the existence of counter examples but still applies to an infinite family of graphs. Furthermore he devised an efficient algorithm to check if a polynomial is reducible. A worked out example of both reduction algorithm and integration via hyperlogarithms applied to the wheel with three spokes can be found in [8] and, together with some more elementary explanations, also in [20].

Reduction algorithm and hyperlogarithm integration are both implemented in (and in the case of the latter even the main task and naming inspiration of) `HyperInt`.

3.2.1 Application to graphical functions.

Let G be a graph (for simplicity with edge weights $\nu_e = +1$ for all $e \in E$) such that the graphical function $f_G^{(1)} \equiv f_G$ exists. Then the affine integral representation of f_G (see eq. (2.55)) is

$$f_G(z) = \Gamma(Y) \int_0^\infty \frac{\mathrm{d}\alpha_2 \ldots \mathrm{d}\alpha_{|E|}}{\hat{\phi}^Y \ \hat{\psi}^{2-Y}\Big|_{\alpha_1=1}}.$$

We will illustrate the typical steps in checking such a graphical function for linear reducibility by an example.

Example 3.2.1.

Let G be the graph (again dismissing the two inverse propagators $e_{z\infty}$and e_{01} that its completed version would have right from the start)

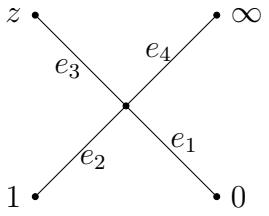

Then its graphical function is (using the projective integral for now and only later deciding which variable to set to 1)

$$f_G(z) = \int_{\Delta_{\mathbb{P}}} \frac{\Omega}{(z\bar{z}\alpha_1\alpha_3 + (z-1)(\bar{z}-1)\alpha_2\alpha_3 + \alpha_1\alpha_2)(\alpha_1+\alpha_2+\alpha_3)}. \tag{3.2}$$

Reduction. Now one can use the `HyperInt` functions `cgReduction`, which computes the reductions, and `reductionInfo`, which gives an overview over the result of the reduction, to check for reducibility. Concretely, the output of `reductionInfo` in this example is

After 1 variables: minimum 4 polynomials
$$\{\{x[2]\},\{x[3]\}\}$$
After 2 variables: minimum 3 polynomials
$$\{\{x[1],x[2]\},\{x[1],x[3]\},\{x[2],x[3]\}\}$$
After 3 variables: minimum 3 polynomials
$$\{\{x[1],x[2],x[3]\}\}$$

where $x[i] \leftrightarrow \alpha_i$. The first line is particularly interesting here, because it indicates that one might have a problem when the integration order begins with α_1. Actually finding a working integration order is then a matter of trial and error informed by the data one can gather from this output[2]. Furthermore it indicates the minimum number of polynomials that will appear after integrating a certain number of variables. This is useful to see if a working integration order that one has found is already optimal or if there might be more efficient integration orders in the sense that they produce less polynomials in intermediate results.

Finding integration orders. Suppose we have somehow found an order of integration that we suspect might work. Now we can use another `HyperInt` function called `checkIntegrationOrder`. Say we want to try the order $\alpha_1, \alpha_2, \alpha_3$. We noticed above that an integration starting with α_1 will most likely be problematic and lo and behold, `checkIntegrationOrder` returns

1. $x[1]$: 2 polynomials, 2 dependent
Error, (in checkIntegrationOrder) Not linear in $x[2]$.

However, in this case all integration orders starting with either α_2 or α_3 will work. Curiously, the order $\alpha_1, \alpha_3, \alpha_2$ will also work, because we set the last variable to 1 in the affine integral. The quadratic terms in α_2 then simply vanish and one finds

1. $x[1]$: 2 polynomials, 2 dependent
2. $x[3]$: 6 polynomials, 4 dependent
Final polynomials
$$\{-1+z,-1+zz,-zz+z\}$$

where $zz \leftrightarrow \bar{z}$. The first two lines contain information about the total number of polynomials in the integrand in each integration step and how many of them actually

[2]For larger graphs with more variables the output does not contain all possible combinations of variables at each step, as it does in this simple example after two and three variables. Which variables occur in such sets gives valuable hints regarding possibly working integration orders.

depend on the next variable, e.g. in the first step there are the two polynomials $\hat{\phi}$ and $\hat{\psi}$ and both depend on α_1 . This can be compared with the minimum number of polynomials from the `reductionInfo` output to judge efficiency of an integration order.

The last line indicates that the denominator of the final integration result will *at most* be a product of z, $\bar{z}$, $z-1$, $\bar{z}-1$ and $z-\bar{z}$ (the single z and $\bar{z}$ are never written explicitly in the output). Consequently, one already knows where the graphical function will at most have singularities without having to do a single integration. While these final polynomials may be more complicated for larger graphs (see section 3.3.1), all graphical functions checked so far are only singular on

$$L = \{(z, \bar{z}) \in \mathbb{C}^2 \mid z\bar{z} = 0 \text{ or } (z-1)(\bar{z}-1) = 0\}. \tag{3.3}$$

which leads to the suspicion that this might be the case in general. A proof however currently seems to be out of reach.

Remark 3.2.2. *It has to be emphasized that the reduction algorithm only makes positive statements about linear reducibility. Even if the reduction does not find an integration order such that at each step there is a suitable variable, an adequate change of variables may change that [30]. However, this has to be done on a case by case basis and is not further pursued in this thesis.*

Another caveat has to be added regarding linearly reducibility of graphical functions in different permutations of $(0, 1, z, \infty)$*. Due to the large number of graphical functions at higher number of vertices, each graph was only checked for reducibility in the four cases that change the position of the* ∞ *vertex, i.e.* $(0, 1, \infty, z)$*,* $(0, 1, z, \infty)$*,* $(0, \infty, 1, z)$ *and* $(\infty, 1, 0, z)$*. These four were chosen because all edges connected to* ∞ *are removed from the graph and moving* ∞ *therefore often changes the structure of the graph immensely. It is in principle possible that permuting one of the three other vertices changes linearly reducibility, but this seems to be a negligible effect and we believe that very few if any linearly reducible graphical functions (of those that can be found with the algorithm) were overlooked by discarding the other 20 permutations. For comparison, of the 88 linearly reducible 9 vertex graphical functions that were found (see below) 59 were found in the first permutation. The second, third and fourth then gave 16, 8 and 5 more respectively, all of which became reducible because the structure of the graph was significantly modified by moving* ∞ *(by far the most common case being a reduction of the total number of edges).*

3.3 Results

7 vertices. At 7 vertices there are a total of 7 graphical functions of which 5 were previously found by hand [38]. Their graphs are drawn in figure 3.1. All seven graphs are linearly reducible. One of the two new functions (bottom left in fig. 3.1) was successfully computed with Panzer's `HyperInt` and added to Schnetz's list of graphical functions. Due to its inverse propagators, the other new graphical function (bottom right in fig. 3.1) produces such a large polynomial η in the numerator that direct computation is for now not possible.

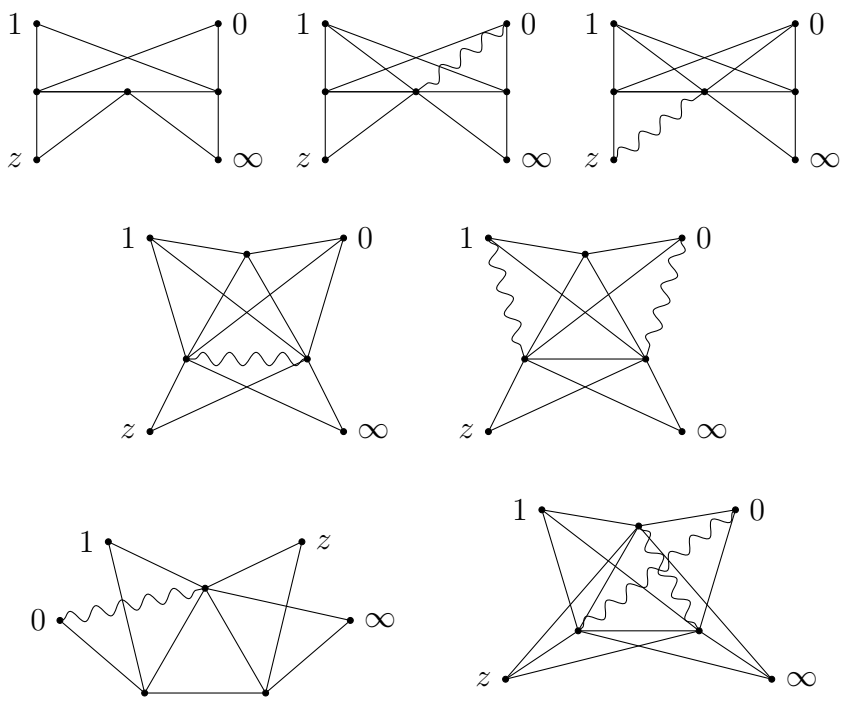

Figure 3.1: The seven 7-vertex graphs that have convergent graphical functions and satisfy the constraints of chapter 3. Edges between external vertices are not drawn. The specific permutation of $(0, 1, z, \infty)$ drawn here was randomly chosen. The two graphs in the bottom row were previously overlooked.

8 vertices. In the case of 8 vertices the script confirmed a list of 19 type 1 graphs. In addition to that it was found that there are 23 graphs of the second kind and 167 of the third. All but four of the 19 graphs without inverse propagators are linearly reducible (see fig. 3.2). The vast majority of type 2 and 3 graphs give graphical functions with enormous numerator polynomials that prohibited computations with them.

9 vertices. 9 vertex graphical functions are currently the most important to investigate, mainly because computing certain specimen leads directly to previously unknown periods of ϕ^4 graphs (see section 3.3.2).Their number is already too large to be reasonably and reliably generated by hand. There are 219, 563 and 8353 of the first, second and third kind respectively but only the 219 without inverse propagators were more thoroughly investigated, seeing that already at 7 and 8 vertices graphical functions with numerator structures due to inverse propagators are inaccessible with current programs. In total 88 of 219 graphs were found to be linearly reducible.

Only five of those 88 graphical functions could be integrated within reasonable time (<1 week). They are depicted in fig. 3.3. All others require excessive amount of time, and memory demands of several dozen GiB per process severely restrict the possibility of parallelization. From the set of graphical functions that are helpful for the computation of currently unknown ϕ^4 periods, only two are linearly reducible. The computation of the easier of the two will be finished in the foreseeable future (cf. section 3.3.2).

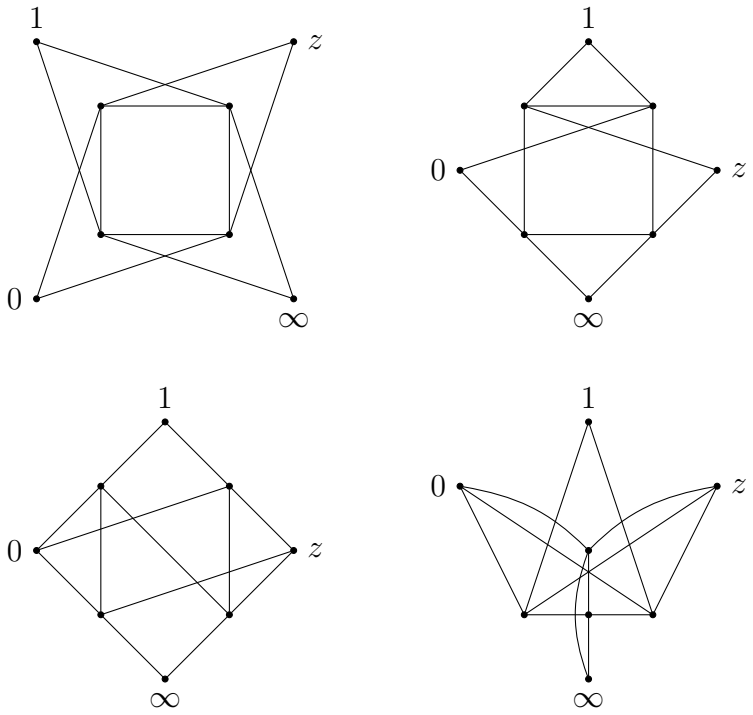

Figure 3.2: The four non-reducible graphs with 8 vertices and no inverse propagators.

10 vertices. For 10 vertices only the number of graphs of first and second kind is known: 1966 and 19914. Two important specimen (depicted in fig. 3.5), that would allow computation of new ϕ^4 periods were checked for linear reducibility. The upper graph depicted in fig. 3.5 was quickly found to be non-reducible but the computation for the other graph is quite time-consuming and still ongoing.

# vertices	7	8	9	10
# g.f. in type 1	1	19	219	1966
2	1	23	563	19914
3	5	167	8353	?
lin. reducible (only type 1)	1	15	88	?

Figure 3.4: Summary of computational results.

3.3.1 Upper bounds for Landau varieties of 9 vertex graphical functions

In definition 2.3.1 we mentioned the Landau variety as the subset of $\mathbb{C}^n$ on which (the analytic continuation of) a graphical function is not defined, which was essentially (see caveat below) the set of zero loci of the polynomials in the denominator. The previous section contained a brief example of an upper bound on that set of

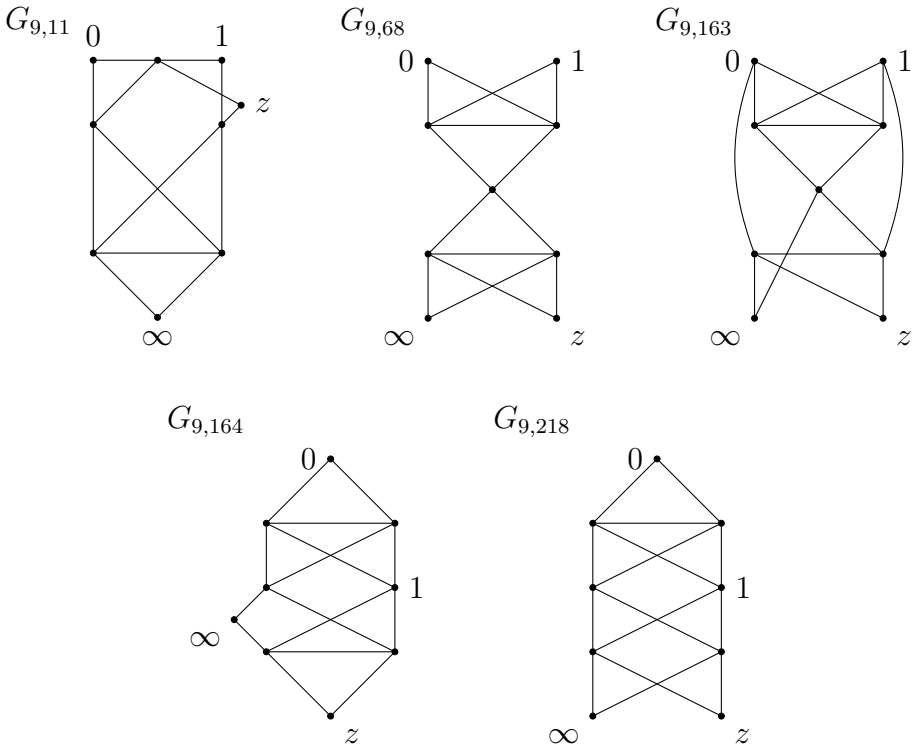

Figure 3.3: The five 9 vertex graphical functions that could be computed with `HyperInt`.

polynomials, as provided by the function `checkIntegrationOrder` for the case of a conformally parametrized graphical function with three external vertices:

Final polynomials

$$\{-1+z, -1+z\bar{z}, -z\bar{z}+z\}$$

We worked out integration orders for all 88 linearly reducible 9 vertex graphical functions and collected the upper bounds provided by `checkIntegrationOrder`. In addition to $\{z, \bar{z}, z-1, \bar{z}-1, z-\bar{z}\}$, which appears in every final polynomial set, we found the following linear combinations of

$$z_0 = z - \bar{z} \qquad z_1 = z\bar{z}$$
$$z_2 = (z-1)(\bar{z}-1) = z\bar{z} - z - \bar{z} + 1 \qquad z_3 = 1$$

with coefficients in $\{0, \pm 1\}$:

$$z_1 - z_2 \leftrightarrow z + \bar{z} - 1 \qquad z_1 + z_2 - z_3 \leftrightarrow 2z\bar{z} - z - \bar{z}$$
$$z_1 - z_3 \leftrightarrow z\bar{z} - 1 \qquad z_1 - z_2 + z_3 \leftrightarrow z + \bar{z}$$
$$z_2 - z_3 \leftrightarrow z\bar{z} - z - \bar{z} \qquad -z_1 + z_2 + z_3 \leftrightarrow 2 - z - \bar{z}$$

$$z_1 \pm z_0 \leftrightarrow z\bar{z} \pm (z - \bar{z}) \qquad z_2 + z_0 \leftrightarrow z\bar{z} + 1 - 2\bar{z}$$
$$z_3 \pm z_0 \leftrightarrow 1 \pm (z - \bar{z}) \qquad z_2 - z_0 \leftrightarrow z\bar{z} + 1 - 2z$$

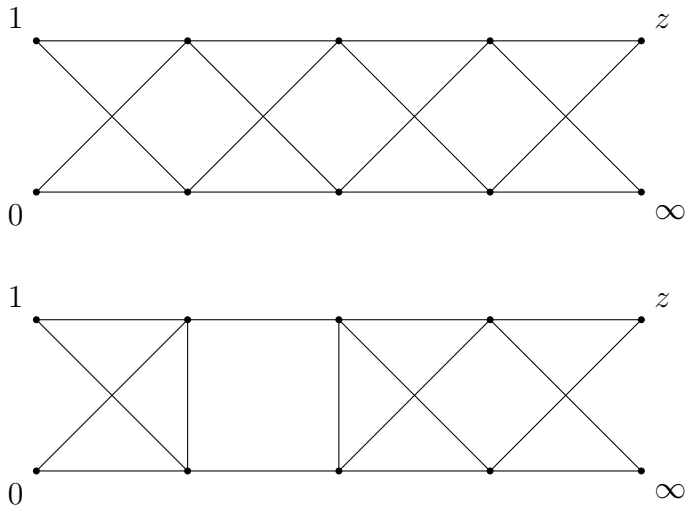

Figure 3.5: Two 10 vertex graphical functions.

We found only a single exception where a polynomial occurred that was not of this form. The reduction of the graph $G_{9,127}$ with external vertices assigned as in fig. 3.6 resulted in the two polynomials

$$z^2 - z - \bar{z} + 1 \quad \text{and} \quad \bar{z}^2 - z - \bar{z} + 1. \tag{3.4}$$

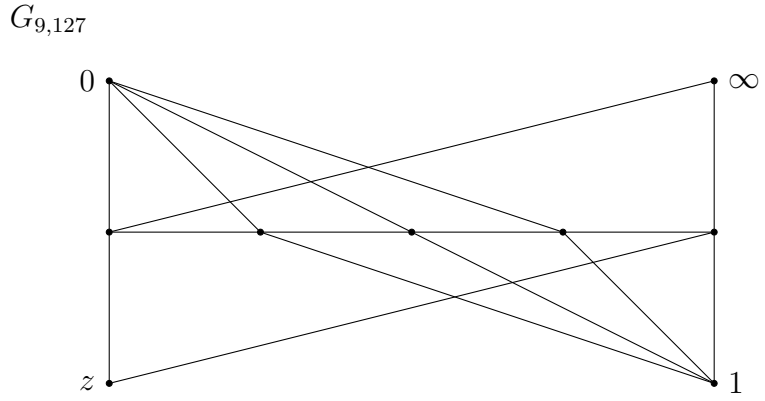

Figure 3.6: The graph $G_{9,127}$.

The zero loci of all these polynomials are upper bounds in two senses. On the one hand we have the fact that the algorithm used for the reduction gives an approximation of the Landau variety $\Sigma \subset \mathbb{C}^3 \ni (z_1, z_2, z_3)$. This means that the output of `checkIntegrationOrder` might contain 'final polynomials' that are not actually in the denominator of the integration result. On the other hand we have an extraordinary property of graphical functions in the conformal parametrization. From the obvious symmetry under exchange of z and $\bar{z}$ (the only $z, \bar{z}$ dependence is in $\hat{\Phi} = z\bar{z}\Phi_{0z} + (z-1)(\bar{z}-1)\Phi_{1z} + \Phi_{01}$) one knows that if a graphical function is of the form

$$f_G(z) = \frac{g(z)}{z - \bar{z}}, \tag{3.5}$$

that is, if it has a denominator polynomial with zero locus $z = \bar{z}$, then $g(z)$ must always be such that it vanishes at $z = \bar{z}$ and removes the apparent singularity. While this particular symmetry only works for $z - \bar{z}$, there might be other hidden symmetries that cancel other poles in a similar fashion. An indication for this is the fact that all graphical functions that have so far been checked by Schnetz with his own program [36] were singular only on

$$L = \{(z, \bar{z}) \in \mathbb{C}^2 \mid z\bar{z} = 0 \text{ or } (z-1)(\bar{z}-1) = 0\} \tag{3.6}$$

and nowhere else. This leads to the hypothesis that this might be a general property of *all* graphical functions. Our results are consistent with the hypothesis. The zero loci of all sets of polynomials found in the reductions have non-empty intersection with L and the one new 7 vertex function did not give a counterexample. At 9 vertices there are 28 linearly reducible (type 1) graphical functions that could not previously be computed with Schnetz's program, but they are so complicated that - while in principle integrable with `HyperInt` - they could not yet be computed to see if they provide a counterexample. Finishing these integrations will take an immense amount of computing time but should be doable in the long run.

3.3.2 The 9 vertex graphical function $G_{9,55}$

So far, all computing power has been concentrated on the integration of the graphical function of $G_{9,55}$ as depicted in fig. 3.7. Knowing this graphical function will provide the periods called $P_{8,26}$ and $P_{8,28}$ in [35].

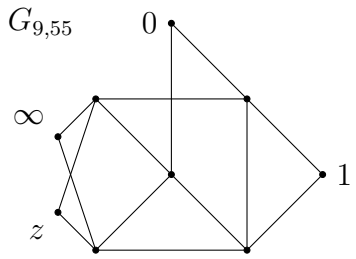

Figure 3.7: The graph $G_{9,55}$.

At the time of writing, the integration of the ninth of 11 variables (there are 12 edges remaining after removal of ∞ and one parameter is set to 1) is under way and approximately half finished. The first seven integration steps can be done in less than one day (on a single core) while the eighth integration already takes roughly 2-4 days, even including parallelization. For the integration of the ninth variable the integrand, which contains already 993,276 polylogarithms, was split into 199 batches of 5000 terms each. Integrating one such batch takes 3 to 7 days, claims 50-70 GiB memory and yields an intermediate result containing $\approx 10^8$ terms[3].

[3]Adding all intermediate results up in the end reduces the number of terms drastically, but will most likely still leave $\approx 10^6$ terms to be integrated in the next step.

Chapter 4

Conclusion

In this thesis we introduced a parametric version of Schnetz's graphical functions and presented various results obtained with it.

We gave a short introduction to the necessary graph theoretical concepts, focussing on the spanning forest polynomials of Brown and Yeats and their dual counterparts. Following that we set up graphical functions as defined by Schnetz (slightly - and straightforwardly - generalizing to an arbitrary number of external vertices). We then discussed some of their properties and applications in physics and mathematics.

The second chapter contains a derivation of a parametric integral representation of graphical functions carried out in the fullest possible detail. The result is a generalization of an integral representation of position space Feynman integrals due to Nakanishi. Using this new representation we introduced analytically continued graphical functions and proved their analyticity for the case that all arguments and edge weights have positive real parts. In the special case of the conformal parametrization we proved one new identity and presented a new proof of an identity originally due to Schnetz.

Apart from these theoretical considerations we also presented results of computations of concrete graphical functions. Specifically, we slightly modified Michael Borinsky's `feyngen` to generate a complete list of completed graphical functions in 4 dimensions with 7, 8 and 9 vertices that satisfy certain properties that make them interesting. These graphical functions were then checked for linear reducibility and if possible integrated with Erik Panzer's `HyperInt` - at least as far as processing power and memory limitations admitted.

There are several starting points for possible future work. The graph theory used so far was very basic. It might be possible to deduce new relations for spanning forest polynomials using one of the many rich theories that exist - graph homology and metric graphs (interpreting what we called weight as length) are keywords that come to mind. Ideally this would lead to further combinatorial criteria for linear reducibility.

On the level of the integral, a deeper understanding of the special functions that occur in the integration process is desperately needed. This includes the multiple polylogarithms briefly mentioned in the introduction but also much more general

objects like modular forms [13] and multiple elliptic polylogarithms [11]. It might be worthwhile to consider graphical functions in the context of moduli spaces, specifically moduli spaces of curves of genus zero with n marked points that have already been applied to Feynman integrals [9], [4]. Finally, it seems promising to consider graphical functions with non-Euclidean metrics. In particular, Penrose's Twistor theory [32] which already found applications in quantum gravity and string theory could be employed to look for deeper results on the behavior of graphical functions.

On a computational level, there will not be much more advances with the currently available programs and technology. In the near future the integration of $G_{9,55}$ will be finished and enable the computation of two new ϕ^4 periods. Integrating the remaining linearly reducible 9 vertex graphical functions would likely take several years and checking even a single 10 vertex graphical function for linear reducibility already takes weeks. However, an upcoming `FORM` implementation of `HyperInt`[1] will be able to deal with the huge number of terms that occur in the integration process much better than the current `Maple` implementation. This will allow for computations of 8 and 9 vertex graphical functions with large numerator structures and open up 10, possibly even 11 vertex graphical functions for integration.

[1] Private communication with E. Panzer.

Bibliography

[1] Maple 16. Maplesoft, a division of Waterloo Maple Inc., Waterloo, Ontario.

[2] Spencer Bloch, Hélène Esnault, and Dirk Kreimer. On motives associated to graph polynomials. *Communications in Mathematical Physics*, 267:181–225, 2006. arXiv:0510011v1 [math.AG].

[3] Christian Bogner. *Mathematical aspects of Feynman integrals*. PhD thesis, Johannes Gutenberg-Universität Mainz, 2009. URL: `http://ubm.opus.hbz-nrw.de/volltexte/2010/2215/`.

[4] Christian Bogner and Francis Brown. Feynman integrals and iterated integrals on moduli spaces of curves of genus zero. 2014. arXiv:14081862 [hep-th].

[5] Christian Bogner and Stefan Weinzierl. Feynman graph polynomials. 2010. arXiv:1002.3458v3 [hep-ph].

[6] Michael Borinsky. Feynman graph generation and calculations in the Hopf algebra of Feynman graphs. *Computer Physics Communications*, 185:3317–3330, 2014.

[7] David J. Broadhurst and Dirk Kreimer. Knots and numbers in ϕ^4-theory to 7 loops and beyond. *International Journal of Modern Physics*, C6:519–524, 1995.

[8] Francis Brown. The massless higher-loop two-point function. *Communications in Mathematical Physics*, 287:925–958, 2009. arXiv:0804.1660v1 [math.AG].

[9] Francis Brown. Multiple zeta values and periods of moduli spaces $\bar{m}_{0,n}$. *Annales scientifiques de l'ENS*, 42:371–489, 2009. arXiv:0606419 [math.AG].

[10] Francis Brown. On the periods of some Feynman integrals. 2010. arXiv:0910.0114v2 [math.AG].

[11] Francis Brown and Andrey Levin. Multiple elliptic polylogarithms. 2011. arXiv:1110.6917 [math.NT].

[12] Francis Brown and Oliver Schetz. A K3 in ϕ^4. 2011. arXiv:1006.4064 [math.AG].

[13] Francis Brown and Oliver Schnetz. Modular forms in quantum field theory. 2013. arXiv:1304.5342 [math.AG].

[14] Francis Brown and Oliver Schnetz. Single-valued multiple polylogarithms and a proof of the zig-zag conjecture. *Journal of Number Theory*, 148:478–506, 2015. arXiv:1208.1890 [math.NT].

[15] Francis Brown and Karen Yeats. Spanning forest polynomials and the transcendental weight of Feynman graphs. *Communications in Mathematical Physics*, 301:357–382, 2011. arXiv:0910.5429v1 [math-ph].

[16] John C. Collins. *Renormalization*. Cambridge Monographs on Mathematical Physics. Cambridge University Press, Cambridge, 1986.

[17] James M. Drummond. Generalised ladders and single-valued polylogs. *Journal of High Energy Physics*, 2013(2), 2013. arXiv:1207.3824 [hep-th].

[18] James M. Drummond, Claude Duhr, Burkhard Eden, Paul Heslop, Jeffrey Pennington, and Vladimir A. Smirnov. Leading singularities and off-shell conformal integrals. *Journal of High Energy Physics*, 2013(8), 2013. arXiv:1303.6909 [hep-th].

[19] Paul Ginsparg. Applied Conformal Field Theory. In Édouard Brézin and Jean Zinn-Justin, editors, *Fields, Strings and Critical Phenomena (Les Houches 1988, Session 49)*. North-Holland, 1990. arXiv:hep-th/9108028 .

[20] Marcel Golz. Evaluation techniques for Feynman diagrams. B.sc. thesis, Humboldt-Universität zu Berlin, Germany, 2013. URL: `http://www2.mathematik.hu-berlin.de/~kreimer/wp-content/uploads/BA_Golz_final.pdf`.

[21] Marcel Golz, Erik Panzer, and Oliver Schnetz. Properties of graphical functions. in preparation.

[22] Claude Itzykson and Jean Bernard Zuber. *Quantum Field Theory*. Dover Publications Inc., Mineola, NY, Dover edition, 2005.

[23] Gustav Kirchhoff. Ueber die Auflösung der Gleichungen, auf welche man bei der Untersuchung der linearen Vertheilung galvanischer Ströme geführt wird. *Annalen der Physik und Chemie*, 72:497–508, 1847.

[24] Maxim Kontsevich and Don Zagier. Periods. In Björn Engquist and Wilfried Schmid, editors, *Mathematics Unlimited - 2001 and Beyond*. Springer-Verlag, Berlin, 2001.

[25] Ivan Aleksandrovich Lappo-Danilevskij. *Mémoires sur la théorie des systèmes des équations différentielles linéaires*, volume I-III. Chelsea, 1953. Individual volumes first published in Travaux Inst. Physico-Math. Stekloff vol. 6-8, (1934-36).

[26] John M. Lee. *Introduction to Smooth Manifolds*. Springer, New York; London, 2nd edition, 2012.

[27] Brendan D. McKay and Adolfo Piperno. Practical graph isomorphism, {II}. *Journal of Symbolic Computation*, 60:94–112, 2014.

[28] Noboru Nakanishi. *Graph theory and Feynman integrals*, volume 11 of *Mathematics and Its Applications*. Gordon and Breach, New York (N. Y.) ; Paris ; London, 1971.

[29] Erik Panzer. Algorithms for the symbolic integration of hyperlogarithms with applications to Feynman integrals. 2014. arXiv:1403.3385v1 [hep-ph].

[30] Erik Panzer. *Feynman integrals and hyperlogarithms*. PhD thesis, Humboldt-Universität zu Berlin, 2015. URL: `http://www2.mathematik.hu-berlin.de/~kreimer/wp-content/uploads/Panzerphd.pdf`.

[31] Giampiero Passarino and Martinus J. G. Veltman. One-loop correction for e^+e^- annihilation into $\mu^+\mu^-$ in the Weinberg model. *Nuclear Physics: B*, 160:151–207, 1979.

[32] Roger Penrose. Twistor algebra. *Journal of Mathematical Physics*, 8(2):345–366, 1967. URL: `http://scitation.aip.org/content/aip/journal/jmp/8/2/10.1063/1.1705200`.

[33] Frédéric Pham. *Singularities of Integrals: Homology, hyperfunctions and microlocal analysis*. Springer, London, 2011.

[34] Friedrich Sauvigny. *Partial Differential Equations: Vol. 1 Foundations and Integral Representations*. Springer, London, 2006.

[35] Oliver Schnetz. Quantum periods: A census of ϕ^4-transcendentals. *Communications in Number Theory and Physics*, 4:1–48, 2010. arXiv:0801.2856 [hep-th].

[36] Oliver Schnetz. `zeta_procedures`, 2012. URL: `http://www2.mathematik.hu-berlin.de/~kreimer/tools/`.

[37] Oliver Schnetz. Graphical functions and single-valued multiple polylogarithms. 2013. arXiv:1302.6445v1 [math.NT].

[38] Oliver Schnetz. unpublished notes. 2013.

[39] Richard P. Stanley. Topics in algebraic combinatorics. `http://math.mit.edu/~rstan/algcomb/algcomb.pdf`. Version of 1 February 2013.

[40] William Thomas Tutte. Lectures on matroids. *Journal of Research of the National Bureau of Standards - B. Mathematics and Mathematical Physics*, 69B:1–47, 1965.

[41] Steven Weinberg. High-Energy Behavior in Quantum Field Theory. *Physical Review*, 118:838–849, 1960.

[42] Hassler Whitney. Congruent graphs and the connectivity of graphs. *American Journal of Mathematics*, 54:150–168, 1932.

[43] Hassler Whitney. Non-separable and planar graphs. *Transactions of the American Mathematical Society*, 34:339–362, 1932.

[44] Arthur S. Wightman and Raymond F. Streater. *PCT, Spin, Statistics and all that*. W. A. Benjamin Inc., New York, Amsterdam, 1964.

Acknowledgements

我谢谢我的女朋友，我的爱人，王潇睿的爱和支持。 Furthermore I thank my parents for their continued support, Oliver Schnetz for his patience when explaining things to me and his rigor when commenting on the nonsense I wrote, Dirk Kreimer for giving me the chance to work in such a fascinating field, Erik Panzer for illuminating discussions and the best 'customer support' imaginable and last but not least all my friends who help me get my mind off math and physics every now and then.

Selbständigkeitserklärung

Hiermit versichere ich, dass ich die vorliegende Arbeit selbständig verfasst und keine anderen als die angegebenen Quellen und Hilfsmittel verwendet habe.

Berlin, den